VECTRA

NEDO-10084-4
MARCH 1995

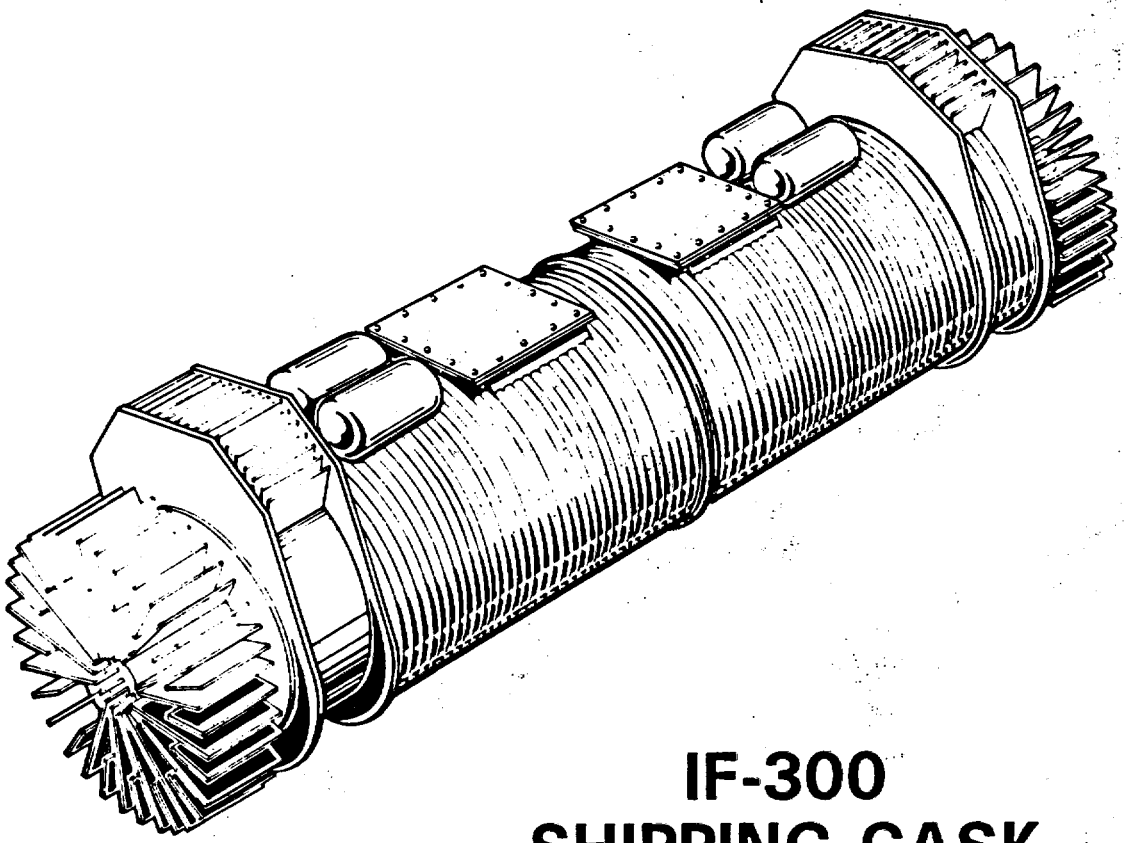

IF-300 SHIPPING CASK

CONSOLIDATED SAFETY ANALYSIS REPORT

VOLUME
2

ML

NOTICE AND DISCLAIMER

See Volume 1

REVISION CONTROL SHEET

See Volume 1

(BLANK PAGE)

TABLE OF CONTENTS

VOLUME 1

			Page
NOTICE AND DISCLAIMER			ii
REVISION CONTROL SHEET			iii
I.	INTRODUCTION		1-i
	1.1	Purpose	1-1
	1.2	IF-300 Cask	1-1
II.	DESIGN SUMMARY		2-i
	2.1	Cask Description	2-1
	2.2	Structural Analysis	2-4
	2.3	Thermal Analysis	2-8
	2.4	Criticality Analysis	2-10
	2.5	Shielding Analysis	2-11
	2.6	Fission Product Release	2-14
	2.7	Regulations	2-14
	2.8	Operation and Maintenance	2-14
	2.9	Fabrication and Quality Assurance	2-15
III.	FUELS AND CONTENT DESCRIPTION		3-i
	3.1	Introduction	3-1
	3.2	Fission Product Activities and Powers for the Design Basis Fuels	3-1
	3.3	Axial Peaking Factor	3-9
	3.4	Fuel Acceptance	3-9
	3.5	Defective Fuel	3-13
	3.6	Non-Fuel Contents	3-16
IV.	EQUIPMENT DESCRIPTION		4-i
	4.1	Shipping Package	4-1
V.	STRUCTURAL INTEGRITY ANALYSIS		5-i
	5.1	Introduction	5-1
	5.2	Design Loads	5-1
	5.3	Materials	5-3
	5.4	Vessel design Stress Analysis	5-10
	5.5	30-Foot Drop - Energy Absorption and Deceleration	5-27
	5.6	30-Foot Drop - Component Stresses	5-48
	5.7	40-Inch Drop Puncture	5-199
	5.8	Cask Tiedown and Lifting	5-207
	5.9	Engagement of Cask and Tiedowns	5-260
	5.10	Corrugated Exterior Water Containment	5-262
	5.11	Cask Reliability Under Normal Conditions of Transport	5-268
	5.12	Section Conclusion	5-307
	5.13	References	5-307

TABLE OF CONTENTS
(Continued)

VOLUME 1
(Concluded)

			Page
VI.	THERMAL ANALYSIS		6-i
	6.1	Introduction	6-1
	6.2	Procedures and Calculations	6-1a
	6.3	THTD Results - Design Basis Conditions	6-24
	6.4	Fuel Cladding Temperatures	6-33
	6.5	Miscellaneous Thermal Considerations	6-42
	6.6	Pressure Relief Devices and Fill, Drain, and Vent Valves	6-51
	6.7	Confirmation of Cask Thermal Performance	6-62
	6.8	Section Conclusions	6-79
	6.9	References	6-80
VII.	CRITICALITY ANALYSIS		7-i
	7.1	Introduction	7-1
	7.2	Discussions and Results	7-1
	7.3	Cask Fuel Loading	7-2
	7.4	Model Specification	7-5
	7.5	Criticality Calculation	7-14
	7.6	Critical Benchmark Experiments	7-18
	7.7	References	7-21
VIII.	SHIELDING		8-i
	8.1	Fuel Bases and Source Terms	8-1
	8.2	Shielding Methodology	8-6
	8.3	Internal Shielding	8-20
	8.4	Air-Filled Cavity Shielding	8-20
	8.5	Dose-Rate Acceptance Criteria	8-20
IX.	SAFETY COMPLIANCE		9-i
	9.1	Introduction	9-1
	9.2	10CFR71	9-1
	9.3	49CFR173	9-4
	9.4	Basic Components	9-5
X.	OPERATION, MAINTENANCE, AND TESTING		10-i
	10.1	Operating Procedures	10-1
	10.2	Maintenance Procedures	10-7
	10.3	Testing	10-8
	10.4	References	10-15

TABLE OF CONTENTS
(Continued)

VOLUME 2

			Page
XI.	APPENDICES		A-i
	APPENDIX V-1	NEDO-21796 - IF-300 CASK - BWR BASKET INTERNAL SHIELDING SAFETY ANALYSIS REPORT	V1-i
		Table of Contents	V1-iii
	I.	Introduction	V1-1
	II.	Modification Description	V1-1
	III.	Material Properties	V1-2
	IV.	Force-Time Justification/Design Basis Loading	V1-4
	V.	Structural Analysis	V1-28
	VI.	Other Analyses	V1-47
	VII.	Fabrication	V1-48
		References	V1-50
		Appendix A - Drawings	V1-A-i
		Appendix B - Effective Area Calculations	V1-B-i
		Appendix C - STARDYNE Description	V1-C-i
		Appendix D - Calculations	V1-D-i
		Appendix E - Thermal Stress Analysis	V1-E-i
	APPENDIX V-2	STRUCTURAL ANALYSIS OF IF-300 CASK FOR SHIPMENT OF GROUP II BWR AND PWR FUELS	V2-i
	APPENDIX V-3	IF-300 BWR FUEL BASKET HORIZONTAL DROP ANALYSIS	V3-i
	APPENDIX VI-1	IF-300 SHIPPING CASK DEMONSTRATION TESTING REPORT CASK #301	VI-i

TABLE OF CONTENTS
(Concluded)

VOLUME 3

		Page
XI.	APPENDICES	B-i
	APPENDIX A - CHANNELLED BWR FUEL BASKET	A-i
	A-1.0 General Information	A-1-1
	A-2.0 Structural Evaluation	A-2-1
	A-3.0 Thermal Evaluation	A-3-1
	A-4.0 Containment	A-4-1
	A-5.0 Shielding Evaluation	A-5-1
	A-6.0 Criticality Evaluation	A-6-1
	A-7.0 Operating Procedures	A-7-1
	A-8.0 Acceptance Tests and Maintenance Program	A-8-1
	A-9.0 Quality Assurance	A-9-1
	APPENDIX B - HIGH BURNUP PWR FUEL	B-i
	B-1.0 Introduction	B-1
	B-2.0 Analysis Methodology	B-2
	B-3.0 Neutron and Gamma Source Strength and Decay Heat Calculation	B-4
	B-4.0 Determination of Activation Product and Crud Source Terms	B-13
	B-5.0 Comparison with IF-300 Package C of C	B-16
	B-6.0 Conclusion	B-21
	B-7.0 References	B-25
	APPENDIX C - OUTER PLASTIC WRAP	C-i
	C-1.0 Introduction	C-1
	C-2.0 Procedures and Calculation Methodology	C-2
	C-3.0 IF-300 Shipping Cask Temperature Distributions	C-11
	C-4.0 Conclusions	C-13
	C-5.0 References	C-14

TABLE OF CONTENTS

XI. APPENDICES

		Page
V-1	NEDO-21796	V1-i
V-2	Structural Analyses of IF-300 Cask for Shipment of Group II BWR and PWR Fuels	V2-i
V-3	IF-300 BWR Fuel Basket Horizontal Drop Analysis	V3-i
VI-1	IF-300 Shipping Cask Demonstration Testing Report Cask #301	VI-i

E

APPENDIX V-1

NEDO-21796

IF-300 CASK - BWR BASKET

INTERNAL SHIELDING SAFETY

ANALYSIS REPORT

DECEMBER 1977

TABLE OF CONTENTS

		Page
I.	Introduction	V1-1
II.	Modification Description	V1-1
III.	Material Properties	V1-2
	A. Components/Materials	V1-2
	B. Physical Properties	V1-2
	1. Stainless Steel	V1-3
	2. Depleted Uranium	V1-3
	C. Dynamic Properties	V1-4
IV.	Force-Time Justification/Design Basis Loading	V1-4
	A. Introduction	V1-4
	B. Fin Bending Analysis	V1-5
	1. Summary	V1-5
	2. Discussion	V1-5
	C. Application of Fin Bending Analysis to the IF-300 Cask	V1-15
	D. Cask Deceleration Analysis	V1-21
	E. Application To The Internal Shielding Assembly Structural Analysis	V1-25
	F. Dynamic Amplification Factor (DAF) Determination	V1-26
	G. Design Basis g-loads	V1-27
V.	Structural Analysis	V1-28
	A. Introduction	V1-28
	B. Limit Stresses	V1-28
	C. Calculational Methods and Computer Codes	V1-31
	D. Analytical Results Summary	V1-32
	1. 30' Drop	V1-32
	2. Thermal Stresses	V1-35
	3. Brittle Behavior of Uranium Metal	V1-40
	4. Other Structural Considerations	V1-46
VI.	Other Analyses	V1-47
	A. Shielding	V1-47
	B. Nuclear Criticality Safety	V1-47
	C. Heat Transfer	V1-47
VII.	Fabrication	V1-48
	A. Processes and Methods	V1-48
	B. Quality Assurance	V1-49
VIII.	References	V1-50
Appendices		
	A. Drawings	V1-A-i
	B. Effective Area Calculations	V1-B-i
	C. STARDYNE Description	V1-C-i
	D. Calculations	V1-D-i
	E. Calculations	V1-E-i

IF-300 CASK - BWR BASKET INTERNAL SHIELDING SAFETY ANALYSIS REPORT

I. Introduction

Dose rate measurements taken during our first Dresden 2 fuel shipping campaign showed higher than expected readings at the IF-300 cask closure flange. The dose rates were not in excess of regulatory limits, however, extrapolation of these measurements to higher exposure BWR fuel showed the possibility of exceeding the prescribed limits at a future time. The source of this radiation was determined to be Cobalt-60 in the BWR upper tie plate and handle assembly. Subsequent measurements on an IF-300 cask loaded with PWR fuel showed that a similar situation does not exist for these assemblies.

Supplementary shielding will be added to the BWR fuel basket to prevent the occurrence of excessive cask flange dose rates on shipments of high exposure BWR fuel. This additional shielding masks the IF-300 closure flange area and will assure that external dose rates remain below unacceptable levels.

This report contains a detailed description of the proposed modification as well as shielding, structural, criticality and heat transfer analyses. The shielding assembly fabrication and quality assurance program are also discussed.

II. Modification Description

An add-on modification to the BWR fuel basket has been selected as the best method of providing supplementary shielding. Due to space limitations, depleted uranium metal is used as the shielding medium. Uranium pieces approximately one inch thick are encased in stainless steel and attached to the fuel basket between the basket top plate and the first support ring. Appendix A contains descriptive drawings of the proposed modification. Drawing 159C5238 sheet 6, Rev. 5 shows the entire BWR basket with shielding pieces; 159C5238 sheet 10, Rev 54 shows just the BWR basket upper end with the shielding pieces in place; and 159C5238 sheet 11, Rev 20 shows details of each shielding piece and its connection to the BWR basket.

In order to conform to the basket geometry, the supplementary shielding consists of fourteen pieces or subassemblies. All subassemblies have the same basic construction with the uranium pinned or threaded to a top and bottom stainless steel block. The uranium is then boxed-in with stainless steel end and side pieces. The steel is welded and makes a water tight, close fitting encapsulation. As in the cask body fabrication, a copper diffusion barrier exists at each steel-uranium interface. Each

clad subassembly is fixed to the basket by pinning and welding.

The depleted uranium pieces are vacuum cast in ceramic molds, rough forged and then machined to shape. The physical properties and chemical composition of these pieces are similar to those of the cask body and head shielding.

In addition to the shielding pieces and their supports, some minor modifications to the BWR basket are required to provide more structural rigidity. First the basket top plate, to which the shielding pieces are pinned, is extended to a full circle by the addition of four crescent shaped pieces. Second, the basket lifting bars are converted into I-beams to which the crescent-shaped pieces have been welded, and third, four L-shaped pieces of high-strength (216 SST) stainless steel are inserted in the "corners" of the top plate replacing the 304 stainless steel. These changes are shown in Appendix A on drawings 159C5238 sheets 6 and 10.

III. Material Properties

A. Components/Materials

The following is a list of the components, by generic description, and their materials of construction.

TABLE 1

Component	Material
1. Shielding pieces	Depleted uranium metal - ASTM B419 - 64T
2. Top and bottom subassembly bars (1/2" thick)	304 stainless steel - ASTM A276
3. Subassembly side plates (.060" Thick)	304 stainless steel - ASTM A240
4. Subassembly end bars (3/16" thick)	304 stainless steel - ASTM A276
5. Studs (3/8" & 7/16" OD)	Nitronic 60, 17-4 PH, 304 SST.
6. Support ribs	304 stainless steel - ASTM A276
7. Basket corner inserts	216 stainless steel - AISI 200
8. I-beam lifting bar	304 stainless steel - ASTM A276
9. Top plate extension	304 stainless steel - ASTM A276
10. All uranium-stainless steel interfaces	Copper, .004" minimum (flame-sprayed)

B. Physical Properties

There are basically three thermal conditions under which the BWR basket modification must be evaluated; these are as follows:

B. Physical Properties (cont'd)

- o low temperature - (-40°F)
- o normal temperature - 450°F(1)
- o high temperature - 1000°F

1. Stainless Steels

Table 2 shows the properties used in these evaluations for the various stainless steels.

TABLE 2

Stainless Steel Properties

Item	Temperature -40°F	450°F	1000°F	References
304 Yield stn, ksi	40.0	20.1	15.6	(1), (2), (2)
304 ultimate stn, ksi	140.0	64.0	57.7	(1), (3), (3)
304 mod. of elasticity, E X 10^6 psi	29.0	26.2	22.5	(3), (1), (4)
304 coeff. of thermal expansion, $\alpha \times 10^{-6}$ in/in/°F	8.4	9.65	10.1	(1), (2), (4)
216 yield stn, ksi	>62.4	44.9	36.3	(15), (15), (15)
216 ult stn, ksi	>100.0	89.9	75.4	(15), (15), (15)
Nitronic 60 yield stn, ksi	>57.0	33.5	28.0	(17), (17), (17)
Nitronic 60 ultimate stn, ksi	>100.0	79.0	74.0	(17), (17), (17)
17-4 PH Cond. A yield stn ksi	>129.0	123.0	93.0	(21), (21), (21)
17-4 PH Cond. A ult. stn, ksi	>140.0	128.6	96.0	(21), (21), (21)

2. Depleted Uranium

TABLE 3

Depleted Uranium Properties

Item	-40°F	RT	450°F	1000°F	References
Yield, stn, ksi	>51.0	51.0	46.0	10.0	(5),(6),(7),(5) & (7)
Ultimate stn, ksi	>110.5	110.5	85.0	40.0	(5),(6),(7),(7)
Mod. of elasticity, E x 10^6 psi	30.2	29.5	26.6	20.1	(8),(5),(8),(8)
Coeff. of thermal exp., $\alpha \times 10^{-6}$ in/in/°F	7.5	-	8.56	10.8	(8),-,(8),(8)

(1) In this case, "normal" means the cask is at maximum heat load with the cooling system inoperative under 130°F still air ambient conditions.

C. Dynamic Properties

A great many materials used in shipping cask construction exhibit increased strength (yield and ultimate) with increased strain rate. BMI-1954 (Reference 9) documents this phenomenon for a number of materials including stainless steel and depleted uranium metal. Also see References 12 and 13.

In this analysis no credit will be taken for this increased strength. However, it should be remembered that the margins of safety based on static properties will be greater under actual conditions.

IV. Force-Time Justification/Design Basis Loading

A. Introduction:

The internal shielding assembly experiences its most severe structural loading under the 30 foot drop defined in 10CFR71, Appendix B. This hypothetical accident condition combined with certain initial conditions forms the assembly design basis.

The force-time behavior of the IF-300 cask under 30' drop conditions was initially defined in 1973 as part of the original design and analysis report, NEDO-10084-1. This definition, based on the correlation of fin bending tests conducted at ORNL, was obtained by dividing the cask drop height (H) by the cask stopping distance (δ) thus:

$$g = \frac{H}{\delta} \quad \text{(cask deceleration)}$$

This relationship was derived as follows

$W \cdot H$ = cask potential energy
W = cask weight
H = cask drop height

$F \cdot \delta$ = cask energy dissipation
F = fin bending force (assumed constant)
δ = cask stopping distance

Since:

$W \cdot H = F \cdot \delta$ (to dissipate all energy)

then by rearranging: $\frac{F}{W} = \frac{H}{\delta} = g$

A. Introduction (Cont'd)

Defining deceleration in this manner required several assumptions:

- the fin bending force (F) is constant
- the cask behaves as a rigid body

The first assumption was believed to be valid because an examination of the force-time histories of the fins tested at ORNL showed essentially constant-force behavior following an early-time, very short duration spike. The second assumption was based on an examination of cask structural parameters; although not absolutely rigid, the cask represented an extremely stiff structure.

The AEC/GE agreed-upon method of analysis, for the IF-300 cask was that components and structures in the immediate vicinity of the point(s) of impact would be evaluated at twice the H/δ deceleration; doubling the G-load was to account for impact effects. All other components would be analyzed at a deceleration of H/δ. This method was used for the cask structural analysis and AEC approval of the results was received.

For this current application where a series of small components within the cask (rather than the massive cask structure) are being evaluated under impact conditions it is necessary to consider the early-time as well as the late-time response of the cask impact fins and evaluate the internal shielding assembly accordingly. The following is a derivation of the early-time behavior of stainless steel fins under high strain-rate, large deformation conditions. This derivation is based on theoretical considerations, computer analyses and actual fin bending tests and represents the latest work on this subject.

B. Fin Bending Analysis(1)

1. Summary

There is substantial agreement between the force-time data taken from the mild-steel fin impact tests conducted at ORNL by Davis (see Reference 10) and the stainless steel fin impact tests conducted by Sandia Laboratories (see Reference 11). Peak stresses that were factors of two or three above the static yield stress were observed in the Sandia tests, while factors of four were observed in Davis' tests. The differences can be attributed to the higher strain-rate dependency of the mild steel. The strain rate effects on stainless steel (see References 12 and 13) are also crucial to any dynamic analysis that might be undertaken.

(1) Information furnished by Mr. R.E. Nickell, Pacifica Technology under contract to General Electric Co.

Numerical analysis of fins has assumed strain-rate independent properties and, as a result, no peak stresses above static yield are seen. A significant reduction of the propagated stress is observed in the cask shells, however, and it would be expected that similar reductions would occur in strain-rate-dependent analysis. This reduction is due to geometric dispersion of wave energy into cask material volume adjacent to the fin.

Correlation of both the Davis and Sandia Laboratories data reveals that the high peak stresses can be eliminated by proper choice of slenderness ratio and aspect ratio, in agreement with Euler and plate buckling formulas. Based upon the slenderness ratios of the various IF-300 fins and the restraint imposed by the lateral or circumferential dimension, the IF-300 fins should expect, under conservative conditions, to see the high peak stresses at impact.

2. Discussion

The planned approach to this investigation consisted of three parts: (1) an evaluation of the data in Reference 10, including load cell instrumentation, in order to determine the validity of the measured early-time force response; (2) early-time analysis of some representative fin geometries, in order to examine the strain-rate-independent response of the fins when attached to realistic cask structures; and (3) an assessment of relevant data available from other sources.

Because of the nature of the findings the tasks will be covered in inverse order.

(a) Impact Data

The only significant impact fin analysis discovered is that reported by Biffle et.al., in Reference 11. More important than the analysis, however, were the static and dynamic experimental results from prototypic fin tests. A pneumatic type of load cell, completely different from the strain gage bridge used by Davis and much better calibrated, recorded similar early-time pulses.

Although the object of these fin tests was primarily to evaluate a number of alternate fin geometries (some stiffened and some cylindrical), comparison tests were run on standard, rectangular fins. These standard fins were referred to as "simple" fins in Reference 11. The simple fins that were tested statically were 4 inches high, 1/4 inches thick, and 9 inches long. An examination of the static load-deflection trace reveals that buckling of the simple fin occurred when the entire cross-sectional

area reached its compressive plastic limit. In this case, the measured peak load was 80 Kips. The cross-sectional area was 2.25 in^2 which yields an average stress of about 35,000 psi (almost precisely the nominal static yield stress of 35 Ksi). After reaching peak load, of course, the fin eccentricity (no matter how small) causes the fin to buckle.

The two simple fin dynamic tests were also illuminating. Because of limitations on the drop table apparatus, the length of the fins was reduced from the 9 inch length used in the static tests to 6 inches. The two fins buckled into two slightly different mode shapes and two substantially different peak loads were recorded (slight differences in eccentricity are probably to blame). These two peak loads were 119 Kips and 160 Kips, respectively, or, taking the smaller cross-sectional area into account, the average stresses at peak load were about 79 Ksi and 107 Ksi. These values represent increases of about 125% and 205%, respectively, over the static yield stress.

These large peak forces are attributed to the strain-rate dependency of the austenitic stainless steels, as documented in References 12 and 13. Based upon data taken on AISI 304 and 316 stainless steels at strain-rates from 10^{-5} per second to about 10 per second, Steichen has concluded that the yield strength increases by about 48 MN/m^2 (7 Ksi) per decade of strain-rate. If the value at 10^{-5} per second is taken to be the static amplitude of the yield stress (35 Ksi), then the extrapolated value at strain-rates typical of impact (10 per second to 1000 per second) is between 77 and 91 Ksi, in reasonable agreement with the peak load stresses reported in Reference 11. It should be noted that even higher strain-rate effects would be expected in impacts involving mild steel.

In addition, Steichen reported two other items of interest. First, the hardening moduli (which determine the longitudinal wave propagation velocity in the fin and, therefore, the peak pulse shape) seem to be independent of strain rate. Second, the strain-rate dependency of the yield stress is reduced at higher temperatures (~400°F). Both of these items are explained by the pinning of dislocations at high strain rates. Once the yield stress is reached, or if the activation temperature is higher, mobility of dislocations returns.

(b) Fin Analysis

Two geometries have been discretized for nonlinear dynamic finite element analysis. One is a plane strain representation of a longitudinal fin attached to a layered surface having no circumferential curvature, as shown in Figure 1. The other is a three-dimensional representation of an actual circumferential fin, including the valve box flare (5° fin inclination) as shown in Figure 2. The analyses were to be carried out with best-estimate

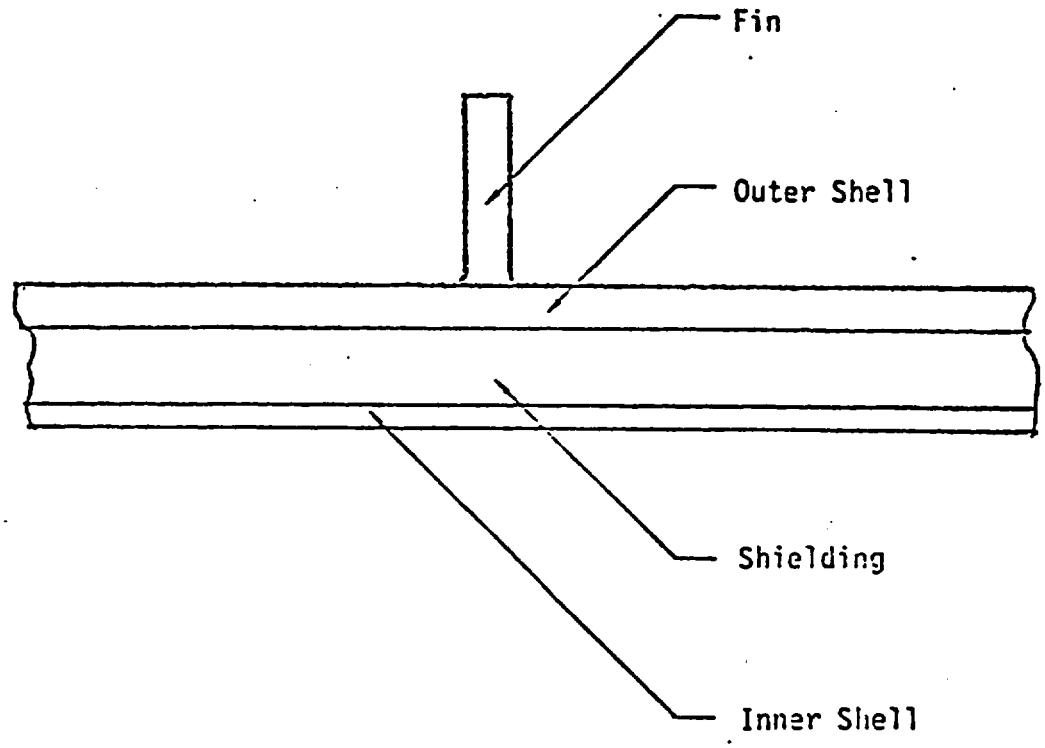

Figure 1. Two-Dimensional, Plane-Strain Model Circumferential Fin

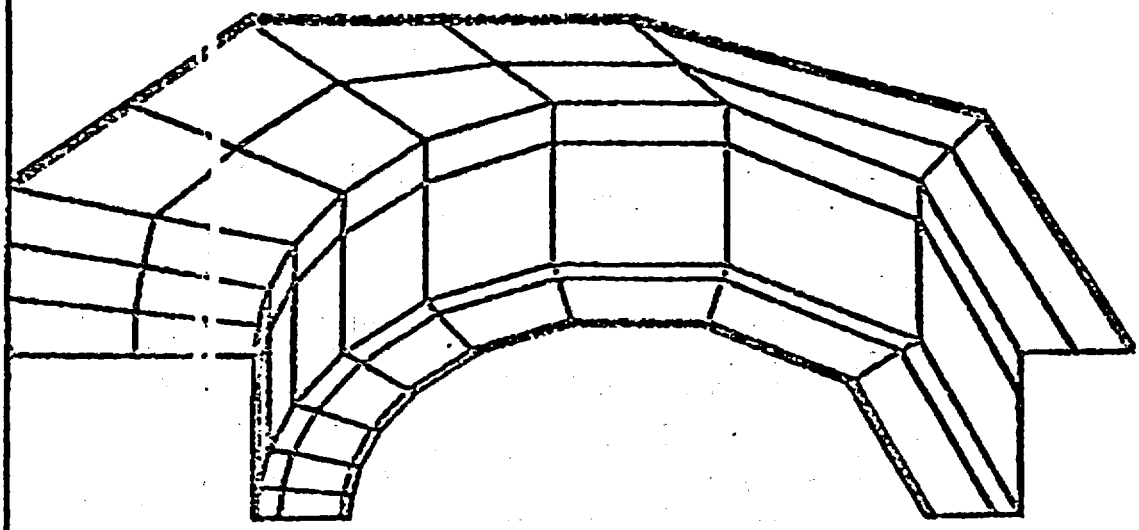

Figure 2. Three-Dimensional Model of Circumferential Fin.

strain-rate-independent properties. Durations of the order of 1 millisecond (early-time) were to be analyzed in order to verify the absence of peak stresses substantially above the static yield stress. Because of the expense of computation associated with the three-dimensional analysis, the plane strain calculations were completed first.

A static yield stress value of 35,700 psi and a hardening modulus of 525,000 psi (as contrasted to Young's modulus of 24×10^5 psi) were used in the plane strain analyses. Both the Sandia Laboratories code HONDO and the M.I.T. code ADINA were exercised and compared. As was expected, stresses from the impact end propagated at velocities dictated by the hardening modulus,

$$c_L \cong \sqrt{\frac{E_T}{\rho}} \quad ,$$

where c_L is the longitudinal wave speed, E_T is the tangent (hardening) modulus, and ρ is the density.

In addition, and as expected, the amplitude of stress was limited by the static yield stress (with a small amount of hardening as a function of plastic straining). No load peaks were observed. The beneficial effect of geometric dispersion of wave energy from the fin into cask containment and shielding material adjacent to the fin was observed. A typical result in a conservative location (in the outer shell, directly under the fin centerline) shows a reduction in peak equivalent stress of about 50%.

(c) Davis Data

An examination of the computer-generated force-time plots from the data of Reference 10 shows a strain-rate effect that is at least as pronounced as the Sandia Laboratories impact results. Peak stresses average out at about 100 Ksi, with the slender fins showing almost no strain-rate effect and the stubby fins showing substantial strain-rate dependence. However, the results are not uniform since some thin, but stubby, fins do not exhibit these effects.

In order to arrive at a reasonable correlation with the experimental data, an elastic buckling model is proposed. The reasoning is that all fins are sensitive to imperfections if the stress is sufficiently large, and that strain-rate effects allow the stress to reach these large compressive values in stubby fins. Also, restraint supplied by fin width should be accounted for through an aspect ratio dependence. In the following, an energy method is used to produce the desired result.

In order to apply an energy method to the buckling of the fins, an approximate buckled profile must be assumed. This displaced shape must satisfy the kinematic boundary conditions and should reflect known information. Here we assume that the fin is restrained against transverse displacement and rotation at its attachment to the cask (or base plate). Therefore,

$$\bar{w}(o,y) = \frac{\partial \bar{w}}{\partial x}(o,y) = 0$$

We also assume that the fin buckles in shape of a "question mark"[1] and that the dynamic loading is conservative (i.e., the applied force always remains directed parallel to the x-axis and remains in the z=o plane). For initial simplicity we also assume that there is no dependence on y (i.e., there is no twisting or warping of the cross section during buckling). It also should be noted that, because of the strain rate effects, uniformity of stress is assumed. Inertia is implicitly included in the strain-rate effects on yield, but is not explicitly considered in the energy balance.

The simplest expression that accomplishes these goals is the deflected shape

$$\bar{w}(x,y)=w_0 x^2(x-\ell).$$

Substituting into the bending strain energy

$$D\iint\left\{\left(\frac{\partial^2\bar{w}}{\partial x^2}+\frac{\partial^2\bar{w}}{\partial y^2}\right)^2 -2(1-\nu)\left[\frac{\partial^2\bar{w}}{\partial x^2}\frac{\partial^2\bar{w}}{\partial y^2}-\left(\frac{\partial^2\bar{w}}{\partial x\partial y}\right)^2\right]\right\}dx\,dy$$

and integrating gives

$$4Dbw_0^2\ell^3,$$

where D is the flexural stiffness ($Eh^3/12(1-\nu^2)$), ν is Poisson's ratio, E is Young's modulus, h is the fin thickness, ℓ is the height, and b is the width. The assumed deflected shape is also substituted into the initial stress membrane energy

$$\iint\left[N_x'\left(\frac{\partial\bar{w}}{\partial x}\right)^2+N_y'\left(\frac{\partial\bar{w}}{\partial y}\right)^2+2N_{xy}'\left(\frac{\partial\bar{w}}{\partial x}\right)\left(\frac{\partial\bar{w}}{\partial y}\right)\right]dx\,dy$$

---

[1] A reasonable assumption based on Davis' tests of 0° and 10° inclined fins all of which bent into this shape.

and integrated to give

$$\frac{2}{15} \quad N_x' \quad b \quad w_0^2 \quad \ell^5 \quad ,$$

where N_x', N_y' and N_{xy}' are the "initial" resultants (per unit length) that are to be scaled by the buckling factor, γ, in order to reach critical values. In our case

$$\gamma = \frac{4 \; D \; b \; w_0^2 \; \ell^3}{\frac{2}{15} N_x' \; b \; w_0^2 \; \ell^5}$$

or

$$(N_x)_{cr} = \gamma \, N_x' = 30 \; \frac{D}{\ell^2} \, .$$

The critical stress is

$$(\sigma_x)_{cr} = \frac{30 \; D}{\ell^2 \; h} \, ,$$

or, for $\nu = 0.3$,

$$\frac{(\sigma_x)_{cr}}{E} = 2.75\left(\frac{h}{\ell}\right)^2 \, .$$

This result is similar to the Euler column buckling formula. It should be noted that no dependence upon aspect ratio is observed.

In order to develop a correlation that involves the aspect ratio, some dependence on the coordinate y must be assumed for the trial buckling shape, or

$$\bar{w}(x,y) = w_0 \, x^2 (x-\ell) y.$$

Carrying out similar steps yields

$$\frac{(\sigma_x)_{cr}}{E} = 2.75\left(\frac{h}{\ell}\right)^2 \left[\frac{1}{1 + \frac{7}{6}\left(\frac{\ell}{b}\right)^2 \frac{N_y'}{N_x'}}\right] \, .$$

where the correction term depends both on the aspect ratio, l/b, and the stress resultant ratio, N_y'/N_x'. This term is the most elementary of its kind, but it describes the effect of lateral restraint on the critical buckling stress. Of course, the stress ratio does not remain constant in either time or space. Therefore, this equation will be replaced by a <u>correlation</u> equation

$$\frac{(\sigma_x)_{cr}}{E} = A\left(\frac{h}{\ell}\right)^2 \left[\frac{1}{1 + B\left(\frac{\ell}{b}\right)^2}\right] .$$

where A and B are correlation coefficients to be determined from existing impact data.

Before attempting to correlate the existing impact data, it is useful to plot the information (see Figure 3) in a dimensionless form, such as normalized peak stress as a function of the square of the slenderness ratio, with aspect ratio as a parameter. Two trends are thus observed. First, for a given slenderness ratio, the peak stress increases as the aspect ratio decreases. This trend can be interpreted as a lateral restraint effect-namely, the tendency to buckle is inhibited somewhat by the fin width. Second, for a given aspect ratio, the peak stress tends to increase as the slenderness ratio decreases, in agreement with the Euler column formula. Both trends are explained, to some extent, by the correlation equation derived above.

In order to fit the data, we choose a slenderness ratio of 16, and aspect ratios of 4 (Davis) and 2/3 (Sandia). This yields values of

$$A = 0.90 , \quad B = 0.16 .$$

The correlations are given in Figure 3 for several values of aspect ratio, in order to compare with the actual data. Plastic buckling is shown by horizontal dashed lines, such as the one representing the static yield stress ratio of 1.2×10^{-3}. This corresponds to a yield stress of 36 Ksi and a modulus of 30×10^6 psi. Strain-rate dependence is represented by higher horizontal lines.

Because of these trends, an assessment of the IF-300 impact fins is possible, provided that some assumption about the "active" fin width can be justified. For example, the slenderness ratios

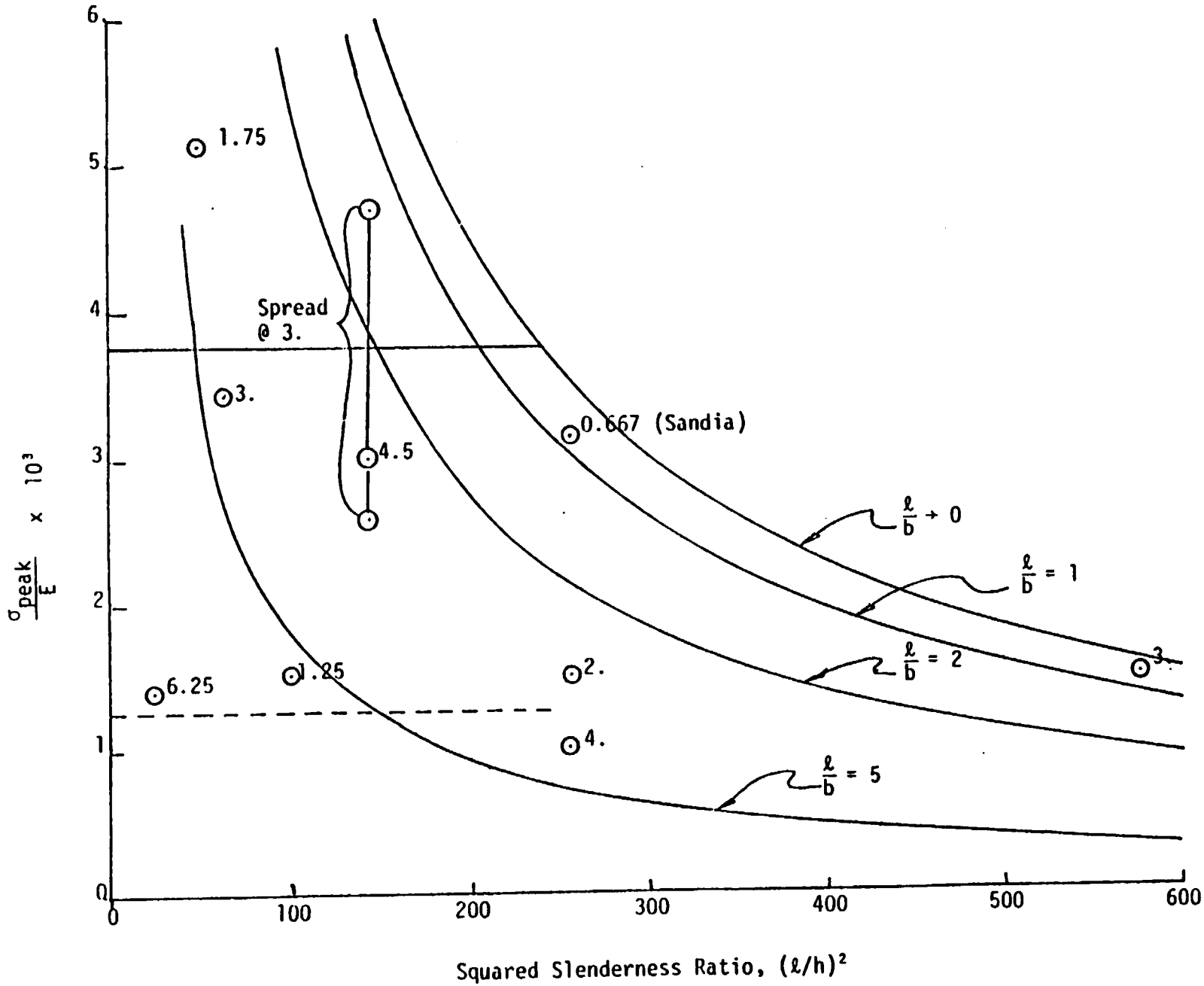
6
5
4
3
2
1
0
0
100
200
300
400
500
600
1.75
Spread
@ 3.
3.
4.5
0.667 (Sandia)
$\frac{\ell}{b} \to 0$
$\frac{\ell}{b} = 1$
$\frac{\ell}{b} = 2$
$\frac{\ell}{b} = 5$
3.
6.25
1.25
2.
4.
$\frac{\sigma_{peak}}{\sigma} \times 10^3$
Squared Slenderness Ratio, $(\ell/h)^2$

Figure 3.

of the IF-300 fins vary from about 5.6 for the four circumferential rings (7" high by 1.25" thick) to 7.0 and 8.4, respectively, for the two sets of top end fins (8" high by 1-1/8" thick and 9.5" high by 1-1/8" thick). A more favorable situation exists with the circumferential fins near the valve boxes, where a slenderness ratio of between 12 and 13 could be used, depending upon impact attitude.

Based upon the data of Steichen, extrapolated to strain rates of 10^3 per second, a maximum stress of 90 Ksi is assumed. With $E = 24 \times 10^6$ psi, this yields the solid horizontal line in Figure 3. This indicates that, for an aspect ratio of unity or less (typical of IF-300 fins), the slenderness ratio would have to be greater to reduce the peak stress. Since this is not the case, the IF-300 fins will see peak stress on the order of 90 Ksi.

Based upon this value and using some knowledge of the wave motion in the fin (see Figure 4), the wave speed is estimated to be between 40,000 and 70,000 in/sec. The force is seen to build up rather linearly to peak stress, depending upon the impedence at each end of the fin. Thus, a stress-time history for the IF-300 fins can be derived and plotted in Figure 5. Note that, following buckling, the force is governed by the static yield stress. In reality, the post-buckling force is difficult to determine, but values that are near the membrane yield force seem to correlate reasonably well with existing data.

C. Application of Fin Bending Analysis to the IF-300 Cask

Figure 5 is a plot of stress as a function of time for the variety of fins found on the IF-300 cask. In order for this plot to be useful in analyzing the internal shielding assembly response to cask impact, Figure 5 must be converted into a force-time or deceleration ("g") - time relationship.

To make the force-time conversion, Nickell suggests multiplying the active or effective fin cross-sectional area by the stress values from Figure 5. This cross-sectional area is simply the product of the fin thickness and the fin effective width. Effective widths of rectangular fins are the actual geometric widths; for circumferential fins the effective widths are based on the hinge (bend) line lengths. The original cask drop analysis used the concept of effective fin width, a detailed discussion of this is found on page 5-31 of the cask DAR (Reference 14). This discussion is reproduced as follows: (Note that what is referred to above as "width" is called "hinge line length" below):

> "As shown in Figure V-8 [Figure 6, this report], the structural rings and fins were assumed to form two hinges with the hinge closest to the cask forming at two times the fin thickness

Figure 4.

Fin Bending Test No. 14, F. Davis - ORNL

b = 2 in., ℓ = 3.5 in., h = 0.5 in.

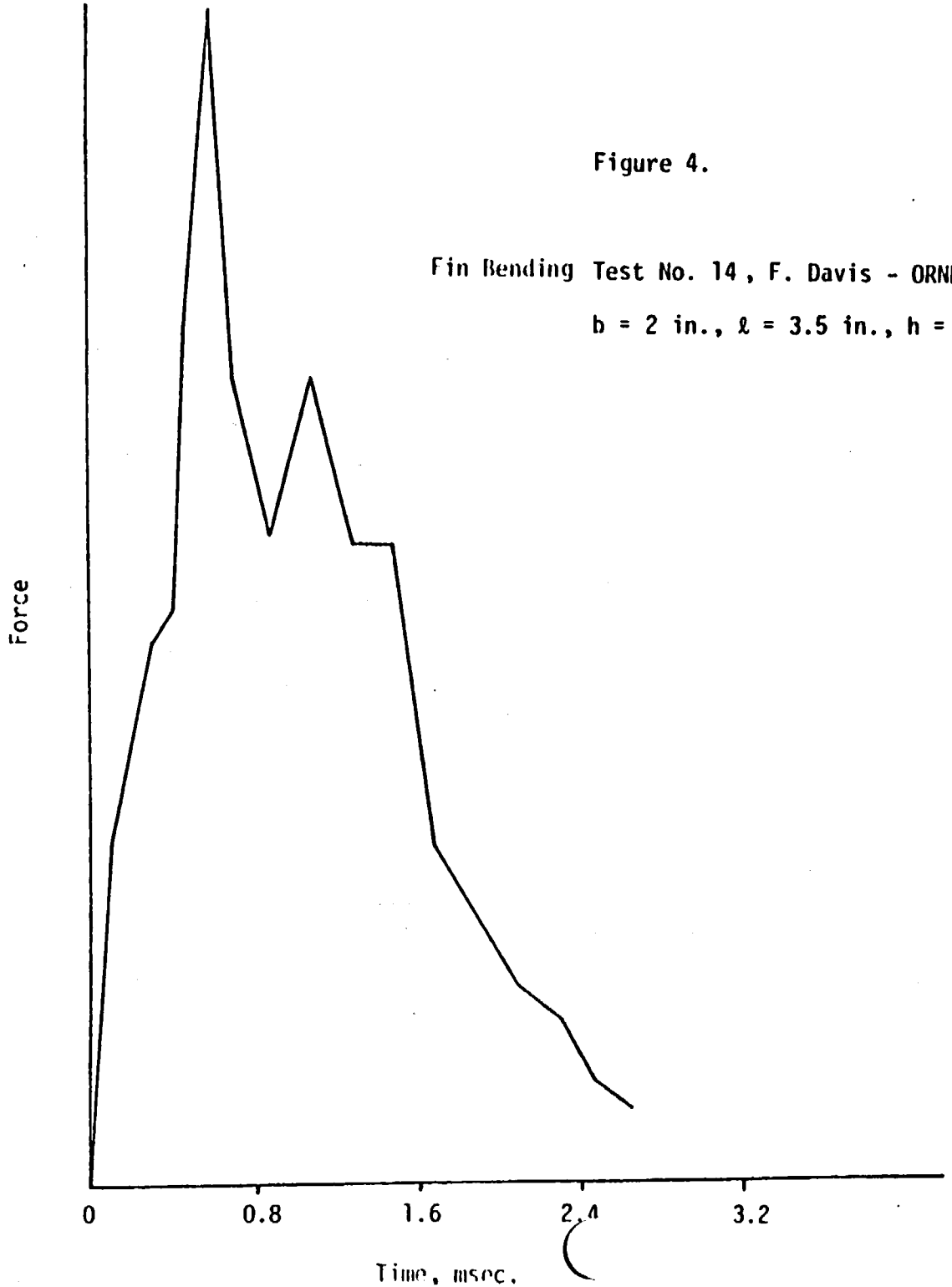

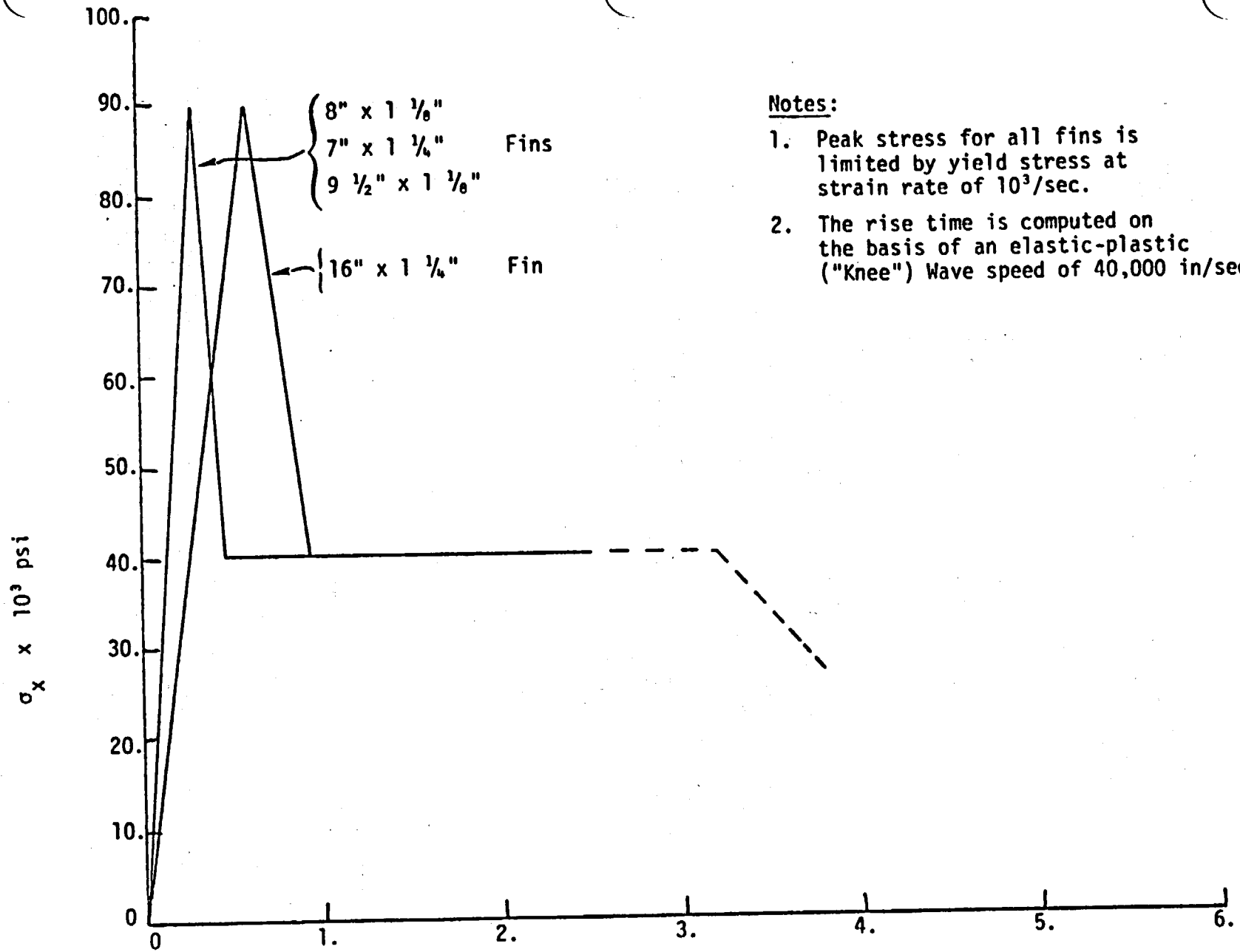

Notes:

1. Peak stress for all fins is limited by yield stress at strain rate of 10^3/sec.
2. The rise time is computed on the basis of an elastic-plastic ("Knee") Wave speed of 40,000 in/sec.

Stress vs Time for Stainless Steel Fins

Figure 5.

away from the cask surface. The second hinge formed at 0.65 times the fin height away from the cask surface. The effective hinge length of the circular structural rings was computed as follows:

$$L_{eff} = \frac{2\ L_o + L_i}{3}$$

where: L_o = length of outer hinge line

L_i = length of inner hinge line

(See Figure V-8)
[Figure 6, this report]

This is based on the fact that the outer hinge absorbs approximately two-thirds of the energy and the inner hinge absorbs the remaining one-third."

It should be noted that the fin deformed shape and location of hinges assumed above was based on measurements of actual test fins.

The internal shielding assembly will be analyzed under 30-foot drop conditions considering 5 cask orientations, three on the side (0°, 45°, 90°) and one on each end (head and bottom). The following table shows these five orientations, the effective impact fin areas and the resultant forces (Figure 5-peak and plateau). Effective area calculations are in Appendix B.

TABLE 4

Areas and Forces

(See Figure 6) Cask Orientation	Total Fin Eff. Area, In^2	Force, Kips Peak	Force, Kips Plateau
0° - Side (1)	318	28620	12720
45° - Side (1)	238	21420	9520
90° - Side (1)	207	18630	8280
Top - End	435	39150	17400
Bottom - End	446	40140	17840

The forces appearing in Table 4 are those which would be applied to the cask body at the appropriate location as a function of time. Figure 7 is an example of the F-t plot for one of the two pairs of impact rings in the 0° side drop orientation. The peak force of 14310 Kips is (by symmetry) half of the peak shown in Table 4 for the 0° drop.

(1) The total side drop area is divided equally between the upper and lower pair of impact rings.

FIGURE WITHHELD UNDER 10 CFR 2.390

FIGURE 6

STRUCTURAL RING, FIN, AND VALVE BOX ARRANGEMENT

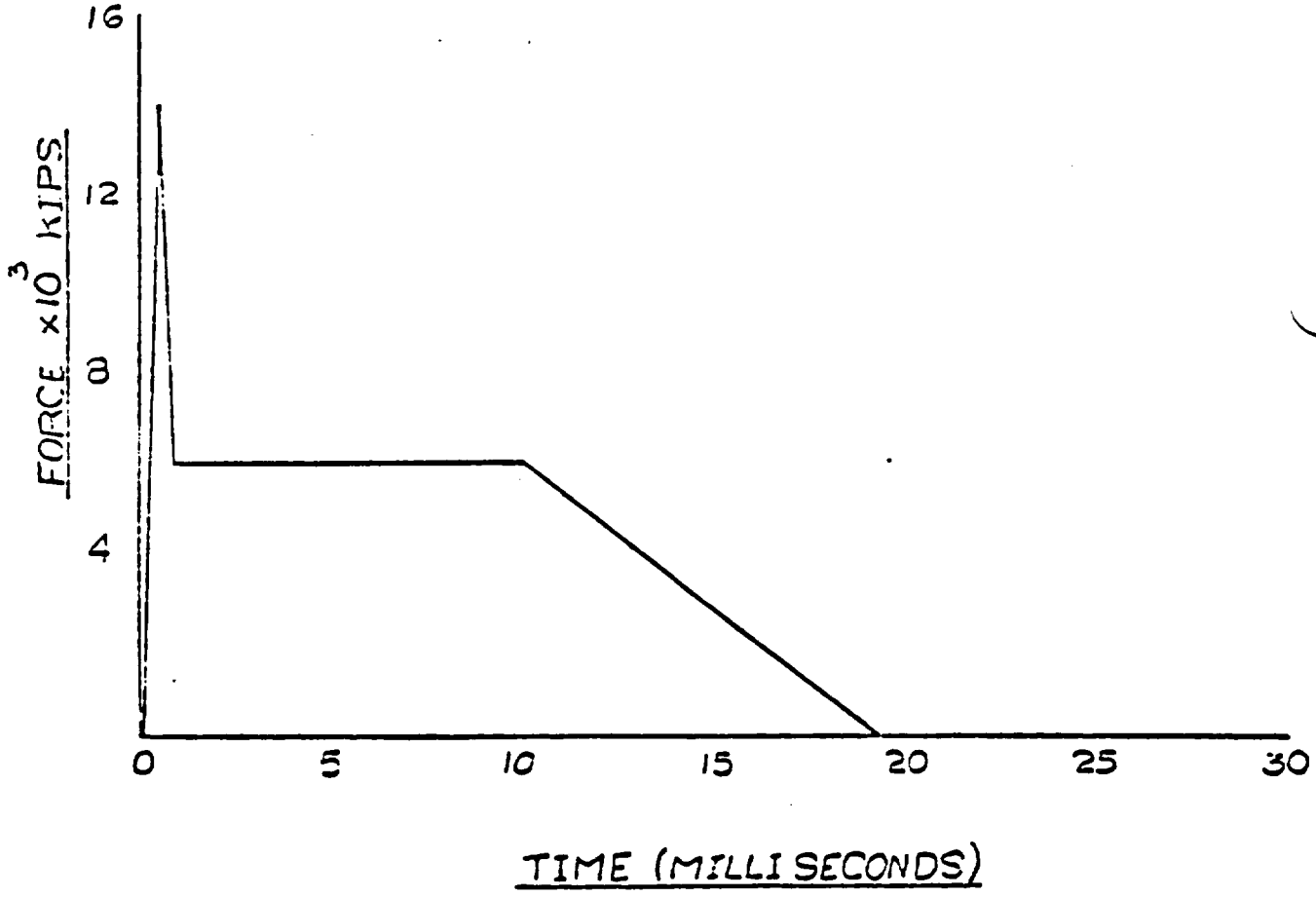

0° Orientation - Forcing Function-Time History

FIGURE 7

The force-time history represented by Figure 7, although typical of what the cask body will experience, is not what will be experienced by the internal shielding assembly. A more usable relationship for the evaluation of this internal structure is deceleration (g) vs time. If the cask were an absolutely rigid body then dividing the forces from Table 4 by the weight of the cask would yield the "g" values. However, there is some deviation from rigid body behavior and further analysis is required to define the cask deceleration as a function of time.

D. Cask Deceleration Analysis[1]

A model has been developed which analyzes the structural response of the IF-300 cask and its contained fuel rods under 30 foot drop conditions. This work is preparatory to a future certificate amendment request. The computer model developed, shown as Figure 8, is a full length representation of the IF-300 cask body and fuel assemblies (modeled in longitudinal bending). The model is non-linear static and dynamic. It was decided to use this model under differing time-related forcing functions to arrive at a comparison between rigid body and flexible body deceleration assumptions. The following three cases were evaluated:

- The model (DRAIN-2D code) supports,nodes 8 and 76, were given a vertical acceleration of 122 g's for 11 milliseconds. This is the maximum side drop deceleration used in the original cask SAR (NEDO-10084-1). This is shown on Figure 9. (Flexible body model- rigid body deceleration assumption).
- The model (DRAIN-2D code) supports, nodes 8 and 76, were given a vertical acceleration corresponding to the wave-form of Figure 7 but making the rigid-body assumption, by dividing the forces by the appropriate cask weights to get "g's". This produces a 204g peak, 91g plateau deceleration as shown on Figure 9. (Flexible body model - rigid body deceleration assumption).
- The model (ANSR-II) was given an initial velocity of 44 feet per second (corresponding to the 30 foot drop) and at t_0 the force-time profile of Figure 7 was applied in the retarding direction at nodes 8 and 76. (Flexible body model - derived fin force/time history.

The results of these three calculations are plotted as Figure 10. This figure shows cask body deflection as a function of location along the cask longitudinal axis. The use of cask body deflection as a comparative measure is appropriate since the impact fins are fixed to the outside diameter of the cask body and the fuel basket is in contact at various locations with the inside diameter of the cask body. It should be noted that the deflections in Figure 10 are first pulse maximums all of which occur at approximately 10 milliseconds.

(1) Material in this section has been developed from work performed by Engineering Design Analysis Company (EDAC) under contract to General Electric Co.

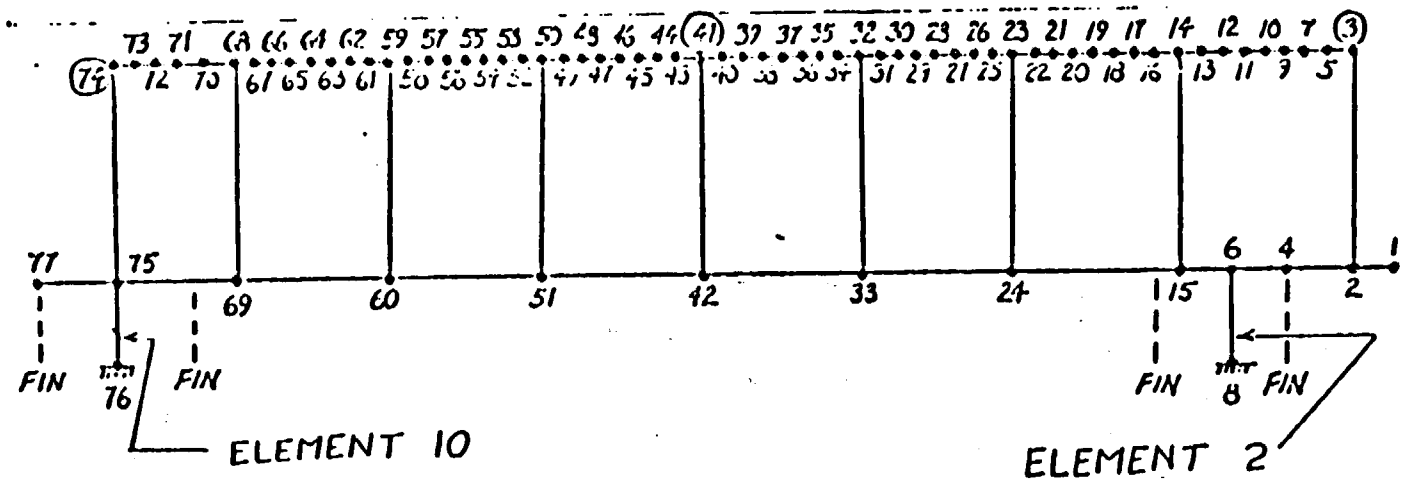

FIGURE 8 ANALYTICAL MODEL FOR NONLINEAR ANALYSIS, BWR CONFIGURATION B

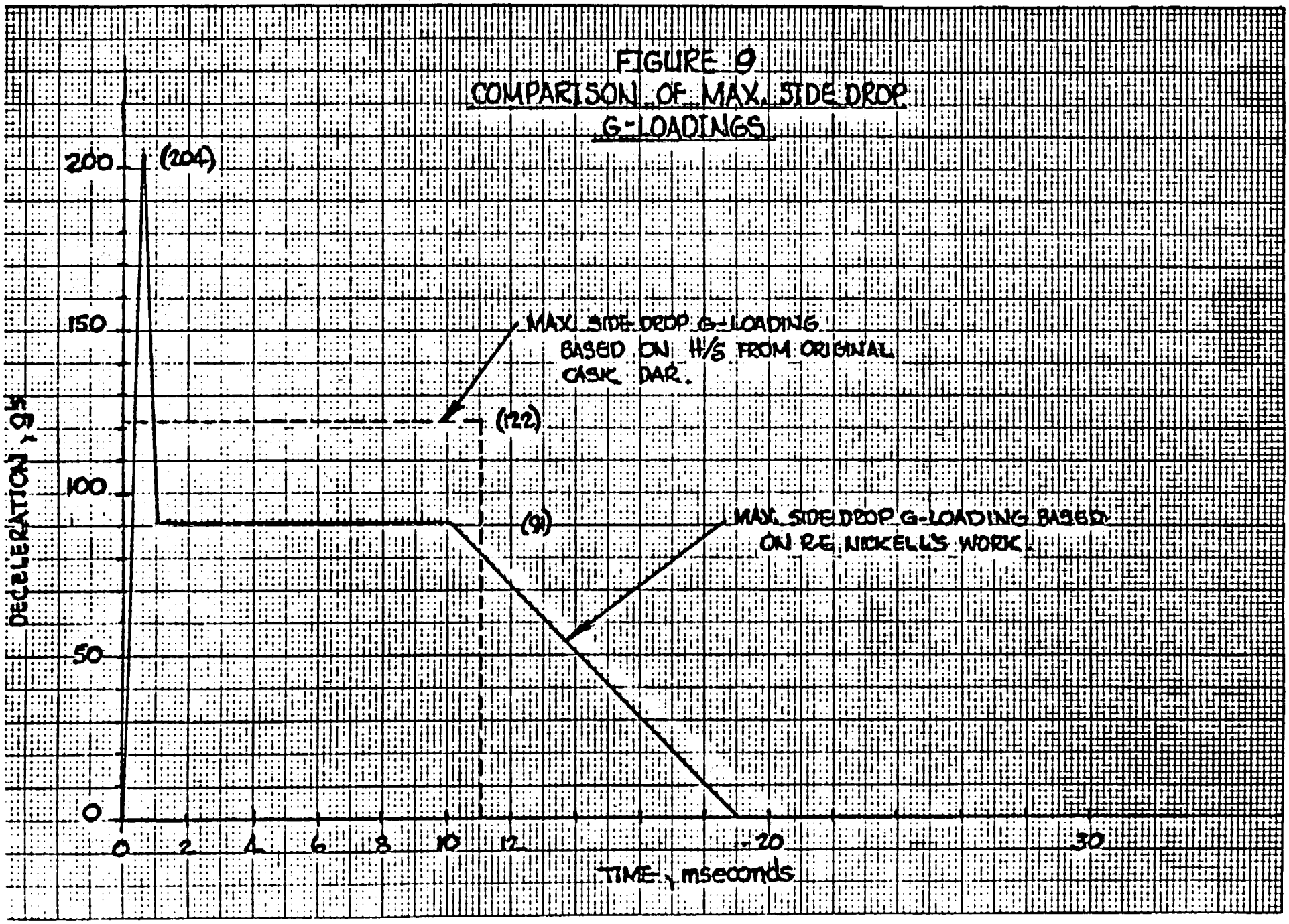

FIGURE 9
COMPARISON OF MAX. SIDE DROP G-LOADINGS

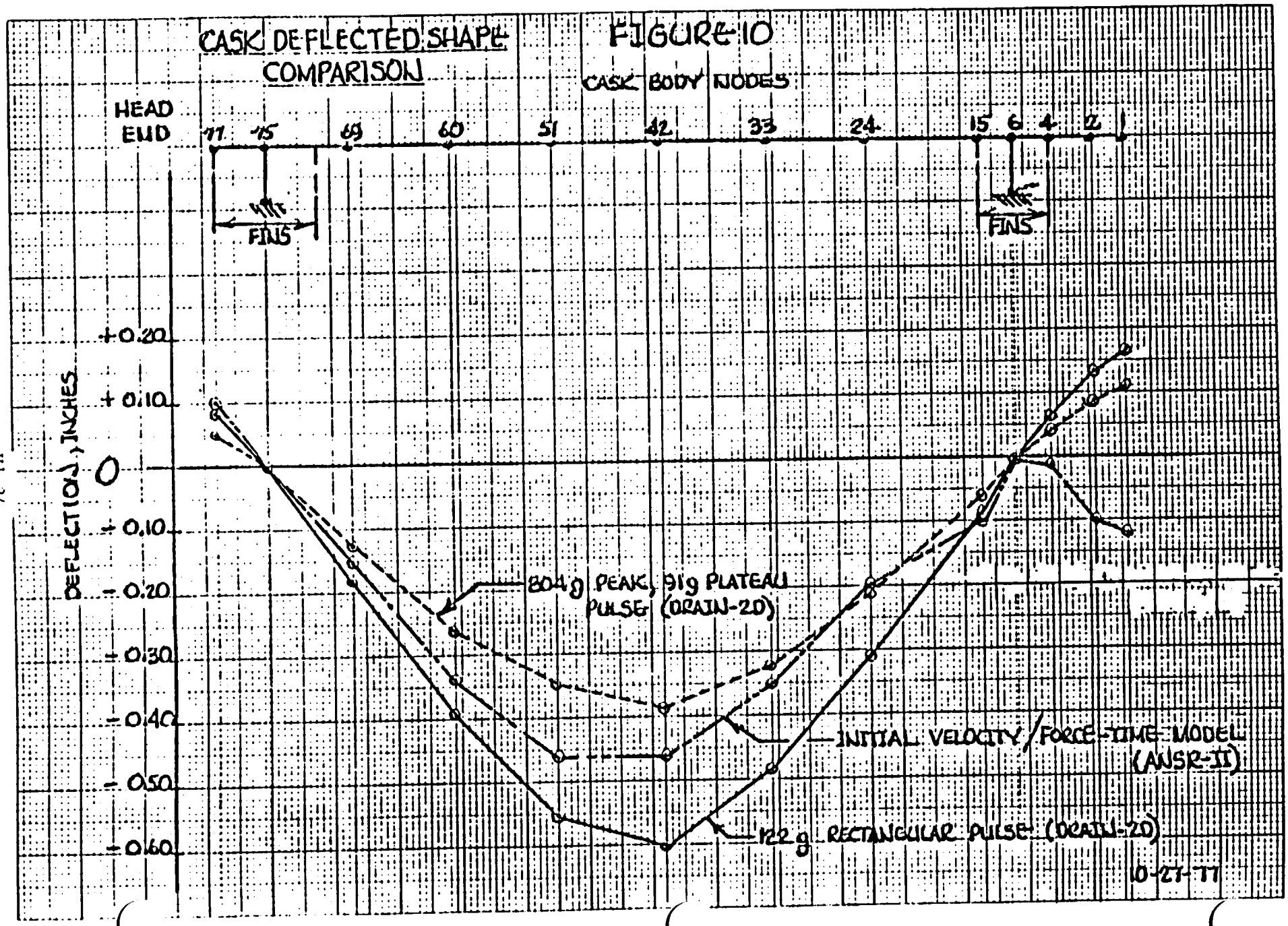
CASK DEFLECTED SHAPE COMPARISON
FIGURE 10
CASK BODY NODES
HEAD END
77
75
69
60
51
42
33
24
15
6
4
2
1
FINS
FINS
+0.20
+0.10
0
-0.10
-0.20
-0.30
-0.40
-0.50
-0.60
DEFLECTION, INCHES
804g PEAK, 91g PLATEAU PULSE (DRAIN-2D)
INITIAL VELOCITY/FORCE-TIME MODEL (ANSR-II)
122g RECTANGULAR PULSE (DRAIN-2D)
10-27-77

Figure 10 shows that at the cask mid-length, node 42, the rectangular 122g deceleration shows the greatest deflection followed by the initial velocity - force/time input and finally the 204g-91g rigid body g-time input. The initial velocity-force/time input is considered the most realistic representation of cask behavior since it does not make the rigid body deceleration assumption. It can be seen from Figure 10 that at the cask mid-length the 204g-91g input is somewhat non-conservative and the 122g rectangular input is somewhat over conservative when compared to the velocity-force/time response. However, as one approaches the points of load application on either end of the cask (nodes 6 and 75) the variations between deflections for the various input functions diminishes significantly from those at the cask mid-length. It is estimated that in the region of the impact fins the 204g-91g rigid body input is only 5% non-conservative relative to the initial velocity - force/time input. The internal shielding assembly to be analyzed is located adjacent to the upper impact fin region and will respond to the local deceleration.

E. Application to the Internal Shielding Assembly Structural Analysis

The internal shielding assembly will be analyzed in Section V by using computer methods (STARDYNE) as well as manual techniques. The most convenient input form for these computations is "g's" or g-time. As demonstrated above the use of Nickell's fin bending correlation with a rigid body deceleration assumption is only about 5% non-conservative in the region of the impact fins where the internal shielding structure is located. On this basis, the use of the rigid body g-loads increased by 5% will produce a reasonable representation of the actual structural response. To account for impact the dynamic amplification factor (DAF) will be computed for the internal shielding assembly at 0°, 45° and 90° orientations (see Figure 6). The shielding structure will then be analyzed statically under loads defined by:

$$g_{analysis} = [g_{peak} \times 1.05 \times DAF] \text{ for } 0°, 45° \text{ and } 90° \text{ orientations}$$

The end drops will be evaluated by assuming a DAF = 2.0, the maximum possible value, and applying this to the peak g-loading. The DAF = 2.0 is assumed to encompass the 5% correction.

F. Dynamic Amplification Factor (DAF) Determination

As is seen in Figure 9 the internal shielding forcing function is in the form of a triangular, short duration pulse followed by a long duration, constant force plateau. The effect of this g-time history on the shielding must be determined. Since the forcing function does not conform to any standardized pulse shapes, it is necessary to utilize a simplified computer model to determine the DAF's. The model is a simple cantilevered beam with a concentrated mass at the end. The mass is identical to that of the actual shielding assembly (top plate, uranium subassemblies and structural members); the weightless beam has the average stiffness of the actual shielding assembly; and, the beam-mass model has the natural frequency of the shielding assembly based on the average deflection of the actual structure. A cantilevered beam model was chosen because the shield assembly is cantilevered from the basket top structural ring when in the side drop orientation. (See Appendix A, 159C5238 Sheet 10).

Three simplified models were written, one for each of the three drop orientations (0°, 45° and 90°). The values for stiffness and natural frequency were taken from the complete shield assembly STARDYNE model described in Section V, Subsection C. The three orientations were run on STARDYNE with an estimated DAF of 1.0 and the output was used to generate the simplified models.

The simplified models use the DYREC program,[1] which is a beam vibration code based on "Timoshenko Beam" theory. In each case the built-in support was subjected to the forcing function appropriate for the drop direction. Figure 9 shows the function for the 0° orientation. The following Table 5 shows the forcing function parameters for each condition.

TABLE 5

Forcing Functions

Drop Orientation	Peak Deceleration, g	Plateau Deceleration, g	Time, msec to Peak	Time, msec To Start of Plateau	Time, msec To End of Plateau	Time, msec To End of Event
0°	214	96	0.6	0.95	10	19.4
45°	161	71.4	0.6	0.95	13.6	26.1
90°	140	62.1	0.3	0.48	15.8	30.3

(1) This code was used to evaluate fuel rods under side drop conditions. See August 13, 1973 submittal to Docket 71-9001, Appendix A 5A-1

To determine the DAF's from the output of the DYREC models the peak response forces were divided by the peak input forces. These peak responses occurred well into the plateau portion of the forcing function. The following Table 6 shows the DAF's for the three side and two end orientations:

TABLE 6

Dynamic Amplification Factors

Drop Orientation	Pulse	DAF
0° - side	long	1.0
45° side	long	1.14
90° - side	short	0.975
end - head	short	2.0
end - bottom	short	2.0

G. Design Basis g-loads

As discussed above the internal shielding assembly will be evaluated under static load conditions. The magnitude of the static load will be determined as follows.

For side drop:

$$\text{g-load} = [g_{peak}]_{orientation} \times 1.05 \times DAF$$

For end drop:

$$\text{g-load} = [g_{peak}]_{orientation} \times 2.0$$

In each case the g-peak is determined by dividing the cask loaded weight (140k) into the product of the peak stress (Figure 7) and the applicable effective fin area (Table 4). The following Table 7 summarizes the design basis g-loads for the internal shielding assembly.

TABLE 7

Design Basis g-loads

Cask Orientation	g peak	1.05 x g peak	DAF	Design Basis g-load
0° - side	204	214	1.0	214
45° - side	153	161	1.14	184
90° - side	133	140	0.975	137
head - end	280	-	2.0	560
bottom-end	287	-	2.0	573

V. Structural Analysis

A. Introduction

The structural analysis of the internal shielding assembly consists of the following:

- o Calculation of the 30 foot drop loading considering three side orientations (0°, 45°, 90° - see Figure 6) and two end orientation (head, bottom) at maximum normal(1) operating temperature, 450°F
- o Calculation of the thermal stresses under the normal and maximum temperature conditions, 450°F and 1000°F(2) respectively
- o Calculation of the thermal stresses under low temperature conditions, - 40°F(3)
- o Consideration of brittle fracture of depleted uranium shielding pieces under 30' drop low temperature conditions, -40°F(3)

The basic design requirement is that the shielding assembly remain essentially fixed in place under the four conditions listed above.

The g-loads which will be used for the 30' drop analyses are shown in TABLE 7. Section III tabulates and justifies the material properties used in this analysis.

B. Limit Stresses

There are three criteria which may be used for evaluating the calculated stresses; these will be applied as appropriate. The criteria are as follows:

1. Ultimate Strength

For those components loaded in simple tension (or compression) or in a combination of tension and shear loading, an effective stress will be computed and the limit stress used will be the ultimate strengths tabulated and referenced in Section III of this report. No credit will be taken for dynamic properties of materials although elevations in strength do occur under high strain-rate conditions. Shear strength will be taken at .577 times yield strength.

(1) "Normal" is somewhat of a misnomer. In this case the cooling system is assumed to be inoperative with the cask at maximum heat load and 130°F ambient air temperat

(2) Maximum temperature of shielding following 30 minute, 1475°F fire per 10CFR71 Appendix B.

(3) Minimum evaluation temperature for normal transport per 10CFR71, Appendix A.

2. Shape Factors

For members in pure bending the concept of shape factors will be used. Shape factor bridges the gap between elastic and plastic action of a beam. It is defined as the ratio of the plastic moment to the elastic moment of a beam and can be applied to materials of good ductility such as stainless steel. It essentially is a multiplier of the material yield strength which accounts for the necessity to plastically stress the entire beam cross section (not just the outer fiber) before collapse can occur. This is based on an idealized stress-strain diagram where the plastic region is horizontal. For rectangular cross-section beams such as found in the internal shielding assembly the shape factor is:

$$SF = \frac{M_p}{M_e} = \frac{\frac{\sigma b h^2}{4}}{\frac{\sigma b h^2}{6}} = 1.5$$

where:
- h is the beam depth
- b is the beam thickness
- σ is a material property

and the limit stress in bending would be:

$$\sigma_{lim} = 1.5 \times \sigma_{yd}$$

If there is a combined stress in the beam from bending and tension then the limit stress is defined by ASME Code (Sections III and VIII), as shown in Figure 12 . This is a modification of the shape factor concept.

3. Maximum Moment Carrying Capability

Whereas the shape factor concept was predicated on the assumption of elastic - perfectly plastic behavior of material, the maximum moment carrying capability concept is based on a bi-linear representation of the actual stress-strain behavior of ductile material. In generating a moment balance within a beam in bending consideration is given to both the yield and ultimate strength of the material. The details of how this concept is applied to the shielding assembly are contained in Appendix D.

FIGURE 12

LIMIT STRESS FOR COMBINED TENSION & BENDING FOR RECTANGULAR SECTIONS

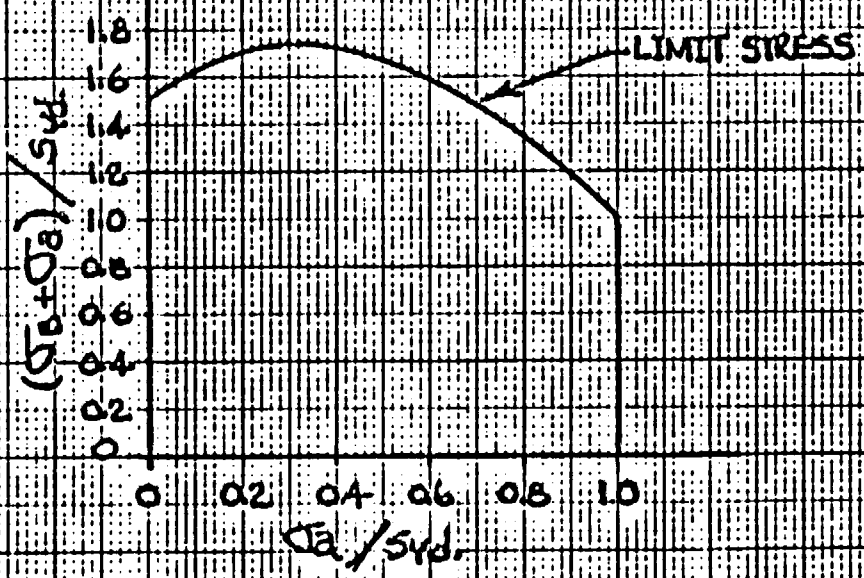

C. Calculational Methods and Computer Codes

The following is a tabulation of the structural analyses performed and the method(s) employed:

Item	Method
Top plate structure - side drop	STARDYNE
Shield Assys #1 & #2 - side drop	STARDYNE
Shield Assys #3 & #4 - side drop	Manual
Thermal Stresses	Manual
Shield Assy attachment welds	Manual
Stud shear out	Manual
End drop - all structures	Manual

1. Manual

Manual calculations were performed using generally accepted rules for structural analysis. For cases where it is not possible or feasible to exactly describe the structure or conditions, a conservative approach will be taken and justified.

2. STARDYNE Code

The MRI/STARDYNE - 3 code is a linear elastic, static and dynamic structural analysis program. The program has been used extensively in the analysis of nuclear power plant structures. STARDYNE is a fully warranted and supported engineering application package available at CDC-6600 data centers. Detailed information on STARDYNE-3 is contained in Appendix C.

a) STARDYNE Model Description

The STARDYNE model of the internal shielding assembly consists of 685 nodes, 572 beams, 144 quadralateral plates and 40 triangular plates. The model is three dimensional, it includes the entire basket top plate, shielding assemblies #1 and #2, and the basket axial structural members. The loads from shielding assemblies #3 and #4 are applied appropriately to the top plate but their stiffnesses against bending in the side drop has been omitted since they lend little to the total assembly stiffness. (These

components are evaluated by hand calculation). The nodes are modeled in a global coordinate system which allows a particular loading direction to be specified; in this instance the 0°, 45° and 90° orientations will be evaluated. Each case will be evaluated statically at the appropriate g-load (see Section IV). The shield assembly STARDYNE model is shown on Page C-5 of Appendix D.

D. Analytical Results Summary

The following tables summarize the computer and manual computations of shielding assembly structural behavior under the conditions described in Subsection A of this section. Appendix D contains the complete stress report for the side drop conditions. Appendix E contains the calculations for the end drop and thermal stress conditions.

1. 30 Foot Drop

a) Side Drop - (See Figure 6 and Appendix D)

As previously mentioned the side drop analysis was performed for the highest decelerations in three drop positions - 0°, 45° and 90°.

The basket top plate together with shielding pieces #1 and #2 and the basket longitudinal structural members were analyzed using the STARDYNE computer code. The small shielding pieces #3 and #4 were analyzed separately using manual techniques.

The stress report for the side drop analysis is contained in Appendix D and is self explanatory. The approach taken regarding the STARDYNE model output was to examine the stress levels of all beams and plates but not report those whose stresses were less than the limit stress refined by 1.5x yield strength. Those elements whose stress exceeds the forementioned limit were evaluated on the basis of maximum moment carrying capability. These evaluations are contained in the Appendix D stress report. The complete analysis of the smaller shielding subassemblies (#3 and #4) is in Appendix D since these are manual calculations. Additionally, all stud connections have been evaluated in the stress report since the computer model was not written to consider this amount of detail.

Due to the number of elements involved no attempt will be made here to tabulate the results. It is sufficient to say that under the highest loading accident conditions experienced by the cask none of the shielding components or the basket structure failed (e.g., exceeded the maximum limit stress for this faulted condition). The design objective of no significant displacement of the shielding has been satisfied.

b) End Drop

The end drop may occur on either the cask head or the cask bottom. When in the head down position the shielding subassemblies hang from their support ribs and are supported by the top plate. When in the bottom down position the shielding subassemblies are carried by the support ribs.

From Table 7 the design decelerations are as follows:

$g_{design} = 280 \times 2.0 = 560$ head down

$g_{design} = 287 \times 2.0 = 573$ bottom down

Detailed calculations are in Appendix E.

Head down - the following table shows the components and their stresses under a static load of 560 "g's".

TABLE 8

Head-Down Drop Stresses

Component	Stress, Ksi	SF
Shield Ass'y #1		
o Rib-to-support ring weld	4.9(1)	12.1
o Rib-to-shielding subass'y.	negligible	-
o Rib-to-top plate weld	5.5	11.6
o Shield Subass'y-to-top plate (shear)	8.4	1.4(2)
Shield Ass'y #2		
o Rib-to-support ring weld	7.5	8.5
o Shield subass'y-to-rib weld	9.8	6.5
o Shield subass'y-to-top plate (shear)	11.1	1.05(2)

(1) No credit taken for top plate support

(2) Safety factors are based on ultimate strength of the material at 450°F except for those in pure shear which will be based on yield strength x .577.

Component	Stress, Ksi	SF
Shield Ass'y #3		
o Rib-to-support ring weld	7.5	8.5
o Shield subass'y-to-rib weld	11.3(1)	5.7
o Shield subass'y stud and clad	12.5	5.1
Shield Ass'y #4		
o Rib-to-support ring weld (shear)	2.9(2)	3.7
o Shield subass'y-to-rib weld (shear)	2.1(2)	4.8
o Shield subass'y studs, clad & top plate (shear)	2.6(2)	4.5

Bottom down - the following table shows the components and their stresses under a static load of 574 "g's". Only minimum areas of the shielding assembly have been considered

TABLE 9

Bottom-Down Drop Analysis

Component	Stress, Ksi	SF(3)
Shield Ass'y #1 Support ribs	11.6	5.5
Shield Ass'y #2 Support ribs	10.0	6.4
Shield Ass'y #3 Support ribs	11.6	5.5
Shield Ass'y #4 Support ribs	5.9	10.8

Conclusion - From above it can be seen that there are no component failures under end drop conditions thus meeting the design objective.

(1) No credit taken for top plate support

(2) Safety factors for components in shear will be based on yield strength x .577.

(3) SF is based on ksi ultimate strength in tension. Under the compressive loading of this case the ultimate strength would be greater.

2. Thermal Stresses

In this section three temperature conditions will be considered for the evaluation of thermal stresses. These conditions are as follows:

- o 450°F - Maximum normal operating temperature. Temperature for the 30' drop structural analysis.
- o 1000°F - Maximum accident temperature. Occurs following drop and fire conditions.
- o -40°F - Minimum normal operating temperature. In actual practice will not be this low due to cask heat load.

The thermal stress evaluation is complex due to the variety of structures involved. Only axial expansion will be considered. The shielding subassemblies are captured between fuel basket components (top structure ring and top plate). The basket is of stainless steel construction; the subassemblies consist of depleted uranium metal encased in stainless steel and supported on stainless steel ribs. There exists the potential for interaction stresses between the uranium and its cladding, the subassemblies and the basket,or both.

a) Derivation

The approach used will be to calculate the unrestrained length at the elevated temperature of each subassembly, accounting for any differential expansion effects between the uranium and its cladding. These lengths will be compared to the unrestrained length, at temperature, of the basket structure. If it is shown that interference will occur then the stresses in the various components will be evaluated by computing the forces required to extend or compress the components an amount equal to the interference.

The change in length of a component due to heating is given by

$$\Delta L = \alpha L \Delta T \qquad (1)$$

where: α is the coefficient of thermal expansion
L is the "cold" length of the component
ΔT is the temperature change of the component

The change in length of a component due to an axial force is given by

$$\Delta L = \frac{PL}{AE} \qquad (2)$$

where: P is the axial force
L is the component length
A is the component cross-sectional area
E is the modulus of elasticity

When evaluating the inneraction of two components in parallel as is the case of the uranium and cladding the net length change for each is:

$$\Delta L = \alpha L \, \Delta T \pm \frac{PL}{AE} \qquad (3)$$

Since the ΔL is the same for each of the components these can be equated and the interaction force, P, determined. This is shown as

$$P = \frac{(\alpha_1 - \alpha_2)\,\Delta T}{\left(\frac{1}{A_2 E_2} + \frac{1}{A_1 E_1}\right)} \qquad (4)$$

Referring to Section III it can be seen that E of stainless steel and E of uranium are quite similar therefore the average value, $\bar{E}$ will be used in these analyses. Equation (4) becomes:

$$P = \frac{(\alpha_1 - \alpha_2)\,\Delta T}{\bar{E}\left(\frac{1}{A_2} - \frac{1}{A_1}\right)} \qquad (5)$$

Equation 5 is used to evaluate the stress in the cladding and the uranium by dividing P by the appropriate area.

The overall length of the unrestrained shielding subassemblies is as follows:

$$L = (L_{rib} + \Delta L_{rib}) + (L_{clad} + \Delta L_{clad})$$

$$\Delta L_{rib} = \alpha_1 L_r \, \Delta T$$

$$\Delta L_{clad} = \alpha_2 L_c \, \Delta T \pm \frac{PL}{AE}$$

$$L = L_r (1 + \alpha_1 \Delta T) + L_c \left(1 + \alpha_2 \Delta T \pm \frac{P}{AE}\right)$$

b) Component Length Summary

o Normal Operating Temperature, 450°F

The following table shows the unrestrained lengths of the components.

TABLE 10

450°F Component Lengths

Component	Length, In
Subassy #1	15.554
Subassy #2	15.555
Subassy #3	15.555
Subassy #4	15.555
Bskt Structure	15.557

As can be seen the maximum interference is .003 inches

o High Temperature, 1000°F

The following table shows the unrestrained lengths of the components.

TABLE 11

1000°F Component Lengths

Component	Length, In
Subassy #1	15.650
Subassy #2	15.650
Subassy #3	15.649
Subassy #4	15.649
Bskt Structure	15.646

As can be seen the maximum interference is .004 inches.

o Low Temperature, - 40°F

The following table shows the unrestricted lengths of the components.

TABLE 12

-40°F Component Lengths

Component	Length, In
Subassy #1	15.486
Subassy #2	15.483
Subassy #3	15.483
Subassy #4	15.483
Bskt. Structure	15.486

As can be seen the maximum interference is .003 inches.

c) Stress Summary

The following table summarizes the combined thermal stresses

TABLE 13

Thermal Stresses

Component	Condition: 450°Normal Stress, Ksi	1000°F Post-Accdt. Stress, Ksi	-40°F Cold Stress, Ksi
Shield Assy #1			
Uranium	3.4	3.6	0.3
Cladding (304 SST)	9.4	12.0	2.1
Support ribs (304 SST)	1.5	1.6	0
Studs	35.4	0	0
Shield Assy #2			
Uranium	3.3	3.5	2.9
Cladding (304 SST)	9.6	12.1	2.1
Support ribs (304 SST)	1.6	1.6	5.4
Studs	35.4 (1)	0	56.1 (1)
Shield Assy #3			
Uranium	4.3	4.8	0.5
Cladding (304 SST)	8.5	10.8	1.9
Support rib (304 SST)	1.6	1.6	0
Studs	0	0	0
Shield Assy #4			
Uranium	4.2	4.6	0.5
Cladding (304 SST)	8.7	11.0	1.9
Support ribs (304 SST)	1.6	1.6	0
Studs	0	0	0
Basket Structure (216 SST, 304 SST)	3.4	3.8	1.5

(1) Cannot be reached since a thermal stress cannot exceed σ_{yd}

Table 13 above combines the stresses due to uranium/clad interaction with the stresses due to assembly/basket structure interaction. As can be seen the stress levels are quite low with the exception of shielding piece #1 and #2 studs. These stresses are, of course, self relieving and do not affect the load carrying capability of the member (see the discussion of thermal stresses in Appendix D). Appendix E contains the thermal stress calculations.

3. Brittle Behavior of Uranium Metal (1)

a) Introduction

It is well known that depleted uranium metal loses ductility at low temperatures. References 5 and 7 show that Charpy V-Notch impact values of uranium metal increase with increasing temperature. Typical values are as follows:

TABLE 14

Typical Charpy V-Notch Values

Test Temp, °F	Charpy Value, Ft-Lbs
-40	8-10
RT	12-14
250	40
450	60

To confirm the published data GE performed Charpy V-Notch testing on six samples of the shield material at a test temperature of -40°F. The values range from a low of 6.0 ft-lbs to a high of 9.5 ft-lbs with the average being 8.4 ft-lbs. A copy of this test report is contained in Appendix E.

Brittle fracture is a phenomenon whereby a crack will propagate in a material from a flaw or other stress rising feature at a stress level possibly lower than the yield strength of the material. For a given material at a specific temperature and stress level a critical flaw size can be determined. Any flaw smaller than the critical value will not propagate a crack and result in failure of the piece. Flaw location and orientation are also important in brittle fracture analysis. ASME Code, Section III Appendix G defines the maximum postulated defect as "... a sharp, surface defect normal to the direction of maximum stress." A defect internal to the piece or in some position other than normal to the maximum stress direction would be of lesser significance.

For common pressure vessel materials testing has been conducted to determine stress intensity factor, K_{ID} as a function of temperature. These rather expensive tests have not been conducted on depleted uranium metal due to the limited use of this material, however, it is possible to derive K_{ID} values from Charpy V-Notch test data; values derived in this manner will be employed in this analysis.

Each uranium piece used in the internal shielding is radiographed to detect the presence of flaws. The sensitivity of this NDT method is such that a flaw size of between 2% and 5% of the 1" shield thickness (.020" to .050") would be detectable (Reference 16). The internal shielding pieces have a 5% rejection level for flaws based on the thickness. Thus any flaw larger than .050 inches will be unacceptable and the piece repaired or replaced.

(1) Information furnished by Mr. R.T. Nickell, Pacifica Technology under contract to General Electric Co.

Based upon correlations that have been developed (References 18, 19, 20) for a variety of materials, including ferritic and austenitic steels, titanium alloys, and aluminum, Charpy V-notch impact test data in the transition and lower shelf regions can be transformed into lower bound fracture mechanics data through the relationship

$$K_{1D}^2 = kE\ (CVN),$$

where k is a conversion factor having units of $in^{-1}ft^{-1}$, E is the elastic modulus in lb/in^2, CVN is the Charpy impact energy in ft-lb, and K_{1D} is the dynamic critical stress intensity in $lb/in^2 \times \sqrt{in}$. The correlation implies that the data are taken at the same temperature.

From data on alpha uranium obtained by Paprocki and Saller (Reference 5), the brittle-to-ductile transition temperature region lies between 100 to 125°C. In view of this, Charpy V-notch impact data were obtained for the actual IF-300 shielding material (U-0.2% Mo) at -40°F, well below the transition temperature and in the lower-shelf portion of the Charpy curve. Using the lowest value of six tests conducted at -40°F on this material (6 ft-lb) and observing the agreement with other data on U-2% Mo at -40°F (5.7 ft-lb), a K_{1D} versus temperature curve was constructed by the above correlation. This curve is shown in Figure 13. It should also be observed that all specimens satisfied the requirements for plane strain fracture toughness

$$t = 2.5\ \left(\frac{K_{1D}}{\sigma_{ys}}\right)^2,$$

Where t is the thickness in inches and σys is the yield strength of the material at the temperature of the test.

An evaluation of the critical flaw is shown below. In this case, the maximum stress from the shielding impact analysis (15.6 ksi) was assumed to be the nominal stress on a flat plate in bending with a thumbnail-shaped crack.

b) Critical Flaw Size Analysis

Consider a flat plate in bending with a thumbnail crack (i.e. thumbnail crack in Mode I) as shown in Figure 14. The Mode I stress intensity is given by

$$K_1 = \left[1 + .12\ \left(\frac{b-a}{b}\right)\right] \frac{\sigma\sqrt{\pi a}\sqrt{\sec\ (\pi a/2t)}}{\phi_o} \qquad \text{(Ref. 18)}$$

Where $\phi_o = \int_o^{\pi/2} \left[1-\left(\frac{b^2-a^2}{b^2}\right) \sin^2\theta\right]d\theta$

= flaw shape correction

FIGURE 13

EST. DYNAMIC FRACTURE TOUGHNESS
VS.
TEMPERATURE

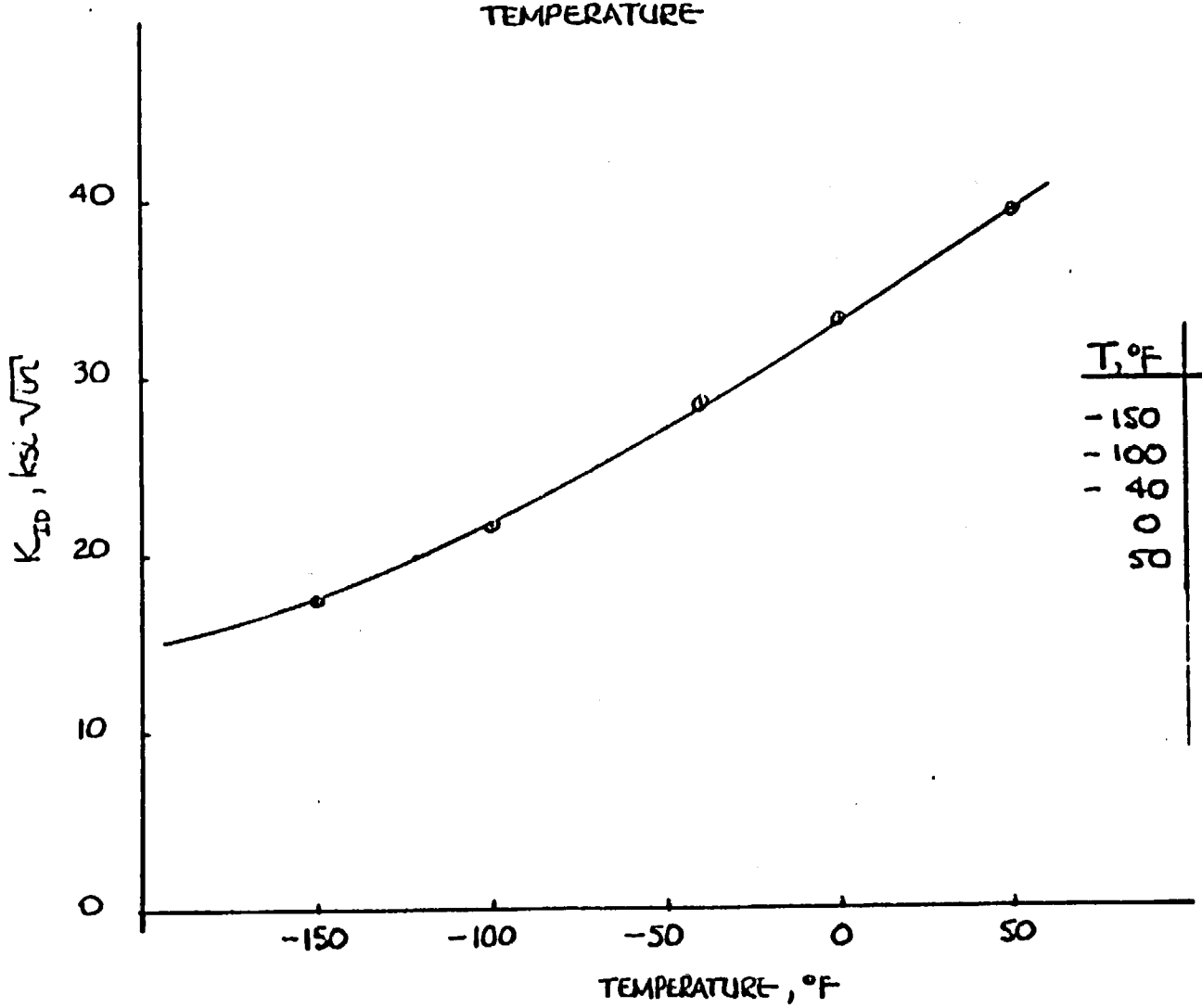

T, °F	CVN, ft-lbs.	K_{ID} ksi $\sqrt{in}$
-150	2.1	17.4
-100	3.3	21.8
-40	5.7	28.7
0	7.6	33.1
50	10.8	39.4

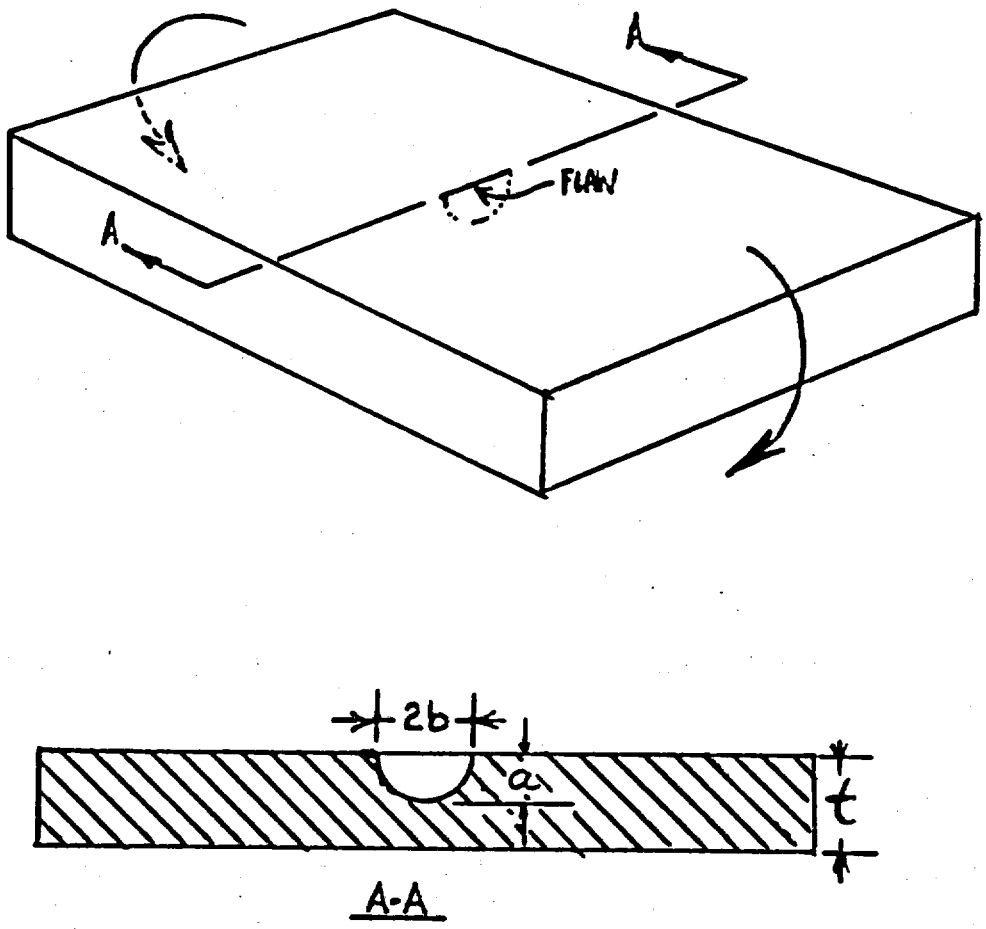

FIGURE 14
PLATE AND FLAW

For b = a, that is a semi-circular crack $\phi_o = \pi/2$ thus:

$$K_1 = \frac{2\sigma}{\pi} \sqrt{\pi a} \cdot \sqrt{\sec\left(\frac{\pi a}{2t}\right)}$$

Now suppose $\frac{a}{t} = \frac{1}{10}$,

then $\frac{\pi a}{2t} = 0.157$, $\sec \frac{\pi a}{2t} = 1.0125$

and $\sqrt{\sec \frac{\pi a}{2t}} = 1.006$

therefore: For σ_{max} of 15.6 ksi @ -40°F

$$a_{cr} = \pi\left(\frac{K_{1D}}{2\sigma_{max}}\right)^2 = \pi\left(\frac{29}{31.2}\right)^2$$
$$= 2.7 \text{ inches}$$

This indicates that a flaw depth of almost 3 inches in a uranium piece stressed to 15.7 ksi at - 40°F would result in a crack propagation to failure. No brittle failure would occur for a lessor depth.

For a part - through (Griffith) crack

$$K_1 = \sigma\sqrt{\pi a}$$

considering = 15.6 ksi and K_{1D} = 28 ksi $\sqrt{in}$ @ - 40°F or

$$a_{cr} = 1.03"$$

c) <u>Conclusion</u>

From this analysis and from the inspectable flaw size (.050"), it can be seen that even for cracks that are a significant fraction of the thickness of the piece, a factor of safety of at least 30 can be demonstrated against dynamic fracture. The two analyses, one for a surface crack and the other for a part-through crack, are felt to be conservative estimates of the type of flaws that would require inspection.

If future stress analyses demonstrates that nominal stresses are higher than the 15.6 ksi maximum here, computed Figure 15 illustrates a method for evaluating flaw criticality for any stress. The safe region is denoted by combinations of nominal stress and flaw size lying below and to the left of the K_{1D} curve. Combinations above and to the right are above the critical value.

FIGURE 15

CRITICAL STRESS VS. CRITICAL FLAW SIZE

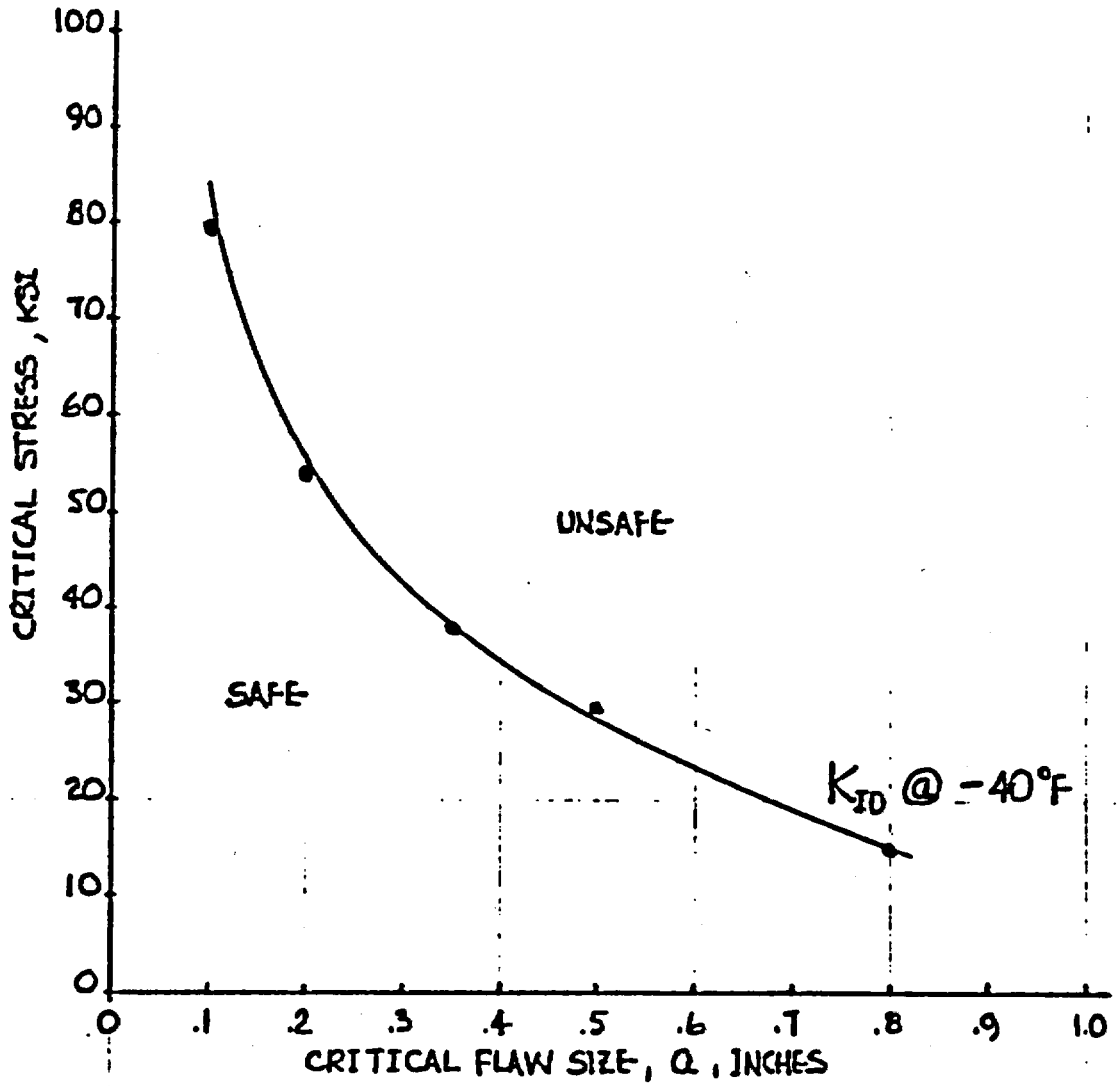

4. Other Structural Considerations

a) Shear Out Of Threads In Uranium

As can be seen in the Appendix A drawings stainless steel studs are threaded into the uranium shielding pieces. Calculations were performed to assure that the depth of stud penetration (thread engagement length) into the uranium is such that the "weakest" area is the stud tensile cross section rather than the threads.

Machinery's Handbook, 16th Edition, gives a method on pages 1050 - 1051 for computing this minimum thread engagement. Detailed calculations are in Appendix D. The minimum computed thread engagement is 0.21 inches; when compared to the design engagement of 0.75 inches this gives a factor of safety against shear out of 3.5.

VI. Other Analyses

A. Shielding

The structural analyses of Section V demonstrate that the internal shielding assembly remains essentially in place under the accident conditions of Appendix B, 10CFR71. Thus, there is no reduction in shielding from that under normal conditions of transport as analized in Reference 14 and consequently no specific additional shielding analysis is required.

B. Nuclear Criticality Safety

The addition of this supplementary internal shielding has no affect on the nuclear safety criticality of the cask and contents since (1) there is no fuel in the region encompassed by the shielding, and (2) the fuel matrix was evaluated in the FSAR with uranium shielding acting as a reflector, and found acceptable.

C. Heat Transfer

The supplementary shielding does not mask or blanket any heated section of the fuel matrix nor does it restrict any coolant flow under normal or accident conditions. Therefore, the additional shielding does not affect the cask thermal capabilities.

VII. Fabrication

A. Processes and Methods

1. Depleted Uranium

The uranium shielding pieces are fabricated from depleted metal. The material is vacuum melted and cast in ceramic molds. The casting are rough forged and then machined to shape.

2. Subassemblies

The depleted uranium pieces are encapsulated in stainless steel. Each subassembly consists of a 1/2" thick top and bottom cap which is pinned or bolted to the uranium. The uranium is then boxed-in with thin stainless steel side plates. All steel pieces are welded together to form a close fitting water-tight seal. All uranium-steel interfaces have a flame-sprayed copper diffusion barrier. The subassemblies are checked for leak-tightness following assembly.

3. Basket Modifications (App. A; 159C5238, Sheet 10)

The basket modification consists of 1) the corner piece replacements, 2) the I-Beam installation, and 3) the curved segment installation.

To install the 216 SST corner pieces it is necessary to remove an equal sized portion of the existing 304 SST top plate, prepare the edges and weld-in the replacement section. The I-Beam is prefabricated and then welded into position. The curved segments are positioned and welded to both the existing top plate edge and the I-Beam. Following the basket structure modification, a jig will be used to drill the shielding subassembly stud holes in the basket top plate.

4. Main Assembly

The shielding assembly consists of fourteen subassemblies. Each subassembly is pinned to the basket top plate and supported from the uppermost basket structural ring by one or more stainless steel ribs. Thes ribs are welded on one end to the subassembly bottom cap and on the other end to the basket structural ring. (See Appendix A, 159C5238, Sheet 11 for details).

B. Quality Assurance

1. General

The fabrication and installation of this supplementary shielding will follow the Quality Assurance plan referenced in the IF-300 Cask Certificate of Compliance No. 9001, latest revision. Work will be accomplished following written and GE-approved procedures.

2. Depleted Uranium Metal

The uranium pieces will be made following GE approved specifications which are similar to those used for the cask body and head shielding. Physical and chemical analyses will be performed. Fissile isotope content will be less than 0.22% U-235. Each piece will be x-rayed for detection of internal flaws and the density of each will be determined using 18.70 grams/cc as the minimum acceptable value. Repairs, if any, will be made following GE-approved procedures and will be documented as to location and method. This data, together with the normal quality control inspection reports, will form part of the fabrication record.

3. Subassemblies, Modifications and Main Assembly

All stainless steel components will be made from material certified to meet the appropriate ASTM specification. All processes, such as welding and copper flame spraying, will be performed following GE approved procedures. Welds and welders will be qualified under ASME Code.

All welds will be nondestructively tested using liquid penetrant or a similar method. All inspection and test reports, welder and weld qualifications, material certifications and procedures will be included in the fabrication record.

REFERENCES

1. Mechanical and Physical Properties of the Austenitic Chromium-Nickel Stainless Steels at Subzero Temperatures, 3rd Edition, March 1970, The International Nickel Company.

2. ASME Code, Section VIII, Division 2, 1977 Edition.

3. ASME Code, Section III, Appendix I, 1977 Edition.

4. Mechanical and Physical Properties of the Austenitic Chromium-Nickel Stainless Steels at Elevated Temperatures, 3rd Edition, November 1968, The International Nickel Company.

5. Reactor Handbook, 2nd Edition, Vol. I-Materials, C.R. Tipton, Jr., 1960.

6. Test Reports #TE-8976 and TE-9006, Hawker-Siddeley Canada, Ltd - Orenda Division. Performed on Heats #368 and #385 for General Electric Co.

7. Docket 71-9061, EXXON Nuclear Company, attachment to letter of March 19, 1976, W.S. Nechodom - EXXON to C.E. MacDonald - NRC, Figure 1. GE room temp data extrapolated for "typical yield".

8. IGR-R/R-287, Uranium Data Manual, IKAEA, 1959.

9. BMI-1954, A Survey of Strain-Rate Effects For Some Common Structural Materials Used In Radioactive Material Packaging and Transport Systems, August 1976.

10. F.C. Davis, "Structural Analysis of Shipping Casks, Energy Absorption Capabilities of Plastically Deformed Struts Under Specified Impact Loading Conditions", ORNL-TM-1312, Vol. 9, February 1971.

11. J.H. Biffle, M.J. Sagartz, and L.I. Weingarten, "Inelastic Response of Metallic Impact Limiters", paper presented at the 4th SMiRT Conference, San Francisco, California, August 15-19, 1977.

12. J.M. Steichen, "High Strain Rate Mechanical Properties of Types 304 and 316 Stainless Steel", HEDL-TME 71-164, November, 1971.

13. J.M. Steichen, "High Strain Rate Tensile Properties of AISI Type 304 Stainless Steel", Journal of Engineering Materials and Technology, Vol. 95, No. 3, July 1973, pp. 182-185.

14. IF-300 Shipping Cask - Design and Analysis Report, NEDO-10084-1, February 1973, Docket 71-9001.

15. Type 216 Data Sheet, Allegheny-Ludlum Steel Corporation, PD21-170A.

16. Communication with Mr. Bill Crawford, Quality Assurance Manager, Eldorado Nuclear Limited, Port Hope, Canada - 10/13/77.

REFERENCES

17. Nitronic 60 - Product Data Sheet, Armco Steel Corporation.

18. S.T. Rolfe and J.M. Barsom, Fracture and Fatigue Control in Structures, Applications of Fracture Mechanics, Prentice-Hall, Inc., Englewood Cliffs, N.J., 1977, Chapters 2 and 6.

19. J.M. Barsom and S.T. Rolfe, "Correlations Between K_{Ic} and Charpy V-Notch Test Results in the Transition-Temperature Range," ASTM STP 466, Impact Testing of Materials, American Society for Testing and Materials, 1970, pp. 281-302.

20. H.T. Corten and R.H. Sailors, "Relationships Between Material Fracture Toughness Using Fracture Mechanics and Transition Temperature Tests", TAM Report No. 346, University of Illinois, Aug. 1971.

21. ARMCO 17-4 PH Product Data Sheet S-6c, ARMCO Steel Corporation.

NEDO-21796

APPENDIX A

DRAWINGS

NEDO-21796

APPENDIX B

EFFECTIVE AREA CALCULATIONS

SUBJECT: TOTAL EFFECTIVE AREA CALCULATIONS FOR SIDE AND END IMPACT FINS

0° Side Orientation

Total no. large impact fins = 4
Thickness of large impact fins = 1.250"
Effective width impact fins = 47.9"
Large fin height = 16"

Large fin area = 4 x 1.25 x 47.9
= 239.5 in^2

Total no. of effective* small fins = 10
Thickness of small fins = 0.5625"
Effective width of small fins = 14"
Small fin height = 7"

Small fin area = 10 x .5625 x 14
= 78.75 in^2

Total 0° drop fin area = 318 in^2

45° Side Orientation

Total No. large impact fins = 4
Thickness of large impact fins = 1.25"
Effective width of large impact fins = 38.21"
Large fin height = 15"

Large fin area = 4 x 1.25 x 38.21
= 191.05 in^2

Total no. effective small fins = 6
Thickness of small fins = .5625"
Effective width of small fins = 14"
Small fin height = 7"

Small fin area = 6 x .5625 x 14
= 47.25 in^2

Total 45° drop fin area = 238 in^2 .

---

* "Effective" small fins are ones which exhibit the double hinge (question mark) behavior under impact conditions.

90° Side Orientation

Total no. large fins = 4
Thickness of large fins = 1.25"
Effective width of large fins = 41.41"
Large fin height = 7"

Large fin area = 4 x 1.25 x 41.41
= 207 in^2

Total no. small fins = 0

Total 90° drop fin area = 207 in^2

Top End Drop

No. acting impact fins = 16
Thickness of impact fins = 1.125"
ΣEffective width of impact fins =
= [(2) (20) + (14) (24.75)]
= 386.5 in
Height of impact fins = 9.5"
Top end drop fin area = 386.5 x 1.125
= 435 in^2

Bottom End Drop

No. acting impact fins = 16
Thickness of impact fins = 1.125
ΣEffective width of impact fins = 16 x 24.75
= 396 in
Height of impact fins = 8 in

Bottom end drop fin area = 396 x 1.125
= 446 in^2

NEDO-21796

APPENDIX C

STARDYNE DESCRIPTION

STARDYNE3 USER'S MANUAL

A Computer System For Structural Engineering

The MRI/STARDYNE3 (Version 3) Structural Analysis System is a fully warranted and supported engineering application package available at CDC-6600 Data Centers. Each data center has one or more Engineering Application Specialists available to provide guidance to STARDYNE users.

If problems are encountered or if information concerning STARDYNE is desired, the user is invited to make immediate contact with Control Data Corporation or the developers, Mechanics Research, Inc., preferably in the order shown below:

- Local Data Center STARDYNE Analyst

or

- Engineering Sciences
  Control Data Corporation
  Minneapolis, Minnesota
  (612) 853-3090
  James Ries, Manager

or

- Mechanics Research, Inc.
  Los Angeles, California
  (213) 670-4650
  Structural Methods Department, Extension 203
  Richard Rosen, Manager
  Raymond Curtis
  Richard Ragle

This manual is compatible only with the CDC 6600 computer and should not be used with STARDYNE versions prior to this date:

April 1, 1974

MRI'S STARDYNE ANALYSIS SYSTEM

SUMMARY

The MRI STARDYNE Analysis System consists of a series of compatible digital computer programs designed to analyze linear elastic structural models. The system encompasses the full range of static and dynamic analyses. These programs provide the analyst with a sophisticated, cost-effective, structural-dynamical analysis system.

The STARDYNE system can be used to evaluate a wide variety of static and dynamic problems:

- The static capability includes the computation of structural deformations and member loads and stresses caused by an arbitrary set of thermal, nodal applied loads and/or prescribed displacements.
- Utilizing the normal mode technique, dynamic response analyses can be performed for a wide range of loading conditions, including transient, steady-state harmonic, random and shock spectra excitation types. Dynamic response results can be presented as structural deformations (displacements, velocities, or accelerations), and/or internal member loads/stresses.

The data input and output formats (both numerical and graphical) have been prepared with one basic philosophy: to enable the user to obtain a meaningful solution in the most logical and straightforward manner possible while keeping the required data input as simple and minimal as practical. The programmed mathematical operations in the matrix decomposition, the eigenvalue-eigenvector extraction, and the error analysis, contain state-of-the-art innovations in the field of numerical analysis. A brief description of the finite element and normal mode analysis methods as they are implemented in STARDYNE is presented. Also included is a discussion on each of the major programs comprising the STARDYNE system.

THE FINITE ELEMENT, NORMAL MODE ANALYSIS METHOD

The basic concept of the "Finite Element" method is that every structure may be considered as a "mathematical" assemblage of individual structural components or elements. There must be a finite number of such elements, interconnected at a finite number of nodal points. The behavior of this finite element structural model will closely approximate the behavioral characteristics of the real structure.

MRI'S STARDYNE ANALYSIS SYSTEM - SUMMARY - CONTINUED

Components of the Structural Model. The physical structure to be modeled must be described in a right-hand cartesian coordinate (global) system and is comprised of the "nodes" and "finite elements".

Nodes. The characteristics of the node point include position in space, movement in space (3 translation x,y,z and 3 rotation $\theta_x, \theta_y, \theta_z$) and connectivity to other nodes via the finite elements. Masses and external forces may be assigned to each node.

Finite Elements. The node points may be interconnected with finite elements in such a way as to realistically represent real physical structures. The most commonly used elements are shown on page A - 53, together with the nodal forces which can be transmitted through the element. The stiffness properties of each of these finite elements are defined in the "STARDYNE Theoretical Manual".

General Solution Procedure. The general solution procedure consists of stiffness matrix formulation, static analysis, eigenvalue/eigenvector determination, and dynamic response analysis.

Stiffness Matrix Formulation. The stiffness matrices of the individual finite elements are first computed and then transformed (if required) from its local coordinate formulation to a form relating to the global coordinate system. Finally, the individual element stiffnesses contributing to each nodal point are superimposed to obtain the total assemblage stiffness matrix [K].

Static Analysis. During a static analysis, the equation

$$[K] \cdot \{\delta\} = \{P\}$$

where $[K]$ = the stiffness matrix
$\{\delta\}$ = the nodal displacement vector
$\{P\}$ = the applied nodal forces

may be solved to determine the nodal displacements and element internal forces and/or stresses given a set of applied nodal forces.

MRI'S STARDYNE ANALYSIS SYSTEM - SUMMARY - CONTINUED

Eigenvalue/Eigenvector Analysis. The eigenvalues (natural frequencies) and eigenvectors (normal modes) of a structural system are determined by solving the equation

$$\omega^2 [m] \{q\} - [K] \{q\} = 0$$

where $[m]$ = the mass matrix (assumed to be diagonal, ie, no mass coupling)
ω = the natural frequencies
$\{q\}$ = the normal modes.

Dynamic Response Analyses. Using the natural frequencies and normal modes together with the related mass and stiffness characteristics of the structure, appropriate equations of motion may be evaluated to determine structure response to dynamic loading.

PROGRAMS COMPRISING STARDYNE ANALYSIS SYSTEM

I. STAR

The STAR program has two distinct functions. They are static load analysis and eigenvalue/eigenvector extraction. The static analysis and modal extraction phases are based on the "Stiffness Method" or "Displacement Method" and the answers are in the realm of "Small Displacement Theory".

CAPABILITY

A. Available Finite Modeling Elements

1. Beam and Pipe elements with shear stiffness in 3-D space.
2. Two Triangular Plate Elements (Thick plate and thin plate)
   a. Plate Bending
   b. Sandwich (Thick plate only)
   c. Inplane (constant strain)
   d. Shear Only (Thick plate only)
3. Quadrilateral Plate Element (Iso-parametric in-plane)
4. Infinitely Rigid Members.
5. Springs, non-standard elements or substructures may be entered in numerical form, by direct alterations to the stiffness matrix.
6. Hexahedron (Cube) Solid Element (Iso-parametric)
7. Wedge Solid Element (Iso-parametric)
8. Tetrahedron Solid Element (constant strain)

NRI'S STARDYNE ANALYSIS SYSTEM SUMMARY - CONTINUED

- Commonly Used Finite Elements

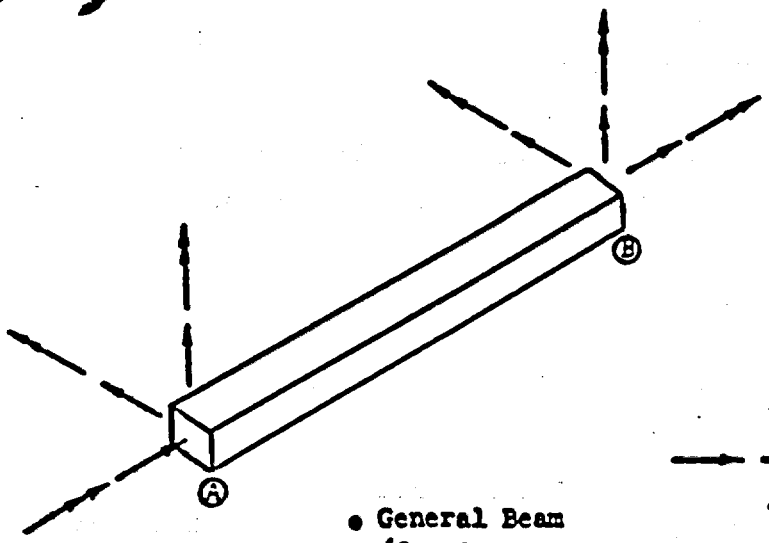

- General Beam
  (2 nodes)

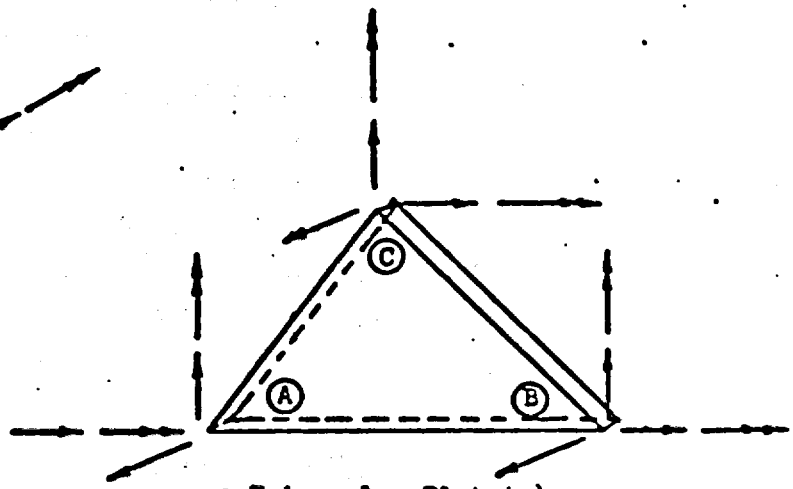

- Triangular Plate(s)
  (3 nodes)

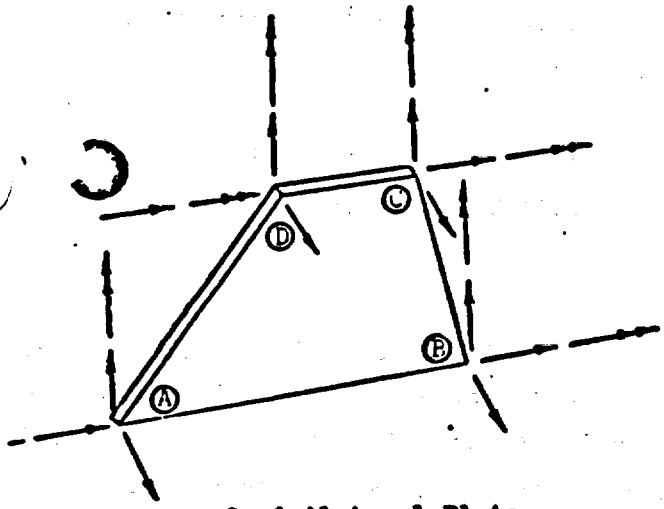

- Quadrilateral Plate
  (4 nodes)

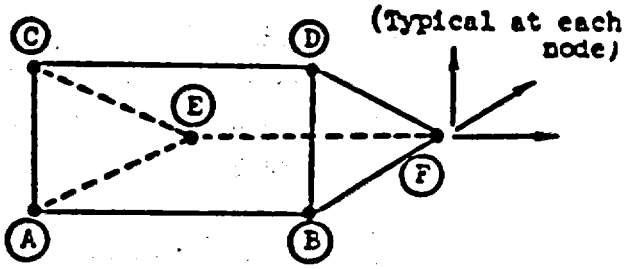

- Wedge Element
  (6 nodes)

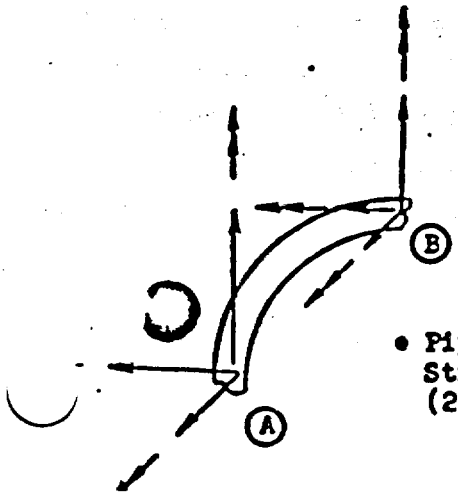

- Pipes-Curved and Straight
  (2 nodes)

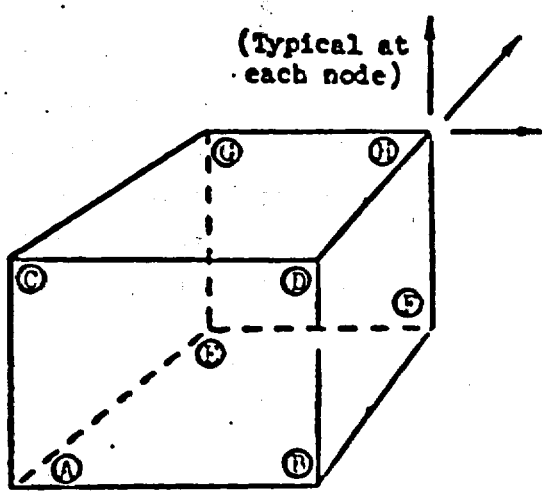

- General Six Sided Solid (Hexahedron)
  (8 nodes)

I. STAR - CONTINUED

B. Static Structural Analysis

1. Applied Nodal Loadings
2. Automated Thermal Analysis
3. Solutions of Free-Free Systems
4. Automated processing of psuedo-static load or displacement vectors as obtained from the dynamic response solutions
5. Element Loadings
6. Inertia Loadings
7. Combined Cases
8. Specified Displacements
9. Substructures

C. Extraction of Eigenvalues and Eigenvectors

1. Inverse Iteration Method for the eigenvalues within specified regions
2. Householder tri-diagonalization and Q-R extraction for all dynamic degrees of freedom

D. Output Section

STAR output processor phase computes element displacements, loads and stress; and nodal equilibrium check. Options are available to present the output in report form.

II. DYNRE1

Transient response to imposed dynamic loadings are treated in DYNRE1. Input forcing functions may be in the form of 1. forces, 2. initial displacements 3. initial velocities, 4. and base accelerations. Output consists of nodal displacements, velocities, accelerations, element loads and stresses.

III. DYNRE2

Steady state frequency response to steady state sinusoidal dynamic loadings are computed by DYNRE2. Input forcing functions may be in the form of distributed forces, base excitations (displacements, velocities or accelerations) and unit sinusoidal excitations (displacements, velocities, accelerations or forces) at specific nodes. Displacements at selected phase angles may be processed in STAR for element stresses.

STARDYNE ANALYSIS SYSTEM SUMMARY - CONTINUED

IV. DYNRE3

Response of multi-degree-of-freedom linear elastic structural models subjected to stationary random dynamic loading. DYNRE3 will compute the RMS nodal responses, RMS element stresses and generate response power spectral density (PSD) curves for selected nodal degrees of freedom. Input forcing power spectrums are defined as shape of spectrum and type of spatial correlation.

V. DYNRE4

Response of multi-degree-of-freedom, linear elastic models subjected to an arbitrarily oriented foundation shock input. The user may enter arbitrary shock spectra, shock spectra computed via DYNRE5, or call for some ratio of the 1940 El Centro (California) earthquake SPECTRA for any of the directions of motion.

DYNRE4 will compute user specified combinations of ABSOLUTE and/or RSS and/or NRL sum nodal and/or element stress responses.

VI. DYNRE5

Computes shock spectrum values from a transient base acceleration time history digitized at equal or unequal time intervals. The user may specify frequencies at which shock spectrum values for displacement, velocity and acceleration will be computed, in turn for each value of damping entered.

VII. PLOT3D

PLOT3D is a versatile graphics program for plotting star finite element structural models.

VIII. PACK4

PACK4 may be used to reduce a STAR math model to fit a smaller DYNRE3 program.

IX. BOP

May be used to consider bottom out, tension only, compression only members, etc., for the STAR statics problem.

STARDYNE STRUCTURAL ANALYSIS SUMMARY

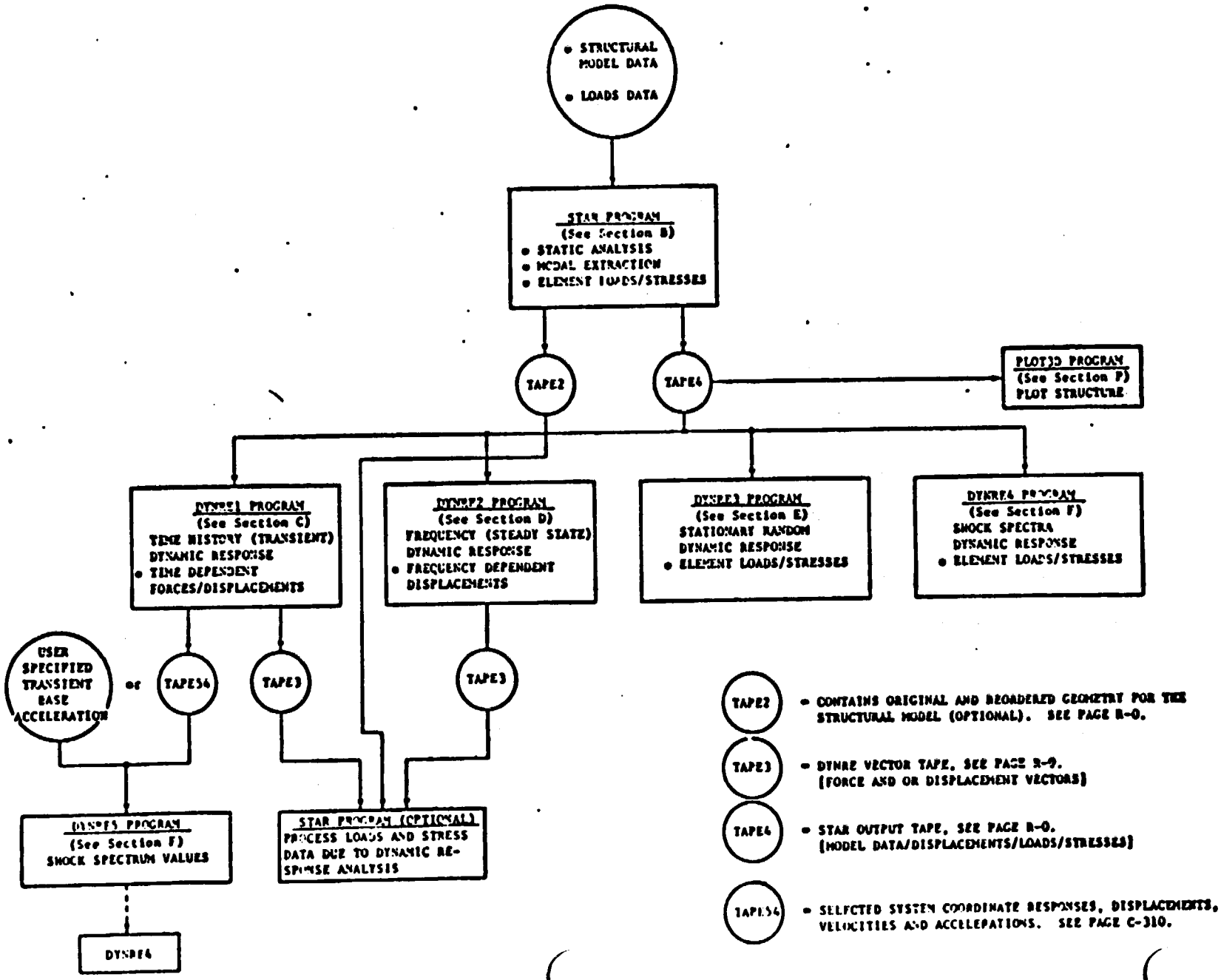

NEDO-21796

APPENDIX D

CALCULATIONS

NEDO-10084-3
September 1984

Stearns-Roger
INCORPORATED

GENERAL ELECTRIC
FUEL RECOVERY OPERATION
ENGINEERING • CONSTRUCTION
Functional Class 3 QAER C VPF No. N/A
☑ APPROVED. No further action required on this document.
☐ APPROVED — WITH COMMENTS. Supplier may proceed with work but must submit revised documents.
☐ DISAPPROVED. Revise and resubmit.
2-8-78
Responsible Engineer Date

STEARNS-ROGER INCORPORATED

STRESS REPORT

C-18813-02-00

GENERAL ELECTRIC COMPANY

IF 300 SHIPPING CASK SHIELDING IMPACT ANALYSIS

PREPARED BY: Bert Van Toornburg DATE: 12-20-77

REVIEWED BY: W. L. Feliss DATE: 12-20-77

APPROVED BY: J. M. Reid DATE: 12-20-77
J. M. Reid
Manager
Engineering Department

TABLE OF CONTENTS

		PAGE
1.0	INTRODUCTION	V1-D-1
2.0	BEAM PROPERTIES	V1-D-2
3.0	LOAD	V1-D-24
4.0	STRESS ANALYSIS OF SHIELDING NO. 1-4	V1-D-26
4.1	Dynamic Load Factors	V1-D-27
4.1.1	Drop Orientation - 0. Degree	V1-D-28
4.1.2	Drop Orientation - 45. Degrees	V1-D-29
4.1.3	Drop Orientation - 90. Degrees	V1-D-30
4.2	Design G-Loads	V1-D-32
4.3	Introduction to Impact Analysis of the Topplate Shielding No. 1 & 2 Assembly	V1-D-33
4.3.1	Drop Orientation - 0. Degree	V1-D-34
4.3.2	Drop Orientation - 90. Degrees	V1-D-53
4.3.3	Drop Orientation - 45. Degrees	V1-D-66
4.4	Shielding No. 3	V1-D-84
4.4.1	Drop Orientation - 90. Degrees	V1-D-85
4.4.2	Drop Orientation - 0. Degree	V1-D-88
4.4.3	Drop Orientation - 45. Degrees	V1-D-91
4.5	Shielding No. 4	V1-D-94
4.5.1	Drop Orientation - 90. Degrees	V1-D-94
4.5.2	Drop Orientation - 0. Degree	V1-D-102
4.5.3	Drop Orientation - 45. Degrees	V1-D-106
4.5.4	Shielding No. 4 - Stud Size Table	V1-D-110
5.0	STUD SUMMARY	V1-D-111
6.0	URANIUM PLATE - COMBINED STRESS VS. IMPACT ORIENTATION	V1-D-113
7.0	THERMAL EVALUATION	V1-D-114
REFERENCES		V1-D-115
APPENDIX A' - FIN BENDING STRESS VS. TIME CURVES		V1-D-117
APPENDIX B' - PROPERTIES OF 304 S.S., 216 S.S. AND URANIUM		V1-D-121
APPENDIX C' - GEOMETRY MODEL OF TOPPLATE - SHIELDING NO. 1 & 2 ASSEMBLY		V1-D-125

1.0 INTRODUCTION

The report describes the design analysis of the additional shieldings assembled to the IF-300 Shipping Cask Basket. The shielding structure shall be examined for the impact loadings resulting from a thirty foot drop. The cask side orientations used in the dropping analysis are 0.0-, 45.- and 90. degrees, considering the most critical G-loading components.

A static elastic analysis of the topplate - shielding assembly is performed using the static portion of the MRI/Stardyne 3 analysis program. The G-load applicable for the drop orientation of the cask is imposed on the assembly as an acceleration. The resulting external load acting on a member is compared to the internal load carrying (collapse load) capacity. The criteria for failure is considered to be the external load exceeding the load carrying capacity of a member, rather than directly comparing the combined stress in a member to a set stress limit. For continuous beam - and plate - elements of ductile material, redistribution of the load occurs above the elastic limit. Although the load redistribution is discussed in the analysis of critical areas of the structure, no credit for this condition is taken into consideration in determining the failure load of a member.

The steady state temperature of the structure during load application is 450°F. and the properties of the materials of the structure is adjusted to reflect this condition.

2.0 BEAM PROPERTIES (i)

1. BEAM NO.'S 3-8 & 82-87

TO INCLUDE THE EFFECT OF THE 3/8 IN. HOLES ON THE OVER ALL STIFFNESS OF THE BEAMS, AVERAGE I_{x_2} & I ARE COMPUTED.

TOTAL BEAM LENGTH = 2 x 5.56 = 11.12 IN.

LENGTH OF BEAM USED FOR 7 HOLES = .375 x 5 + 2 x .375/2 = 2.25 IN

LENGTH OF SOLID BEAM = 8.87 IN.

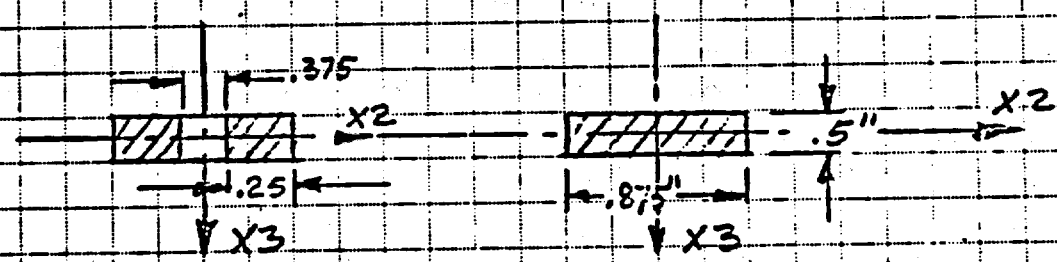

I_{x_i} AT HOLE FOR 2.25 IN. OF TOTAL BEAM LENGTH.

$I_{x_{2_H}} = 1/12 \times .5^3 \times .5 = .0052 \text{ IN}^4$

$I_{x_{3_H}} = 2 \times \left(1/12 \times .25^3 \times .5 + .25 \times .5 \times \left(\frac{.375+.25}{2}\right)^2\right) = .026 \text{ IN}$

I_{x_i} OUTSIDE HOLE FOR 8.87 IN. OF TOTAL BEAM LENGTH.

$I_{x_{2_O}} = 1/12 \times .5^3 \times .875 = .0091 \text{ IN}^4$

$I_{x_{3_O}} = 1/12 \times .875^3 \times .5 = .028 \text{ IN}^4$

2.0 CONT'D

AVERAGE I_{x_1} FOR OVERALL BEAM.

$$I_{x_2} = \frac{.0052 \times 2.25}{11.12} + \frac{.0091 \times 8.87}{11.12} = .0083 \text{ IN}^4$$

$$I_{x_3} = \frac{.026 \times 2.25}{11.12} + \frac{.028 \times 8.87}{11.12} \approx .0280 \text{ IN}^4$$

TORSIONAL RESISTANCE = J [IN^4]

(PER REF. 1 - P. 210-2)

J_H AT HOLES FOR 2.25 IN. OF TOTAL BEAM LENGTH.

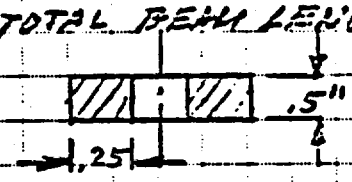

$b = .50$ IN, $d = .25$ IN

$b/d = .5/.25 = 2.0 \Rightarrow \beta = .229$

$$\Sigma J_H = 2 \times \beta \times b \times d^3 = 2 \times .229 \times .5 \times .25^3 = .0036 \text{ IN}^4$$

J_o OUTSIDE HOLES FOR 8.87 IN. OF TOTAL BEAM LENGTH.

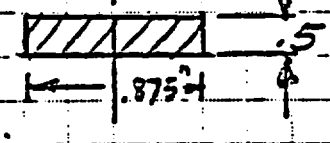

$b = .875$ IN, $d = .5$ IN

$b/d = .875/.5 = 1.75 \Rightarrow \beta = .214$

$$J_o = \beta \times b \times d^3 = .214 \times .875 \times .5^3 = .023 \text{ IN}^4$$

AVERAGE J FOR OVERALL BEAM

$$J = \frac{.0036 \times 2.25}{11.12} + \frac{.023 \times 8.87}{11.12} = .019 \text{ IN}^4$$

AREA $= .875 \times .5 = .44$ IN^2

2.0 CONT'D

$H2 = .875$ IN., $H3 = .50$ IN., CTORS $= t = .5$ IN.

2. BEAM NO.'S 43-47, 58-61 & 516-524

$I_{x_2} = I_{x_3} = 10^3$ IN^4 ∴ NO DEFLECTION DUE TO MOMENT IN LOAD TRANSFER.

EFFECTIVE AREA OF PLATE IN COMPRESSION $= A_e$

$A_e = t \times (t \times 3) = .5^2 \times 3 = .75$ IN^2

$J = 1.0$ IN^4

THE WELDS AT THE PLATES ARE CONSIDERED TO BE INCAPABLE OF TRANSFERING M_2, M_3 & T.

$\rho = 0.0$ LB/IN^3

3. BEAM NO.'S 525-542

TO INCLUDE THE EFFECT OF THE SLOTS ON THE OVER-ALL STIFFNESS OF THE BEAMS ; AVERAGE I_{x_i} & J ARE COMPUTED.

TOTAL BEAM LENGTH = 15.75 IN.

LENGTH OF BEAM USED FOR SLOTS ≅ 12.0 IN.

LENGTH OF SOLID BEAM = 3.75 IN.

2.0 CONT'D

AT SLOTS

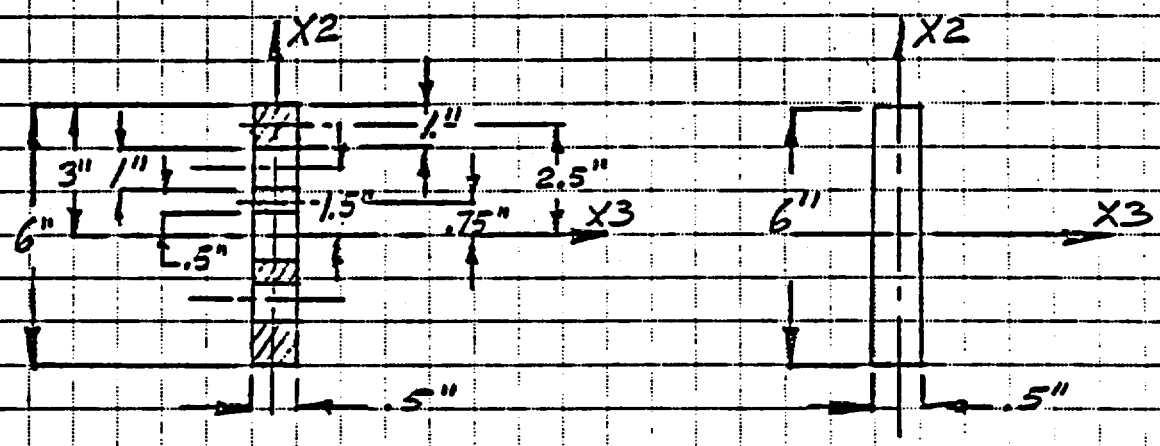

$I_{x_{i,S}}$ AT SLOTS FOR 12.0 IN OF TOTAL BEAM LENGTH

$I_{x_{2,S}} = 2 \times 1/12 \times (.5^3 \times 1. + .5^3 \times .5) = .031 \ IN^4$

$I_{x_{3,S}} = 2 \times (1/12 \times .5 \times (1.^3 + .5^3) + .5 \times 2.5^2 + .5^2 \times .75^2) = 6.63 \ IN^4$

$I_{x_{i,O}}$ OUTSIDE SLOTS FOR 3.75 IN OF TOTAL BEAM LENGTH

$I_{x_{2O}} = 1/12 \times .5^3 \times 6. = .063 \ IN^4$

$I_{x_{3O}} = 1/12 \times 6.^3 \times .5 = 9.0 \ IN^4$

AVERAGE I_{x_i} FOR OVERALL BEAM.

$I_{x_2} = \frac{.031 \times 12.0}{15.75} + \frac{.063 \times 3.75}{15.75} = .039 \ IN^4$

$I_{x_3} = \frac{6.63 \times 12.0}{15.75} + \frac{9.0 \times 3.75}{15.75} = 7.20 \ IN^4$

$J = 10^{-3} \ IN^4 \Rightarrow$ NO CREDIT TAKEN FOR TORSILE RESISTANCE OF PLATE.

AREA = $6 \times .5 = 3.0 \ IN^2$. $H2 = 6.0 IN$ & $H3 = .5 IN$

2.0 CONT'D

4. BEAM NO.'S 88-89 & 154-155

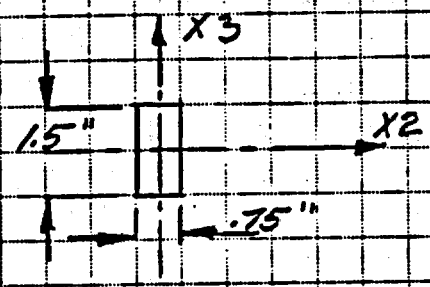

$I_{X2} = 1/12 \times 1.5^3 \times .75 = .21\ IN^4$

$I_{X3} = 1/12 \times .75^3 \times 1.5 = .053\ IN^4$

$b/d = 1.5/.75 = 2.0 \Rightarrow \beta = .229$ (REF. 1-P.2.10-2)

TORSIONAL RESISTANCE = J [IN⁴]

$J = \beta \times b \times d^3 = .229 \times 1.5 \times .75^3 = .145\ IN^4$

AREA = $1.5 \times .75 = 1.13\ IN^2$

H2 = .75 & H3 = 1.5 & CTORS = t = .75

5. BEAM NO.'S 92-93 & 158-159

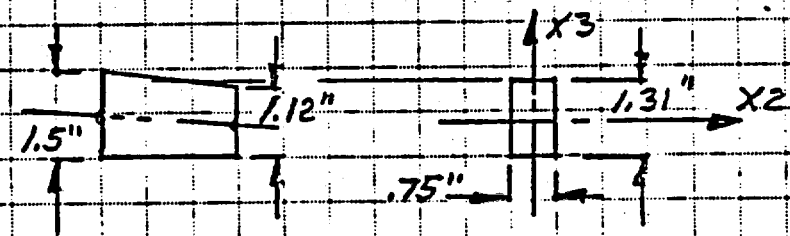

H2 = .75 IN
H3 = 1.12 IN
CTORS = .75 IN

$I_{X2} = 1/12 \times 1.31^3 \times .75 = .14\ IN^4$ $b/d = 1.31/.75 = 1.75 \Rightarrow \beta = .214$

$I_{X3} = 1/12 \times .75^3 \times 1.31 = .046\ IN^4$ $J = .214 \times 1.31 \times .75^3 = .12\ IN^4$

AREA = $.75 \times 1.12 = .84\ IN^2$

2.0 CONT'D

6. BEAM NO.'S 94-95 & 160-161

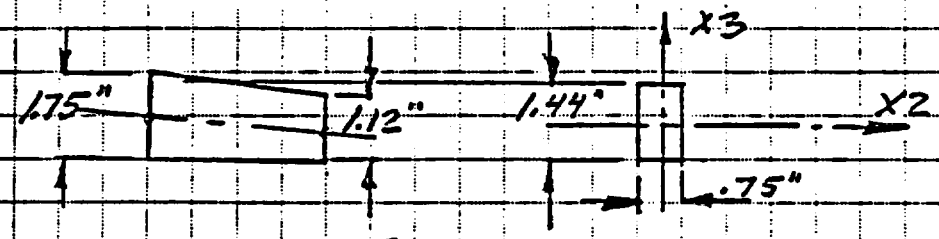

H2 = .75 IN
H3 = 1.12 IN
CTRS = .75 IN

$I_{x2} = 1/12 \times 1.44^3 \times .75 = .187\ IN^4$

$I_{x3} = 1/12 \times .75^3 \times 1.44 = .05\ IN^4$

AREA = $.75 \times 1.12 = .84\ IN^2$, $b/d = 1.44/.75 = 1.92 \Rightarrow \beta = .224$

$J = .224 \times 1.44 \times .75^3 = .136\ IN^4$

7. BEAM NO.'S 90-91 & 156-157

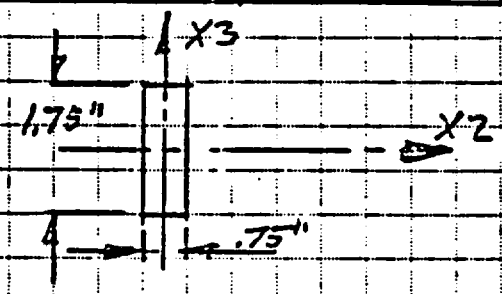

$I_{x2} = 1/12 \times 1.75^3 \times .75 = .335\ IN^4$, H2 = .75 IN
H3 = 1.75 IN

$I_{x3} = 1/12 \times .75^3 \times 1.75 = .062\ IN^4$, CTRS = .75 IN

$b/d = 1.75/.75 = 2.33 \Rightarrow \beta = .242$

$J = .242 \times 1.75 \times .75^3 = .18\ IN^4$

AREA = $1.75 \times .75 = 1.31\ IN^2$

2.0 CONT'D

8. BEAM NO.'S 96-99, 117-122, 124-129, 162-165
182-187, 188-193, 234-243, 260-271,
272-283, 380-389, 408-419, 422-433,
352-359, 508-515, 1-2, 9-42, 78-81, 543-55
316-321, 322-327, 340-345, 346-351,
516-524, 466-471, 472-477, 490-495, 496-50
502-507, 555-566, 567-572.

RIGID BEAM MEMBERS ASSURING 100% LOAD TRANSFER BETWEEN FLEXIBLE BEAMS AND ARE APPLIED AT SHIFTS IN NEUTRAL AXIS OF CONNECTED BEAMS AND AT BEAM TO PLATE ELEMEN CONNECTIONS IN ORDER TO DISTRIBUTE THE LOAD OVER THE ENTIRE ARE AT THE CONNECTIONS.

9. BEAM NO.'S 100-109, 166-175, 244-245, 420-421,
390-391, 406-407

TO INCLUDE THE EFFECT OF THE 3/8 IN. HOLES ON THE OVERALL STIFFNESS OF THE BEAMS, AVERAGE I_{x_L} & J ARE COMPUTED.

TOTAL BEAM LENGTH = 5.56 x 2 = 11.12"
LENGTH OF BEAM USED FOR 7 HOLES = .375 x 5 + 2 x $\frac{.375}{2}$ = 2.25"
LENGTH OF SOLID BEAM = 8.87"

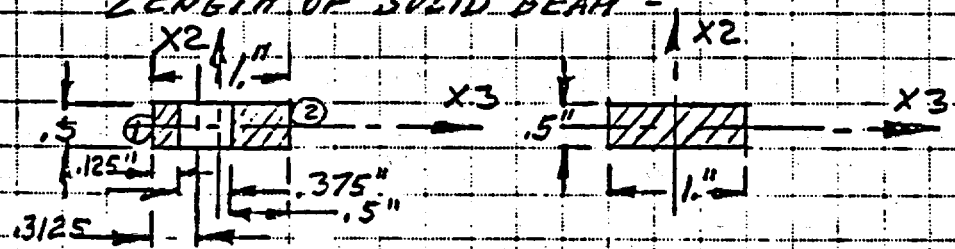

2.0 CONT'D

No.	A IN^2	X3i	A×X3i	A×X3i^2	I0 IN^4
1	.0625	.0625	.0039	.00024	—
2	.25	.75	.1875	.141	.0052
Σ	.3125		.1914	.1412	.0052

$$\bar{X}3 = \frac{.1914}{.3125} = .612 \text{ IN}$$

J_H & $I_{x_{iH}}$ AT HOLE FOR 2.25 IN. OF TOTAL BEAM LENGTH

$$I_{x_{2H}} = .0052 + .1412 - .612^2 \times .3125 = .03 \text{ IN}^4$$

$$I_{x_{3H}} = 1/12 \times (.5^3 \times .125 + .5^3 \times .5) = .007 \text{ IN}^4$$

① $b_1/d_1 = .5/.125 = 4.0 \Rightarrow \beta_1 = .281$

$$J_{H_1} = .281 \times .5 \times .125^3 = .0002 \text{ IN}^4$$

② $b_2/d_2 = .5/.5 = 1.0 \Rightarrow \beta_2 = .141$

$$J_{H_2} = .141 \times .5^4 = .0088 \text{ IN}^4$$

$$\sum_{i=1}^{n=2} J_{H_i} = .009 \text{ IN}^4$$

J_0 & $I_{x_{i0}}$ OUTSIDE HOLES FOR 8.87 IN. OF TOTAL BEAM LENGTH

$$I_{x_{2O}} = 1/12 \times 1.^3 \times .5 = .042 \text{ IN}^4, \quad b/d = 1./.5 = 2.0 \Rightarrow \beta = .229$$

$$I_{x_{3O}} = 1/12 \times .5^3 \times 1. = .010 \text{ IN}^4, \quad J_0 = .229 \times 1. \times .5^3 = .029 \text{ IN}^4$$

AVERAGE I_{x_i} & J FOR OVERALL BEAM.

$$I_{x_2} = \frac{.03 \times 2.25}{11.12} + \frac{.042 \times 8.87}{11.12} = .040 \text{ IN}^4$$

2.0 CONT'D

$I_{x3} \cong \frac{.007 \times 2.25}{11.12} + \frac{.010 \times 8.87}{11.12} = .009\ IN^4$

$J \cong \frac{.009 \times 2.25}{11.12} + \frac{.029 \times 8.87}{11.12} = .025\ IN^4$

AREA = .50 IN^2, H2 = .5 IN, H3 = 1.0 IN, CTOS = t = .5 IN.

10. BEAM NO.'S 110-116, 137-143, 123, 176-181, 201-207, 298-311, 448-461

THE STUDS OF SHIELDING NO. 1 AT THE CONNECTION BETWEEN THE 1/2" x 1.0" BAR & TOP PLATE ARE CONSIDERED TO HAVE NEGLIGIBLE MOMENT CARRYING CAPABILITY.

THE STUDS OF SHIELDING NO. 2 AT BOTH THE RIB- & TOP PLATE-CONNECTION ARE CONSIDERED TO HAVE NEGLIGIBLE MOMENT CARRYING CAPABILITY.

THE STUDS AT THE ABOVE LOCATIONS CAN SLIDE IN THE HOLES (NO WELDS).

INCORRECTLY STATED ANALYSIS

$J = \pi/32 \times .375^4 = .002\ IN^4$

$I_{x2} = I_{x3} = 10^{-3}\ IN^4 \Rightarrow \theta_{x2} = \theta_{x3} \sim 0.0$

3/8" STUD SHEAR AREA = $\frac{\pi \times .375^2}{4} = .110\ IN^2$

SHEAR DISTORTION FOR THIS BEAM TYPE ⇒ SF2 = SF3 = .85 (PER REF. 5-B1-112)

11. BEAM NO.'S 130-136, 194-200, 246-259, 284-297, 392-405, 434-447.

$J = \pi/32 \times .375^4 = .002\ IN^4$

$I_{x2} = I_{x3} = 10^{-3}\ IN^4 \Rightarrow$ NO DEFLECTION DUE TO MOMENT IN LOAD TRANSFER.

SF2 = SF3 = .85 (SEE ITEM # 10).

2.0 CONT'D

3/8 IN.-STUD SHEAR AREA = .110 IN^2

CTORS = d/2 = .18 IN

12. BEAM NO.'S 152-153, 212-213

MATERIAL : URANIUM-SHIELDING NO.2

$I_{x_2} = 1/12 \times 1.0^3 \times 11.5 = .96$ IN^4

$I_{x_3} = 1/12 \times 11.5^3 \times 1.0 = 126.7$ IN^4

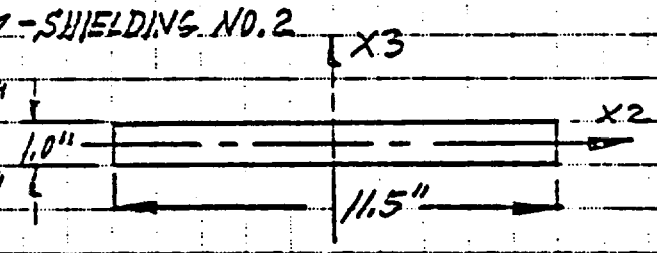

b/d = 11.5 ⇒ β = .333

J = .333 × 11.5 × 1.0^3 = 3.83 IN^4 H2 = 11.5 IN.

H3 = 1.0 IN.

AREA = 11.5 IN^2 CTORS = t = 1.0 IN

TO INCLUDE THE WEIGHT OF THE CLADDING IN THE INTERNAL WEIGHT COMPUTATION OF THE STARDYNE PROGRAM A COMBINED DENSITY OF THE URANIUM-CLADDING MEMBER IS COMPUTED.

URANIUM DENSITY = ρ_u = .679 LB/IN^3

S.S. 304 DENSITY = ρ_{304} = .283 LB/IN^3

COMBINED DENSITY = ρ_c LB/IN^3

SHIELDING NO. 2

WEIGHT OF URANIUM = 52.0 LB & CLADDING = 7.0 LB

2.0 CONT'D.

VOLUME OF BEAM NO.'S (152-153) & (212-213) = V IN^3

$$\rho_c = \frac{W_U + W_{CLAD}}{V} = \frac{52.+7.}{6.5 \times 1.0 \times 11.5}$$

$$\rho_c = .789 \text{ LB/IN}^3$$

13. BEAM NO.'S 312-315, 462-465

MATERIAL: URANIUM-SHIELDING NO.1

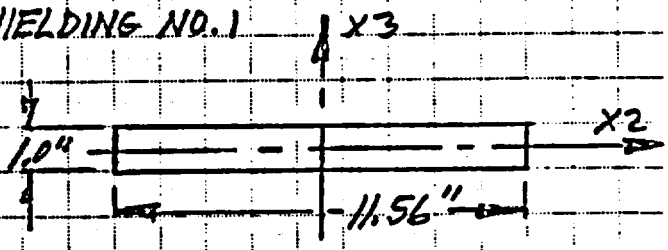

$I_{x2} = 1/12 \times 1.0^3 \times 11.56 = .96 \text{ IN}^4$

$I_{x3} = 1/12 \times 11.56^3 \times 1.0 = 128.7 \text{ IN}^4$

$b/d = 11.56 \Rightarrow \beta = .333$

$J = .333 \times 11.56 \times 1.0^3 = 3.85 \text{ IN}^4$. $H2 = 11.56$ IN. $H3 = 1.0$ IN.

AREA $= 11.56 \text{ IN}^2$ CTRES $= \ell = 1.0$ IN.

TO INCLUDE THE WEIGHT OF THE CLADDING A COMBINED DENSITY ρ_c [LB/IN^3] IS COMPUTED.

SHIELDING NO. 1

URANIUM WEIGHT = 76.0 LB & CLADDING = 9.0 LB

$$\rho_c = \frac{76.+9.}{11.56 \times 9.5} = .774 \text{ LB/IN}^3$$

2.0 CONT'D

14. BEAM NO.'S 62-77

TO INCLUDE THE EFFECT OF THE HOLES IN THE OVER-ALL STIFFNESS OF THE BEAMS, AVERAGE I_{X_2} & AREA ARE COMPUTED.

TOTAL BEAM LENGTH = 2 × 12.67 = 25.34 IN
LENGTH OF BEAM USED FOR HOLES = 30 × (35/64) IN = 16.41 IN
LENGTH OF SOLID BEAM = 8.93 IN

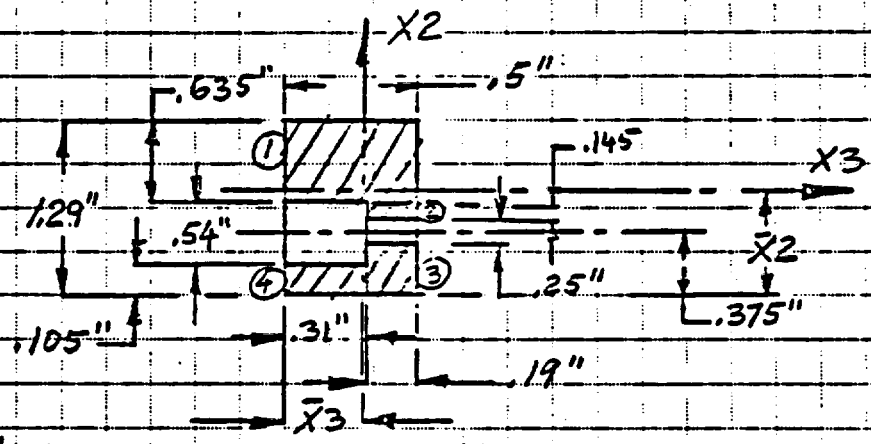

$I_{X_{2H}}$ & AREA$_H$ AT HOLE FOR 16.41 IN. OF TOTAL BEAM LENGTH

NO.	A IN^2	$\bar{X}_{2i}$	A × $\bar{X}_{2i}$	A × $\bar{X}_{2i}^2$	I_0 IN^4
1	.3175	.9625	.3056	.294	.0107
2	.0276	.5725	.0158	.009	—
3	.0475	.125	.0059	.0007	—
4	.0325	.0525	.0017	—	—
Σ	.425		.329	.304	.0107

AREA$_H$ = .425 IN^2, $\bar{X}2 = \frac{.329}{.425} = .775$ IN

$I_{X_{2H}} = .0107 + .304 - .775^2 \times .425 = .060$ IN^4

2.0 CONT'D

NO.	$A\ IN^2$	$\bar{X}3_i$	$A \times \bar{X}3_i$	$A \times \bar{X}3_i^2$	I_o
1	.3175	.25	.0794	.0198	.0066
2	.0276	.405	.0112	.0045	—
3	.0475	.405	.0192	.0078	—
4	.0325	.155	.0050	.0008	—
Σ	.425		.1148	.0329	.0066

$$\bar{X}3 = \frac{.1148}{.425} = .27\ IN$$

$$I_{X2H} = .0066 + .0329 - .27^2 \times .425 = .009\ IN^4$$

$I_{X_{i0}}$ & AREA$_o$ OUTSIDE HOLE FOR 8.93 IN. OF TOTAL LENGTH.

$$I_{X20} = 1/12 \times .5^3 \times 1.29 = .014\ IN^4$$

$$I_{X30} = 1/12 \times 1.29^3 \times .5 = .090\ IN^4$$

$$AREA_o = 1.29 \times .5 = .65\ IN^2$$

AVERAGE I_{X_i} AND AREA FOR OVERALL BEAM.

$$I_{X2} = \frac{.009 \times 16.41}{25.34} + \frac{.014 \times 8.93}{25.34} = \underline{.010\ IN^4}$$

$$I_{X3} = \frac{.06 \times 16.41}{25.34} + \frac{.090 \times 8.93}{25.34} = \underline{.070\ IN^4}$$

$$AREA = \frac{.425 \times 16.41}{25.34} + \frac{.65 \times 8.93}{25.34} = \underline{.50\ IN^2}$$

$$b/d = 1.29/.5 = 2.58 \Rightarrow \beta \cong .25 \quad , \quad H2 = 1.29\ IN$$

$$H3 = .5\ IN$$

$$J = .25 \times 1.29 \times .5^3 = \underline{.040\ IN^4} \qquad CTOCS = t \cong .5\ IN$$

2.0 CONT'D.

15. BEAM NO.'S 48-55

TO INCLUDE THE EFFECT OF THE HOLES ON THE OVERALL STIFFENESS OF THE BEAMS, AVERAGE I_{X_i} & AREA ARE COMPUTED.

TOTAL BEAM LENGTH = 2 × 6.06 = 12.12 IN
LENGTH OF BEAM USED FOR HOLES = 9 × (35/64) = 4.92 IN.
LENGTH OF SOLID BEAM = 7.20 IN

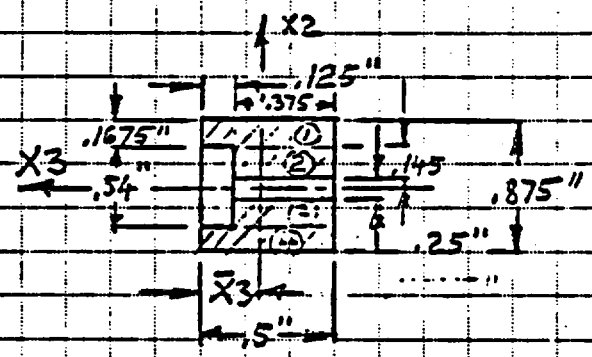

$I_{X_{iH}}$ & $AREA_H$ AT HOLE FOR 4.92 IN. OF TOTAL BEAM LENGTH.

NO.	A IN²	$\bar{X}_{2i}$	$A \times \bar{X}_{2i}$	$A \times \bar{X}_{2i}^2$	I_{OH} IN⁴	$\bar{X}_{3i}$	$\bar{X}_{3i} \times A$	$X_{3i}^2 \times A$	I_i IN⁴
1	.084	.354	—	.011	—	.25	.021	.0053	.0017
2	.054	.198	—	.002	—	.3125	.017	.0053	.0006
3	.054	.198	—	.002	—	.3125	.017	.0053	.0006
4	.084	.354	—	.011	—	.25	.021	.0053	.0017
Σ	.276		—	.026			.076	.021	.0046

$I_{X_{3H}} \cong \Sigma A \times \bar{X}_{2i}^2 = .026\ IN^4$ $\bar{X}_3 = \frac{.076}{.276} = .275\ IN$

$I_{X_{3H}} = .0046 + .021 - .275^2 \times .276 = .005\ IN^4$

$AREA_H = .276\ IN^2$

2.0 CONT'D

$I_{x_{2_0}}$ & $AREA_0$ OUTSIDE HOLE FOR 7.2 IN. OF TOTAL LENGTH.

$I_{x2_0} = 1/12 \times .5^3 \times .875 = .009 \ IN^4$

$I_{x3_0} = 1/12 \times .875^3 \times .5 = .028 \ IN^4$

$AREA_0 = .5 \times .875 = .438 \ IN^2$

AVERAGE I_{x_i} AND AREA FOR OVERALL BEAM.

$I_{x2} = \frac{.005 \times 4.92}{12.12} + \frac{.009 \times 7.2}{12.12} = .007 \ IN^4$

$I_{x3} = \frac{.026 \times 4.92}{12.12} + \frac{.028 \times 7.2}{12.12} = .027 \ IN^4$

$AREA = \frac{.276 \times 4.92}{12.12} + \frac{.438 \times 7.2}{12.12} = .372 \ IN^2$

$b/d = .875/.5 = 1.75 \Rightarrow \beta = .214$ ∴ $H2 = .875 \ IN.$

∴ $H3 = .5 \ IN.$

$J = .214 \times .875 \times .5^3 = .023 \ IN^4$ ∴ $CTORF = t = .5 \ IN.$

2.0 CONT'D

16. BEAM NO.'S 222, 227, 228, 233 & 368, 373, 374, 379

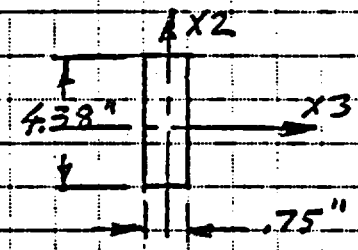

$I_{x2} = 1/12 \times .75^3 \times 4.38 = .154\ IN^4$

$I_{x3} = 1/12 \times 4.38^3 \times .75 = 5.25\ IN^4$

$AREA = 4.38 \times .75 = 3.28\ IN^2$

$b/d = 4.38/.75 = 5.84 \Rightarrow \beta = .298$

$J = .298 \times 4.38 \times .75^3 = .551\ IN^4$

H2 = 4.38 IN.
H3 = .75 IN.
CTORS = t = .75 IN.

17. BEAM NO.'S 223, 226, 229, 232 & 369, 372, 375, 378

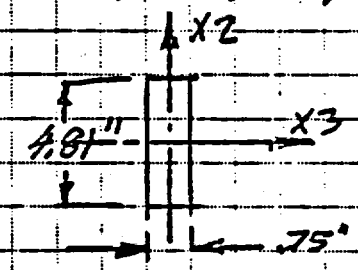

$I_{x2} = 1/12 \times .75^3 \times 4.81 = .169\ IN^4$

$I_{x3} = 1/12 \times 4.81^3 \times .75 = 6.96\ IN^4$

$AREA = 4.81 \times .75 = 3.61\ IN^2$

$b/d = 4.81/.75 = 6.41 \Rightarrow \beta = .30$

$J = .30 \times 4.81 \times .75^3 = .61\ IN^4$

H2 = 4.81 IN
H3 = .75 IN
CTORS = .75 IN.

2.0 CONT'D

18. BEAM NO.'S 224, 225, 230, 231 & 370, 371, 376, 377

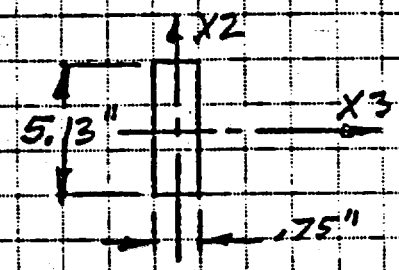

$I_{x2} = 1/12 \times .75^3 \times 5.13 = .180\ IN^4$

$I_{x3} = 1/12 \times 5.13^3 \times .75 = 8.44\ IN^4$

AREA $= .75 \times 5.13 = 3.85\ IN^2$

$b/d = 5.13/.75 = 6.84 \Rightarrow \beta = .302$

$J = .302 \times 5.13 \times .75^3 = .654\ IN^4$

H2 = 5.13 IN.
H3 = .75 IN.
CTORS = .75 IN

19. BEAM NO.'S 328, 329, 334, 335 & 478, 479, 480, 481

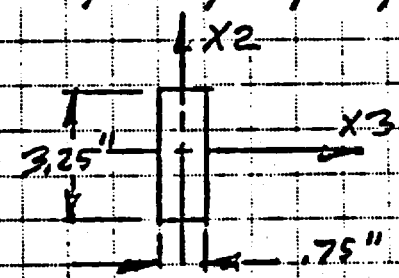

$I_{x2} = 1/12 \times .75^3 \times 3.25 = .114\ IN^4$

$I_{x3} = 1/12 \times 3.25^3 \times .75 = 2.15\ IN^4$

AREA $= 3.25 \times .75 = 2.44\ IN^2$

$b/d = 3.25/.75 = 4.33 \Rightarrow \beta = .284$

$J = .284 \times 3.25 \times .75^3 = .389\ IN^4$

H2 = 3.25 IN.
H3 = .75 IN.
CTORS = .75 IN.

2.0 CONT'D

20. BEAM NO.'S 330, 331, 336, 337 & 482, 483, 484, 485

$I_{x2} = 1/12 \times .75^3 \times 3.69 = .130\ IN^4$

$I_{x3} = 1/12 \times 3.69^3 \times .75 = 3.14\ IN^4$

AREA $= 3.69 \times .75 = 2.77\ IN^2$

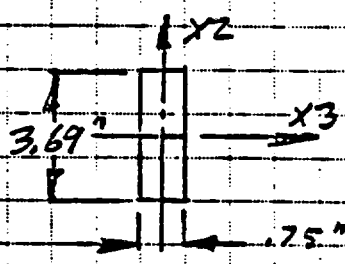

$b/d = 3.69/.75 = 4.92 \Rightarrow \beta = .289$

$J = .289 \times 3.69 \times .75^3 = .450\ IN^4$

H2 = 3.69 IN.
H3 = .75 IN.
CTORS = .75 IN

21. BEAM NO.'S 332, 333, 338, 339 & 486-489.

$I_{x2} = 1/12 \times .75^3 \times 4.0 = .141\ IN^4$

$I_{x3} = 1/12 \times 4.0^3 \times .75 = 4.0\ IN^4$

AREA $= 4.0 \times .75 = 3.0\ IN^2$

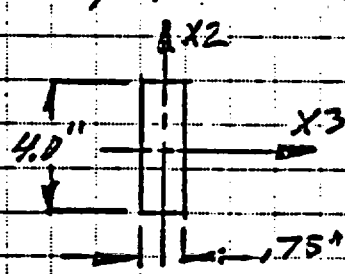

$b/d = 4.0/.75 = 5.33 \Rightarrow \beta = .293$

$J = .293 \times 4.0 \times .75^3 = .494\ IN^4$

H2 = 4.0 IN.
H3 = .75 IN.
CTORS = .75 IN.

2.0 CONT'D

22. BEAM NO.'S 56 & 57

TO INCLUDE THE EFFECT OF THE HOLES IN THE OVER-ALL STIFFNESS OF THE BEAMS, AVERAGE I_{X_i} & AREA ARE COMPUTED.

TOTAL BEAM LENGTH = 5.94 IN
LENGTH OF BEAM USED FOR HOLES = $4 \times \left(\frac{35}{64}\right)$ = 2.19 IN
LENGTH OF SOLID BEAM = 3.75 IN

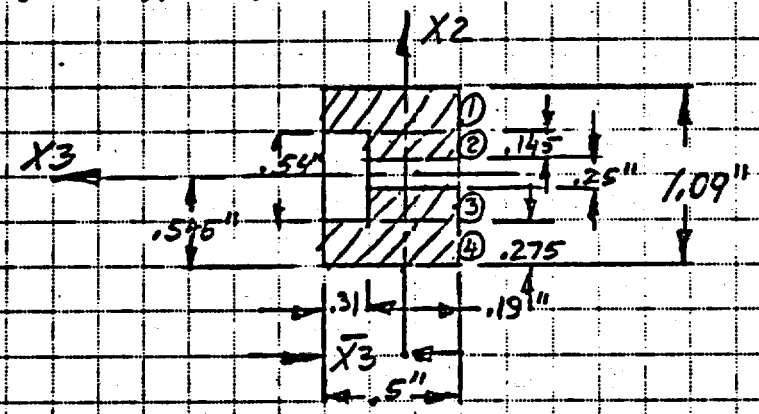

NO.	A IN²	$\bar{X}2_i$	$\bar{X}2_i \times A$	$\bar{X}2_i^2 \times A$	I_0 IN⁴	$\bar{X}3_i$	$A \times \bar{X}3_i$	$A \times X3_i^2$	I_0 IN⁴
1	.1375	.4075	—	.023	—	.25	.0344	.0086	.0029
2	.0276	.1975	—	.0011	—	.405	.0112	.0045	—
3	.0276	.1975	—	.0011	—	.405	.0112	.0045	—
4	.1375	.4075	—	.023	—	.25	.0344	.0086	.0029
Σ	.33			.048			.0912	.0262	.0058

$I_{X_{iH}}$ & $AREA_H$ AT HOLES FOR 2.19 IN. OF TOTAL BEAM LENGTH

$I_{X3_H} \cong \Sigma A \times \bar{X}_{2_i}^2 = .048\ IN^4$, $\bar{X}3 = \frac{.0912}{.33} = .276\ IN$

$I_{X2_H} = .0058 + .0262 - .276^2 \times .33 = .007\ IN^4$

$AREA = .33\ IN^2$

2.0 CONT'D

$I_{x_{1_0}}$ & AREA, OUTSIDE HOLES FOR 3.75 IN. OF TOTAL LENGTH.

$I_{x2_0} = 1/12 \times .5^3 \times 1.09 = .011 \ IN^4$

$I_{x3_0} = 1/12 \times 1.09^3 \times .5 = .054 \ IN^4$

$AREA_0 = 1.09 \times .5 = .545 \ IN^2$

AVERAGE I_{x_1} & AREA FOR OVERALL BEAM.

$I_{x2} = \frac{.007 \times 2.19}{5.94} + \frac{.011 \times 3.75}{5.94} \cong .0095 \ IN^4$

$I_{x3} = \frac{.048 \times 2.19}{5.94} + \frac{.054 \times 3.75}{5.94} = .052 \ IN^4$

$AREA = \frac{.33 \times 2.19}{5.94} + \frac{.545 \times 3.75}{5.94} = .466 \ IN^2$

$b/d = 1.09/.5 = 2.18 \Rightarrow \beta = .236$, $H2 = 1.09$ IN.
$H3 = .5$ IN.

$J = .236 \times 1.09 \times .5^3 = .032 \ IN^4$, CTORS = .5 IN.

23. BEAM NO.'S 144-147 & 208-211

BEAM DIA. = 2.25 IN.

$I_{x2} = I_{x3} = \pi/64 \times 2.25^4 = 1.26 \ IN^4$

$AREA = \frac{\pi \times 2.25^2}{4} = 3.97 \ IN^2$

$J = \pi/32 \times 2.25^4 = 2.51 \ IN^4$, $H2 = H3 = 2.25$ IN.
CTORS = 1.12 IN.

JOB NO. _____ DATE _____ BY G.V.T. CH'K _____

CUSTOMER _____ PROJECT _____

SUBJECT _____

2.0 CONT'D

24. BEAM NO.'S 148 - 151

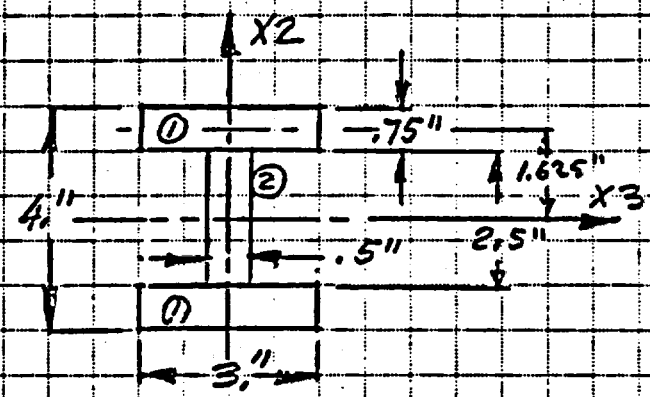

$I_{X2} = 1/12 \times ((3.0^3 \times .75) \times 2 + .5^3 \times 2.5) = \underline{3.40\ IN^4}$

$I_{X3} = 2 \times 1/12 \times .75^3 \times 3.0 + 1/12 \times 2.5^3 \times .5 + 2 \times (3 \times .75 \times 1.625^2)$

$I_{X3} = \underline{12.74\ IN^4}$

$AREA = 2 \times 3 \times .75 + 2.5 \times .5 = \underline{5.75\ IN^2}$

① $b_1/d_1 = 3.0/.75 = 4.0 \Rightarrow \beta_1 = .281$

② $b_2/d_2 = 2.5/.5 = 5.0 \Rightarrow \beta_2 = .291$

$J = 2 \times .281 \times 3.0 \times .75^3 + .291 \times 2.5 \times .5^3 = \underline{.80\ IN^4}$

$H2 = 4.0\ IN.$
$H3 = 3.0\ IN$
$CTOCS = t_{MAX} = .75\ IN.$

2.0 CONT'D

25. BEAM NO.'S 214-217, 360-363

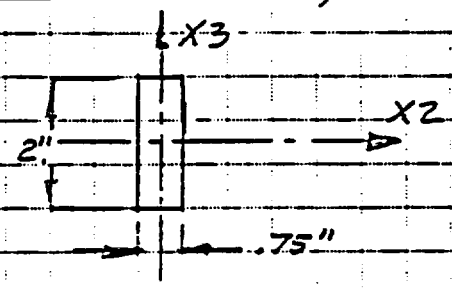

I_{x2} : $1/12 \times 2.^3 \times .75 = .50\ IN^4$

$I_{x3} = 1/12 \times .75^3 \times 2. = .070\ IN^4$

b/d : $2./.75 = 2.67 \Rightarrow \beta = .254$

$J = \beta \times b \times d^3 = .254 \times 2. \times .75^3 = .214\ IN^4$

AREA = $2. \times .75 = 1.5\ IN^2$. $H2 = .75"$. $H3 = 2."$. CTORS = .75"

26. BEAM NO.'S 218-221, 364-367

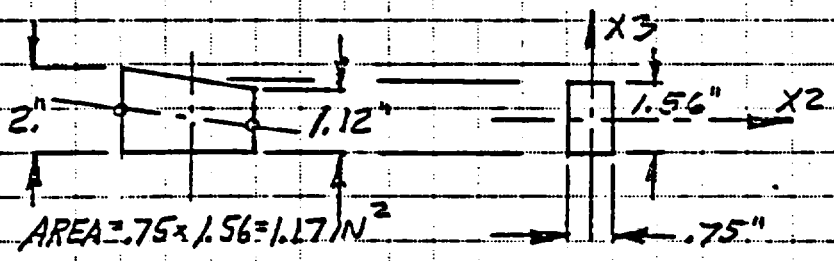

HZ = .75 IN.
H3 = 1.12 IN.
CTORS = .75 IN.

AREA = $.75 \times 1.56 = 1.17\ IN^2$

$I_{x2} = 1/12 \times 1.56^3 \times .75 = .24\ IN^4$. $b/d = 1.56/.75 = 2.08 \Rightarrow \beta = .232$

$I_{x3} = 1/12 \times .75^3 \times 1.56 = .055\ IN^4$. $J = .232 \times 1.56 \times .75^3 = .153$ IN

27. BEAM NO.'S 346-351, 543-545 (RIGID)

AREA = 1.0×10^4 IN., $J = I_{x2} = I_{x3} = 1.0 \times 10^4$. $\rho = 0.0\ LB/IN^3$.

3.0 LOAD

THE CONTRIBUTION OF THE STIFFNESS OF SHIELDINGS 3 & 4 TO THE OVERALL STIFFNESS OF THE ASSEMBLY IS CONSIDERED NEGLIGIBLE.
SHIELDING NO. 3 & 4 IS EXCLUDED FROM THE STRUCTURAL GEOMETRY MODEL.
THE END REACTIONS OF SHIELDINGS 3 & 4 ARE COMPUTED AND TRANSFERED TO THE TOP PLATE AT THE LOCATION OF THE STUD ATTACHMENT AS NODE WEIGHTS.

SHIELDING NO. 3 - END REACTIONS

WEIGHT OF URANIUM PLATE = 14.0 LB
WEIGHT OF CLADDING = 3.0 LB
$W_U + W_C = W_{UC}$ 17.0 LB

WEIGHT OF RIBS = W_R = 3.0 LB

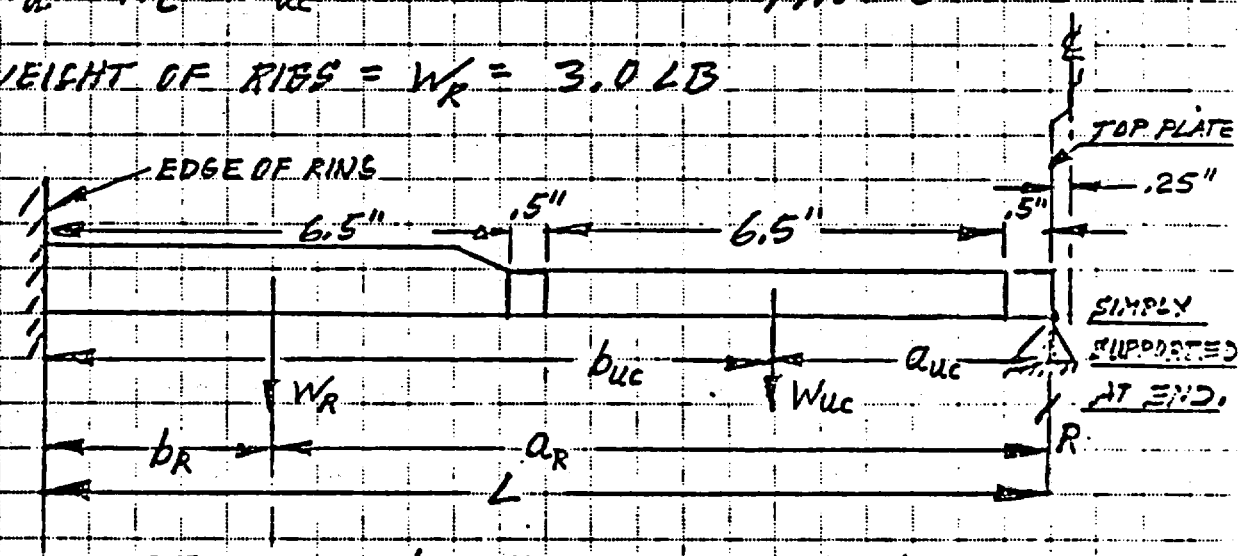

$b_R = 3.25$ IN , $b_{UC} = 10.25$ IN , $L = 14.0$ IN
$a_R = 10.75$ IN , $a_{UC} = 3.75$ IN

$$R = \frac{W_{UC} \times b_{UC}^2 \times (a_{UC} + 2 \times L)}{2 \times L^3} + \frac{W_R \times b_R^2 \times (a_R + 2 \times L)}{2 \times L^3}$$

$$R = \frac{17. \times 10.25^2 \times (3.75 + 2 \times 14.0)}{2 \times 14.^3} + \frac{3. \times 3.25^2 \times (10.75 + 2 \times 14.)}{2 \times 14.^3} = 10.6 \text{ LB}$$

3.0 CONT'D

NO. OF STUDS AT TOP PLATE CONNECTION = 2

REACTION PER NODE = R_i

R_i TO BE APPLIED AS A WEIGHT AT NODES 47, 48, 57, 58, 209, 210, 219 & 220.

$R_i = R/2 = 10.6/2 = 5.3$ LB

SHIELDING NO. 4 - END REACTION

WEIGHT OF URANIUM PLATE =	9.7 LB
WEIGHT OF CLADDING =	1.8 LB
$W_u + W_c = W_{u_c}$ =	11.5 LB

WEIGHT OF RIBS = W_R = 1.3 LB

DIM'S ARE THE SAME AS PER SHIELDING NO. 3

$$R = \frac{11.5 \times 10.25^2 \times (3.75 + 2 \times 14.0)}{2 \times 14.0^3} + \frac{1.3 \times 3.25^2 \times (10.75 + 2 \times 14.0)}{2 \times 14.0^3}$$

R = 7.10 LB ∴ NO. OF STUDS AT TOP PLATE CONNECTION = 1

REACTION PER NODE = R_i

R_i TO BE APPLIED AS A WEIGHT AT NODES 16, 28, 239 & 251.

$R_i = R = 7.10$ LB

4.0 STRESS ANALYSIS OF SHIELDING NO.'S 1-4

POSITION DIAGRAM OF THE VARIOUS SHIELDINGS IN THE TOP PLATE ASSEMBLY AND WITH RESPECT TO THE IMPACT ORIENTATIONS CONSIDERED IN THE ANALYSIS.

POSITION DIAGRAM

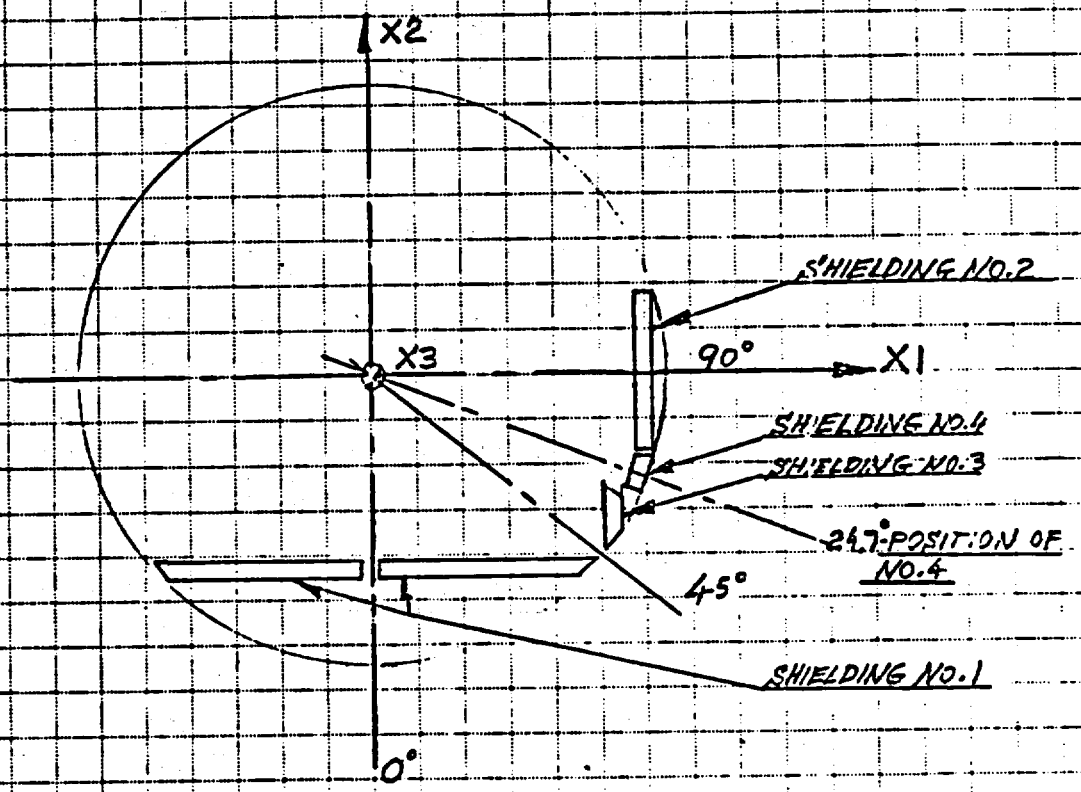

THE SHIELDING NO.'S 1-4 LOCATIONS ARE TYPICAL.

4.1 DYNAMIC LOAD FACTOR CONSIDERED FOR THE SHIELDING ASSY'S.

IN ORDER TO OBTAIN THE NATURAL FREQUENCY OF THE OVERALL TOP PLATE - SHIELDING ASSEMBLY AN APPROXIMATE METHOD IS USED. THE TOP PLATE - SHIELDING ASSEMBLY STRUCTURE IS IDEALIZED AS A CANTILEVERED BEAM WITH THE SAME MASS AS THE ACTUAL STRUCTURE. TO OBTAIN THE APPROXIMATE EQUIVALENT STIFFNESS OF THE CANTILEVERED BEAM AS COMPARED TO THE ACTUAL STRUCTURE, THE STIFFNESS EVALUATION OF THE BEAM IS BASED ON THE AVERAGE ACTUAL DEFLECTION OF THE ASSEMBLY WHEN SUBJECTED TO A LOAD.

THE COMPUTATION OF THE FIRST MODE NATURAL FREQUENCY OF THE ASSEMBLY IS BASED ON A SINGLE DEGREE OF FREEDOM SYSTEM WITH THE MASS AND STIFFNESS AS DESCRIBED ABOVE.

COMPUTATION OF DYNAMIC LOAD FACTORS FOR THE VARIOUS IMPACT ORIENTATIONS.

SINGLE DEGREE OF FREEDOM MODEL

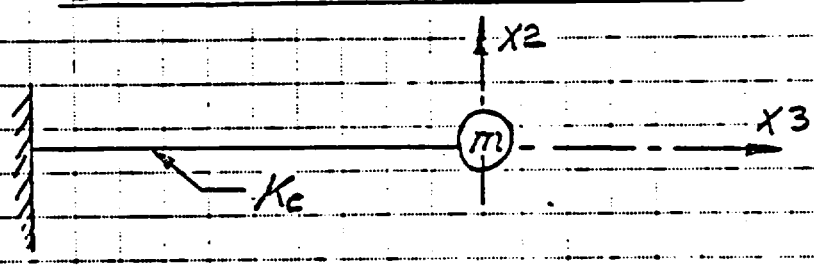

THE DAMPING COEFFICIENTS WERE CONSERVATIVELY CONSIDERED = 0.0 %

(PER REF. 3 - GEOMETRY OUTPUT)

WEIGHT OF TOP PLATE SHIELDING ASSEMBLY = W = 1009.3 Lb

THE AVERAGE DEFLECTION OF ASSEMBLY IN X_i - DIRECTION = ΔX_i

4.1 CONT'D

STIFFNESS COEFFICIENT OF THE CANTILEVERED BEAM = K_{X_J}

$K_{X_J} = \frac{F_{X_J}}{\Delta X_J}$ [LB/IN], WHERE F_{X_J} IS THE FORCE APPLIED TO THE ASSEMBLY IN THE X_J - DIRECTION.

4.1.1 DROP ORIENTATION - 0 DEGREE. (i)

FOR $G_i = G_0 = 214.$ (PER PAR. 4.2)

$\Delta X_J = \Delta X2 = .039$ IN (PER REF. 3 - LOAD CASE #1)

$F_{X2} = 216.0 \times 10^3$ LB

THE NATURAL FREQUENCY = f_{N_i} [CPS]

$$f_{N_i} = \frac{1}{2 \times \pi} \times \sqrt{\frac{K_{X2}}{m}} \text{ [CPS]}$$

$$f_{N_0} = \frac{1}{2 \times \pi} \times \sqrt{\frac{F_{X2} \times g}{\Delta X2 \times W}} \quad g = 386.4 \text{ IN/SEC}^2$$

$$f_{N_0} = \frac{1}{2 \times \pi} \times \sqrt{\frac{216. \times 10^3 \times 386.4}{.039 \times 1009.3}}$$

$$f_{N_0} = 232. \text{ CPS}$$

$$T_{N_0} = 1/f_{N_0} = 1/232. = 4.31. \text{ MSEC.}$$

THE FORCING FUNCTION FOR THE FINS AT 0 DEG. ORIENTATION IS GIVEN IN APPENDIX "A".

THE DYNAMIC LOAD FACTOR (PER P.30) = DLF_i

$DLF_0 = 1.0$

4.1.2 DROP ORIENTATION - 45 DEGREES. (i)

FOR $G_i = G_{45} = 161.$ (PER PAR. 4.2)

$\Delta X_{45} = \sqrt{\Delta X1^2 + \Delta X2^2}$ (PER REF. 3 - LOAD CASE # 2)

$\Delta X_{(45°)} = \sqrt{.0148^2 + .015^2}$

$\Delta X_{(45°)} = .0210$ IN

$F_{X(45°)} = \sqrt{F_{X1}^2 + F_{X2}^2} = \sqrt{114862.^2 + 114862.^2}$

$F_{X(45°)} = 162.439 \times 10^3$ LB

THE NATURAL FREQUENCY $= f_{N_i}$ [CPS]

$f_{N_{45}} = \frac{1}{2 \times \pi} \times \sqrt{\frac{F_{X(45°)} \times g}{\Delta X_{(45°)} \times W}}$, $g = 386.4$ IN/SEC^2

$f_{N_{45}} = \frac{1}{2 \times \pi} \times \sqrt{\frac{162439. \times 386.4}{.021 \times 1009.3}}$

$f_{N_{45}} = 274.$ CPS

$T_{N_{45}} = 1/f_{N_{45}} = 1/274. = 3.65$ MSEC.

THE FORCING FUNCTION FOR THE FINS AT 45 DEG. ORIENTATION IS GIVEN IN APPENDIX "A".

THE DYNAMIC LOAD FACTOR (PER P.30) = DLF_i

$DLF_i = DLF_{45} = \underline{1.14}$

4.1.3 DROP ORIENTATION - 90 DEGREES. (i)

FOR $G_i = G_{90} = 140.$ (PER. PAR. 4.2)

$\Delta X_S = \Delta X1$ IN (PER REF. 3 - LOAD CASE #3)

$\Delta X1 = .0177$ IN.

$F_{X1} = 141.31 \times 10^3$ LB

THE NATURAL FREQUENCY $= f_{N_i}$ [CPS]

$$f_{N_{90}} = \frac{1}{2\times\pi} \times \sqrt{\frac{F_{X1} \times G_i}{\Delta X1 \times W}} \quad g = 386.4 \text{ IN/SEC}^2$$

$$f_{N_{90}} = \frac{1}{2\times\pi} \times \sqrt{\frac{4.510. \times 386.4}{.0177 \times 1004.3}}$$

$f_{N_{90}} = 278.$ CPS

$T_{N_{90}} = 1/f_{N_{90}} = 1/278. = 3.60$ MSEC.

THE FORCING FUNCTION FOR THE FINS AT 90 DEG. ORIENTATION IS GIVEN IN APPENDIX "A".

THE DYNAMIC LOAD FACTOR (PER P.30) $= DLF_i$

$DLF_i = DLF_{45} = .97$

JOB NO. _____ DATE _____ BY F.K.T. CH'K _____

CUSTOMER _____ PROJECT _____

SUBJECT PAR. 4.1.1 - 4.1.3

(PER REF. 11)

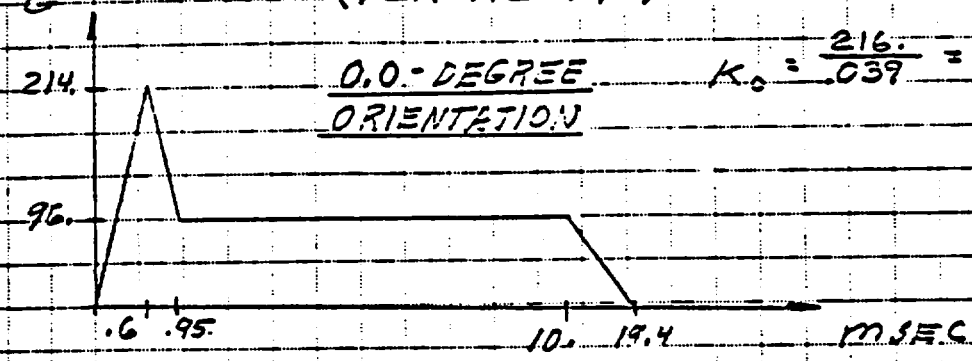

0.0-DEGREE ORIENTATION

$K_0 = \frac{216.}{.039} = 5538.$ K/IN

$W = 1009.3$ LB

$DLF_0 = 1.0$

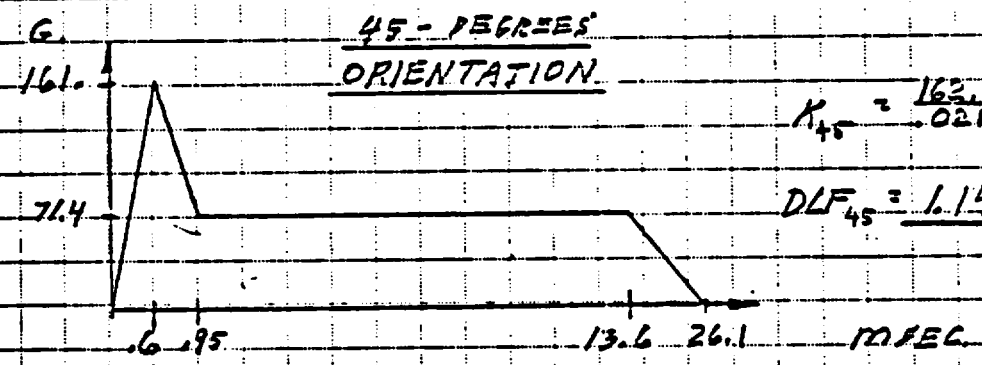

45-DEGREES' ORIENTATION

$K_{45} = \frac{162.4}{.021} = 7733.$ K/IN

$DLF_{45} = 1.14$

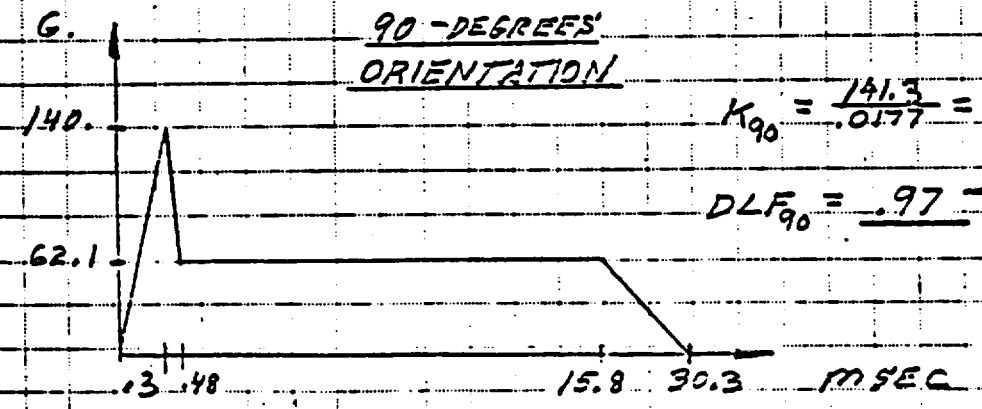

90-DEGREES' ORIENTATION

$K_{90} = \frac{141.3}{.0177} = 7983.$ K/IN

$DLF_{90} = .97$

4.2 DESIGN G-LOADS

TABLE 1

PEAK ORIENTATIONS DROP ORIENTATION	PEAK G	TOPPLATE ASSEMBLY & SHIELDINGS NO. 3 & 4 $G_i = G \times 1.05$	DYNAMIC LOAD FACTOR = DLF$_i$	STATIC INPUT FOR TOPPLATE - SHIELDING ASSEMBLY $G_i = G_i \times DLF_i$
0	204	214	1.0	214.0
45	153	161	1.14	184.0
90	133	140	.975	137.0
TOP	280	—	2.0	560.
BOTTOM	287	—	2.0	574.

4.3 INTRODUCTION TO IMPACT ANALYSIS OF THE TOPPLATE-SHIELDING NO. 1 & 2-ASSEMBLY.

THE TOPPLATE-SHIELDING ASSEMBLY IS MODELLED IN THREE DIMENSIONS BY FINITE ELEMENTS SUCH AS BEAM, TRIANGULAR PLATE- AND QUADRILATERAL PLATE-ELEMENTS.

THE BEAM IS A 6 DOF/NODE ELEMENT, THE TRIANGULAR AND QUADRILATERAL PLATES ARE 5 DOF/NODE ELEMENTS. IN ORDER TO TRANSFER TORSION FROM AN OUT-OF-PLANE (PLATE X3-AXIS) BEAM TO A NODE OF A PLATE ELEMENT, THE BEAM CENTERLINE IS CONNECTED TO THE PLATE NODE AND BY RIGID BEAM ELEMENTS TO SEVERAL ADJACENT PLATE NODES LIKE THE SPOKES OF A WHEEL.

THE BEAMS WHICH ARE OFFSET ARE CONNECTED TO EACH OTHER BY RIGID BEAM ELEMENTS.

THE CONTRIBUTION OF THE STIFFNESS OF SHIELDINGS 3 & 4 TO THE OVERALL STIFFNESS OF THE ASSEMBLY IS CONSIDERED NEGLIGIBLE. SHIELDINGS 3 & 4 IS EXCLUDED FROM THE STRUCTURAL GEOMETRY MODEL. THE END REACTIONS OF SHIELDINGS 3 & 4 ARE COMPUTED (SEE PAR. 3.2) AND TRANSFERED TO THE TOPPLATE AT AT THE LOCATION OF THE STUD ATTACHMENT AS NODE WEIGHTS.

SHIELDINGS 3 & 4 ARE ANALYSED SEPERATELY (PAR. 4.4 & 4.5) FOR THE DIFFERENT IMPACT ORIENTATIONS.

THE SEGMENTS WELDED TO THE TOPPLATE HAVE THE SAME RADIUS AS THE STRUCTURAL RINGS SPACED AT EQUAL DISTANCE ALONG THE AXIS OF THE CASK.

FOR EACH IMPACT ORIENTATION THE GAP BETWEEN THE DEFLECTED TOPPLATE AND THE INNER SURFACE OF THE ADJACENT SHELL IS CHECKED AND THE ASSEMBLY IS ANALYSED WITH OR WITHOUT CONTACT

4.3 CONT'D

FORCES FOR THE APPROPRIATE IMPACT ORIENTATION. THE RIB SUPPORTS OF SHELDINGS 1 & 2, THE DIVIDER PLATES AND THE 2 1/4 IN. DIA. SHAFTS ARE CONSIDERED FIXED AT THE STRUCTURAL RING AND THE PLATE OF THE RING.
THE FORSING FUNCTIONS OF THE FINS (δ VS. TIME) AND THE RESULTING DYNAMIC LOAD FACTORS AND G-LOADS FOR THE VARIOUS IMPACT ORIENTATIONS ARE DESCRIBED IN PAR. 4.1 AND 4.2.
THE RESULTING G-LOADS FOR THE APPROPRIATE IMPAC ORIENTATIONS ARE IMPOSED ON THE ASSEMBLY AS TRANSLATIONAL ACCELERATIONS AND INPUT AS SUCH IN THE STARDYNE 3 FINITE ELEMENT PROGRAM (REF. 5) AND A STATIC ANALYSIS IS PERFORMED ON THE ABOVE DESCRIBED MODEL OF THE ASSEMBLY.

4.3.1 DROP ORIENTATION - 0. DEGREE.
(REF. 3 - LOAD CASE # 4)
FOR THE 0. DEGREE ORIENTATION THERE IS NO GAP BETWEEN THE CIRCLE SEGMENT AND THE INNER SURFACE OF THE ADJACENT SHELL AS THE STRUCTURAL RINGS AND THE SEGMENT HAVING THE SAME RADIUS WILL CONTACT THE SHELL AT THE SAME TIME.

CONTACT AREA AND FORCE-DIAGRAM.

(PER REF. 6 - TABLE XIV - PAGE 320)

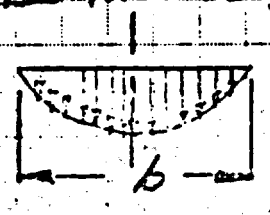

WIDTH OF RECTANGULAR CONTACT AREA = b IN.

4.3.1 CONT'D

$b = 2.15 \times \sqrt{\frac{G}{E} \times \frac{D_1 \times D_2}{D_1 - D_2}}$ FOR A SOLID DISC.

INNER DIA. OF SHELL = D_1 = 37.5 IN, SEGMENT DIA. = D_2 = 37.31 IN.

AT 450°F $E \cong 26.0 \times 10^6$ LB/IN^2, PLATE THICK. = t_{pl} = .5 IN.

TOTAL CONTACT FORCE FOR THE NODES BELOW = ΣP_{x2}

$\sigma_{x2} = \frac{\Sigma P_{x2}}{t_{pl}} \cong \frac{600 \times 214}{159} = 81.0$ K WHERE THE ASSUMED G-LOAD WAS 159.0 G AND ΣP_{x2} IS OBTAINED PER REF. 3 LOAD CASE # 4 - MEMBER LOADS.

PER PAR. 4.2 THE G-LOAD = G_0 = 214.

$b = 2.15 \times \sqrt{\frac{81 \times 10^3}{26 \times 10^6} \times \frac{37.5 \times 37.31}{(37.5 - 37.31)}} \cong 10.3$ IN.

ASSUMED CONTACT LENGTH EQUAL TO THE CHORD BETWEEN NODE NO. 120 & 130 = b_a.

b_a = 13.22 IN. > b = 10.3 IN. COMPUTING THE COMBINED RESULT OF THE DEFLECTIONS (REF. 3 - LOAD CASE # 4 - NODE DEFLECTIONS) IN THE X1-, X2-DIRECTIONS, CONTACT OCCURS FOR 13.22 < b < 15.0 IN (REF. TOPPLATE MODEL APPENDIX C)

RESULTING IN: 13.22 IN < b_{ACTUAL} < 15.0 IN ⇒ b_a CONSERVATIVE.

NODES 120-130 ARE FIXED WITH RESPECT TO TRANSLATION IN THEIR INDIVIDUAL X2-COORD. DIRECTIONS, WHERE THE X1-AXIS IS TANGENT TO THE CIRCLE AT THE NODE.
THE TOPPLATE ASSEMBLY IS ANALYSED AS DESCRIBED IN PAR. 4.3.

4.3.1 CONT'D

LIMIT STRESS FOR COMBINED TENSION & BENDING FOR RECTANGULAR SECTIONS.

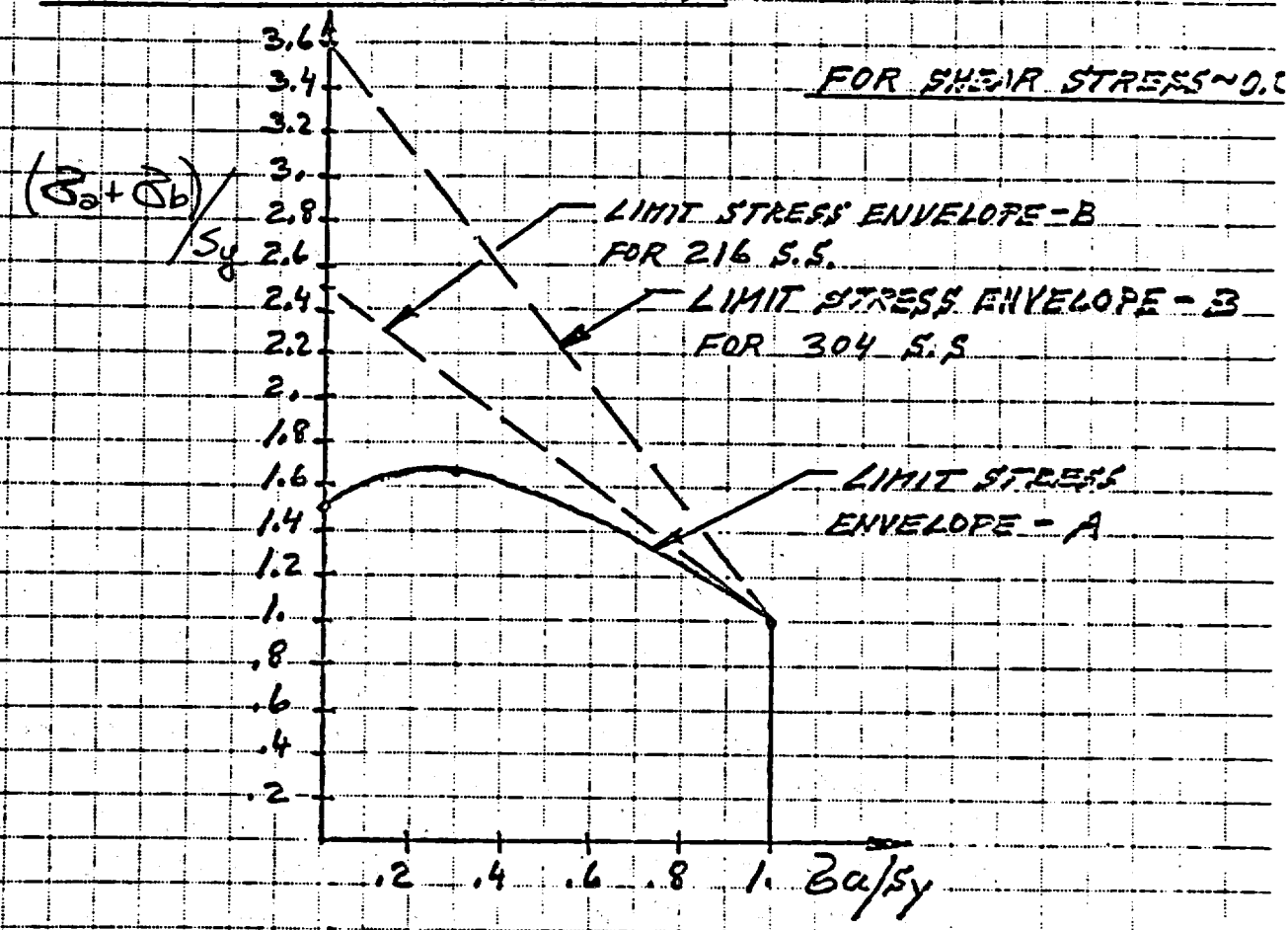

THE LIMIT STRESS ENVELOPE - A IS DEVELOPED FROM REF. 7 - P.7 - FIG. 2 AND BASED ON THE CONSERVATIVE ASSUMPTION OF PERFECT PLASTICITY WITH NO STRAIN-HARDENING.

THE LIMIT STRESS ENVELOPE - B IS BASED ON A BI-LINEAR REPRESENTATION CONSIDERING STRAIN-HARDENING.

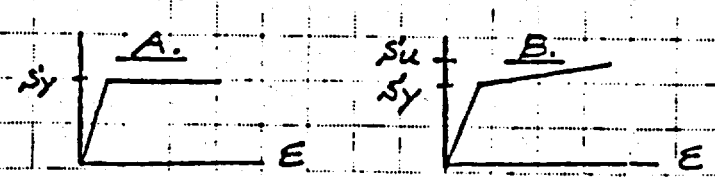

4.3.1 CONT'D

CONSIDERING CURVE "A" THE EQUIVALENT ELASTIC STRESS (σ_e) AT WHICH FAILURE WILL OCCUR FOR $\sigma_a/S_y = 0.0$ IS $= \sigma_e = 1.5 \times S_y$

CONSIDERING CURVE "B" THE EQUIVALENT ELASTIC STRESS AT FAILURE FOR $\sigma_a/S_y = 0.0$ IS $= \sigma_e$

BASED UPON A TRAPEZIODAL STRESS STRAIN DISTRIBUTION ACROSS THE THICKNESS THE EQUATION FOR σ_e IS : (REF. 9)

$$\sigma_e = S_y \times 1.5 + (S_u - S_y)$$

$$\sigma_e = S_y \times .5 + S_u \quad \text{OR} \quad \frac{\sigma_e}{S_y} = .5 + \frac{S_u}{S_y}$$

FOR 304 SS. AT 450°F : $S_u = 64.0$ KSI (REF. 8)
$S_y = 20.1$ KSI
FOR 216 S.S AT 450°F
$S_y = 44.9$ KSI & $S_u = 89.9$ KSI
(PER TABLE 2 - APPENDIX B)

FOR SIMPLIFICATION A STRAIGHT LINE IS CONNECTING THE TWO POINTS FOR THE BOUNDARY CONDITIONS $\sigma_a/S_y = 0.0$ & 1.0

FOR $\sigma_a/S_y = 0.0 \Rightarrow \sigma_e/S_{y_{304}} = (\sigma_a + \sigma_e)/S_{y_{304}} = .5 + \frac{64.}{20.1}$

$(\sigma_a + \sigma_3)/S_{y_{304}} \cong 3.6$ & $(\sigma_a + \sigma_B)/S_{y_{216}} = .5 + \frac{89.9}{44.9} = 2.50$

FOR ALL THE BEAM ELEMENTS IN THE ASSEMBLY THE MOMENTS COMPUTED IN REF. 3 ARE CONSERVATIVE AT THE ENDS WHERE AN ELASTIC LOAD DISTRIBUTION RESULTS IN A LOCAL PLASTIC DEFORMATION. THE E [LB/IN²] VALUE IS ACTUALLY CHANGING ALONG THE BEAM RESULTING IN A REDISTRIBUTION OF THE LOAD TO REGIONS BELOW

4.3.1 CONT'D

THE ELASTIC LIMIT FOR BEAMS SUPPORTED ELASTICALLY AT THE ENDS FAILURE DOES FIRST OCCUR WHEN A COMBINATION OF TENSILE FORCES AND BENDING MOMENTS BETWEEN THE ENDS PRODUCES TENSILE AND BENDING STRESS RATIOS OUTSIDE THE LIMIT STRESS ENVELOPE. ASSURING THAT THE MAXIMUM ELASTIC STRESS RATIO ALONG A BEAM IS WITHIN THE ENVELOPE PROVES IN A CONSERVATIVE WAY THAT THE INTEGRITY OF THE BEAM IS MAINTAINED DURING LOAD APPLICATION OF THE ASSEMBLY.

IN BEAMS WITH HOLES AVERAGE I_{xi} & AREA WERE COMPUTED TO INCLUDE THE EFFECT OF THE HOLES ON THE OVERALL BEAM STIFFNESS. IN THESE BEAMS THE STRESSES BASED ON THE ACTUAL CROSS-SECTION AT THE NODE ARE COMPUTED.

MOMENT IN BEAM NO. i AT NODE NO. J ABOUT THE LOCAL K-AXIS = $M_{i,J,K}$

THE AXIAL FORCE IN BEAM NO. i = P_i

STRESS IN BEAM NO. i AT NODE NO. J = $\sigma_{i,J}$

FOR MOMENTS AND FORCES SEE REF. 3 - LOAD CASE #4 - ELEMENT LOADS & FOR STRESSES SEE ELEMENT STRESSES.

4.3.1 CONT'D

THE MAXIMUM STRESS FOR BEAMS WITH PROPERTY NO. 15 OCCUR IN BEAM NO.'S 52 & 55.

BEAMS 52 & 55

(PER PAR. 2.0 - PROPERTY NO. 15)

$I_{X2_0} = .009\ IN^4$

$I_{X3_0} = .028\ IN^4$

$AREA_0 = .438\ IN^2$

$$\sigma_{55,282} = \frac{P_{55}}{.438} + \frac{M_{55,2.52,2} \times C_2}{.009} + \frac{M_{55,2.92,3} \times C_3}{.028}$$

$$\sigma_{55,282} = \frac{1.977}{.438} + \frac{.117 \times .5}{.009 \times 2} + \frac{1.665 \times .875}{.028 \times 2} = 33.79\ KSI$$

$$\sigma_i = \sigma_{55} = \frac{P_{55}}{.438} = \frac{1.977}{.438} = 4.51\ KSI$$

$$\sigma_a = \sigma_{55} = 4.51\ KSI$$

$$\sigma_B = \frac{.117 \times .5}{.009 \times 2} + \frac{1.665 \times .875}{.028 \times 2} = 29.26\ KSI$$

S_y FOR 304 SS = 20.1 KSI (PER APPENDIX B)

$$(\sigma_a + \sigma_B)/S_y = (4.51 + 29.26)/20.1 = 1.68$$

$$\sigma_a/S_y = 4.51/20.1 = .22$$

THE COORD. (.22, 1.68) IS WITHIN THE ENVELOPE

THE EFFECT OF SHEAR IS NEGLIGIBLE.

4.3.1 CONT'D

THE MAXIMUM STRESS FOR BEAMS WITH PROPERTY NO. 14 OCCUR IN BEAM NO.'S 62 & 70.

BEAMS 62 & 70

(PER PAR. 2.0 - PROPERTY NO. 14)

$I_{x20} = .014\ IN^4$

$I_{x30} = .090\ IN^4$

$AREA_0 = .65\ IN^4$

$$\sigma_{62,272} = \frac{P_{62}}{.65} + \frac{M_{62,272,2} \times C_3}{.014} + \frac{M_{62,272,3} \times C_2}{.090}$$

$$\sigma_{62,272} = \frac{3.50}{.65} + \frac{.036 \times .5}{.014 \times 2} + \frac{5.0 \times 1.29}{.090 \times 2} = 41.8\ KSI$$

$$\sigma_{62} = \frac{P_{62}}{.65} = \frac{3.50}{.65} = 5.3\ KSI$$

$\sigma_a = \sigma_{62} = 5.3\ KSI$

$\sigma_B = \sigma_{62,272} = 41.8\ KSI$

$S_y = 20.1\ KSI$

$(\sigma_a + \sigma_B)/S_y = 41.80/20.1 = 2.07$

$\sigma_a/S_y = 5.30/20.1 = .26$

THE COORD. (.26, 2.07) IS WITHIN THE ENVELOPE

THE EFFECT OF SHEAR IS NEGLIGIBLE.

4.3.1 CONT'D

THE MAXIMUM STRESS FOR BEAMS WITH PROPERTY NO. 4 OCCUR IN BEAM NO.'S 88 & 154

BEAMS 88 & 154

(PER PAR. 2.0 - PROPERTY NO. 4)

$I_{x2} = .21\ IN^4$

$I_{x3} = .053\ IN^4$

$\sigma_{88,310} = .346 + \frac{M_{88,310,2} \times C_2}{.21} + \frac{M_{88,310,3} \times C_3}{.053}$

$\sigma_{88,310} = .346 + \frac{.617 \times 1.5}{.21 \times 2} + \frac{4.41 \times .75}{.053 \times 2} = 33.75\ KSI$

$\sigma_a = .346$

$\sigma_{88,310} = \sigma_a + \sigma_B$

$(\sigma_a + \sigma_B)/S_y = 33.75/20.1 = 1.68$

$\sigma_a/S_y = .346/20.1 = .02$

THE COORD. (.02, 1.68) IS WITHIN THE ENVELOPE

THE EFFECT OF SHEAR IS NEGLIGIBLE

4.3.1 CONT'D

THE MAXIMUM STRESS FOR BEAMS WITH PROPERTY NO. 9 OCCUR IN BEAM NO.'S 104 & 170

BEAMS 104 & 170

(PER PAR. 2.0 - PROPERTY NO. 9)

$I_{x20} = .042\ IN^4$, AREA = $.5\ IN^2$

$I_{x30} = .01\ IN^4$

$$\sigma_{104,323} = .84 + \frac{M_{104,323,2} \times C_3}{.042} + \frac{M_{104,323,3} \times C_2}{.01}$$

$$\sigma_{104,323} = .84 + \frac{.042 \times 1.}{.042\ 2} + \frac{2.038 \times .5}{.01 \times 2} = 52.3\ KSI$$

$\sigma_a = .84\ KSI$

$\sigma_{104,323} = \sigma_a + \sigma_B$

$(\sigma_a + \sigma_B)/S_y = 52.3/20.1 = 2.60$

$\sigma_a/S_y = .84/20.1 = .04$

THE SHEAR FORCE = $V_{104,323,2} = 3.13\ K$, $V_{104,323,3} \sim 0.0K$

THE COORD. (.04, 2.60) IS WITHIN THE ENVELOPE

PER REF. 10-P. 62 THE SHEAR REDUCTION FACTOR IS = C

$$C \sim \left(1 - \left(\frac{V_{104,323,2}}{V_p}\right)^4\right) = \left(1 - \left(\frac{3.13}{20.1 \times .577 \times .5}\right)^4\right) = .92$$

BY INSPECTION OF THE ENVELOPE IT CAN BE SEEN THAT A

4.3.1 CONT'D

REDUCTION OF THE LOAD CARRYING CAPABILITY BY APPROX. 8% IS NEGLIGIBLE WHEN COMPARING TO THE INTERNAL LOAD CONDITION OF THE ELEMENT.

SHIELDING NO. 2 - STUD ANALYSIS

THE COMBINATION OF AXIAL FORCES AND MOMENTS ACROSS THE STUD ELEMENTS WHICH PRODUCES THE HIGHEST RESULTING AXIAL TENSILE FORCE IS CONSIDERED. IN ORDER TO ASSURE THAT NO ROTATION OF THE ELEMENTS WOULD OCCUR DUE TO MOMENT TRANSFER ACROSS THE ELEMENTS, HIGH VALUES OF I_{x_i} WERE USED. THE DEFORMATION OF THE ELEMENTS ARE THE RESULT OF ONLY SHEAR FORCES, WHICH IS THE CASE IN THE ACTUAL ASSEMBLY AT THE STUD CONNECTIONS.

THE HIGHEST RESULTING AXIAL TENSILE FORCE IN THE STUDS (PROPERTY NO.'S 10 & 11) OCCUR IN BEAM NO.'S 111 & 176.
STUD MATERIAL: 304 S.S. - 450°F ⇒ S_y = 30.1 KSI & S_u = 64.0 KSI
BEAMS 111 & 176 AT RIB-URANIUM PLATE CONNECTION.

(PER PAR. 2.0 - PROPERTIES 10 & 11)

THE MOMENTS ACROSS THE ELEMENTS ARE NEGLIGIBLE.

AXIAL TENSILE FORCE = P_i, STUD SIZE: 7/16 IN - 14 UNC

P_{115} = 2.32 K, TENSILE STRESS AREA = .106 IN^2

STRESS THROUGH THE THREADS = $\sigma_{x1} = \frac{2.32}{.106} = 21.89$ KSI

STRESS OUTSIDE THREADS = $\frac{2.32}{.150} = 15.5$ KSI

4.3.1 CONT'D

THE RESULTING SHEAR STRESS $= \tau_{x1,x2}$

$$\tau_{x1,x2} = \frac{\sqrt{V2^2 + V3^2}}{.106} = \frac{\sqrt{.557^2 + .113^2}}{.106}$$

$$\tau_{x1,x2} = 5.36 < .577 \times S_y = .577 \times 20.1 = 11.60 \text{ KSI}$$

THE FOLLOWING STRESS-STRAIN CURVE IS ASSUMED.

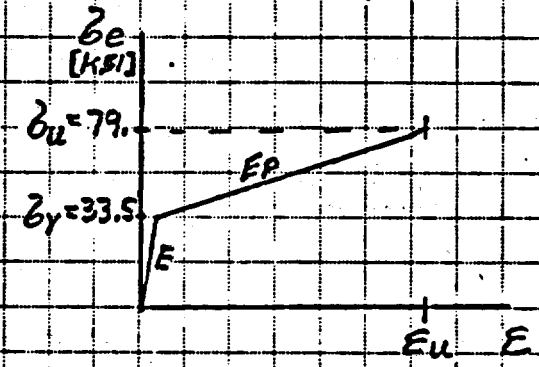

THE COMBINED STRESS IS OBTAINED FROM THE EQUATION FOR THE EFFECTIVE STRESS $= \sigma_e$ (PER REF. 9-P.102)

THE HIGHER STRAIN VALUE IN THE STUDS DUE TO THE CHANGE IN E [LB/IN²] DURING LOAD APPLICATION AS COMPARED TO THE COMPUTED VALUE BASED ON AN ELASTIC BEHAVIOR, IS CONSIDERED TO HAVE NEGLIGIBLE INFLUENCE ON THE LOAD DISTRIBUTION THROUGH THE ASSEMBLY. THE COMPUTATION OF THE TOTAL STRAIN HAS THEREFORE BEEN OMITTED.

FOR AXIAL STRESS & SHEAR σ_e OF REF. 9 REDUCES TO:

$$\sigma_e = \frac{1}{\sqrt{2}} \times \sqrt{2 \times \sigma_{x1}^2 + 6 \times \tau_{x1,x2}^2}$$

4.3.1 CONT'D

$$\sigma_e = \frac{1}{\sqrt{2}} \times \sqrt{2 \times 21.89^2 + 6 \times 5.36^2}$$

$$\sigma_e = 23.80 \text{ KSI} < \sigma_u = 64.0 \text{ KSI}$$

FOR STUD ENGAGEMENT LENGTH SEE PAR. 4.4.1 SHIELDING NO. 1 – STUD ANALYSIS.

AS THE STUDS ARE YIELDING DURING LOAD APPLICATION, AN AVERAGE LOAD DISTRIBUTION WILL OCCUR AMONG THE STUDS.
THE MAXIMUM COMBINATION OF FORCES AMONG THE STUDS OCCUR AT THE LOCATION OF RIB-URANIUM PLATE.
(i, j) BELOW ARE COORD. DIRECTIONS.
THE AVERAGE MOMENT = M_{a_i}
THE AVERAGE AXIAL TENSILE FORCE = P_{a_i}
THE AVERAGE SHEAR FORCE = $S_{a_{i,j}}$

$$M_{a_2} = \frac{34.0}{7} = 4.86 \text{ KIN}$$

$$P_{a_1} = \frac{2.98}{4} = .750 \text{ K}$$

$$S_{a_{2,3}} = \sqrt{\left(\frac{8.69}{7}\right)^2 + .05^2} = 1.24 \text{ K}$$

THE METHOD USED FOR MODELLING OF STUD CONNECTIONS FOR SHIELDING NO. 1 IS IDENTICAL TO THE METHOD DESCRIBED FOR NO. 2.

TENSILE STRESS IN THREADS AT RIB-URANIUM CONNECTION = σ_x.

STUD SIZE: 3/8 IN – 16 UNC ⇒ $A_t = .0775 \text{ IN}^2$, $N_s = 7$

MATERIAL: 17-4 PH S.S. CONDITION "A" ⇒ $S_y = 123.0$ KSI & $S_u = 128.6$ KSI

4.3.1 CONT'D

ASSUME $\sum_{i=1}^{n} A_{t_i} \times X_i = 0$

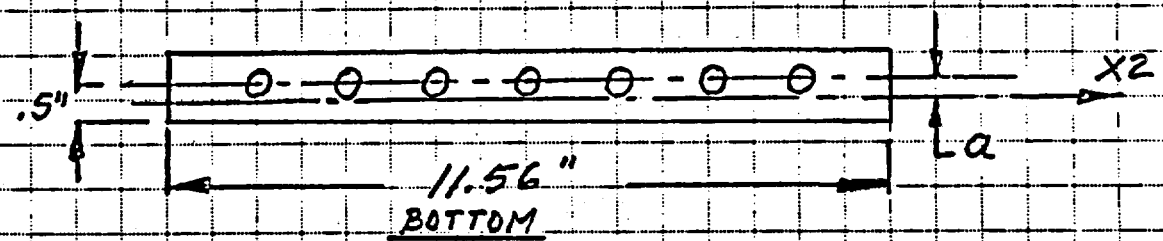

$$N_s \times A_t \times a - 11.56 \times (.5 - a)^2 \times \frac{1}{2} = 0$$

$$a = \frac{(N_s \times A_t + 11.56 \times .5)}{11.56} \pm \sqrt{\left(\frac{N_s \times A_t + 11.56 \times .5}{11.56}\right)^2 - .5^2}$$

$$a = .325 \text{ IN}$$

$$I_{X2} = 7 \times .0775 \times .325^2 + 1/12 \times 11.56 \times (.5 - .325)^3 + 11.56 \times (.5 - .325)^3 \times \frac{1}{4}$$

$$I_{X2} = .078 \text{ IN}^4$$

$$\sigma_{X1} = \frac{P_{a1}}{A_t} + \frac{M_{a2} \times a}{I_{X2}} = \frac{.75}{.0775} + \frac{4.96 \times .325}{.078}$$

$$\sigma_{X1} = 29.92 \text{ KSI}$$

SHEAR STRESS AT THREADS = τ_{X1}

$$\tau_{X1} = \frac{S_{a2,3}}{A_t} = \frac{1.24}{.0775} = 16.0 \text{ KSI} < .577 \times S_y = .577 \times 123.0 = 70.97 \text{ KSI}$$

$$\sigma_e = \frac{1}{\sqrt{2}} \times \sqrt{2 \times 29.92^2 + 6 \times 16.0^2}, \text{ AT RIB-URANIUM PLATE.}$$

$$\sigma_e = 40.78 \text{ KSI} < S_y = 123.0 \text{ KSI}$$

FOR STUD ENGAGEMENT LENGTH SEE PAR. 4.4.1

4.3.1 CONT'D

TENSILE STRESS IN THREADS AT TOPPLATE-URANIUM PLATE CONNECTION = σ_{x1}

$$M_{a_2} = \frac{\Sigma M_2}{N_S} = \frac{15.25}{7} = 2.18 \text{ KIN}$$

$$P_{a_1} = \frac{\Sigma P_1}{4} = \frac{2.06}{4} = .515 \text{ K}$$

$$S_{a_{2,3}} = \sqrt{\left(\frac{2.78}{7}\right)^2 + \left(\frac{8.47}{7}\right)^2} = 1.27 \text{ K}$$

STUD SIZE: 3/8 IN - 16 UNC $\Rightarrow A_t = .0775 \text{ IN}^2$

* MATERIAL: NITRONIC-60 AT 450°F $S_y = 33.5$ KSI & $S_u = 79.0$ KS.

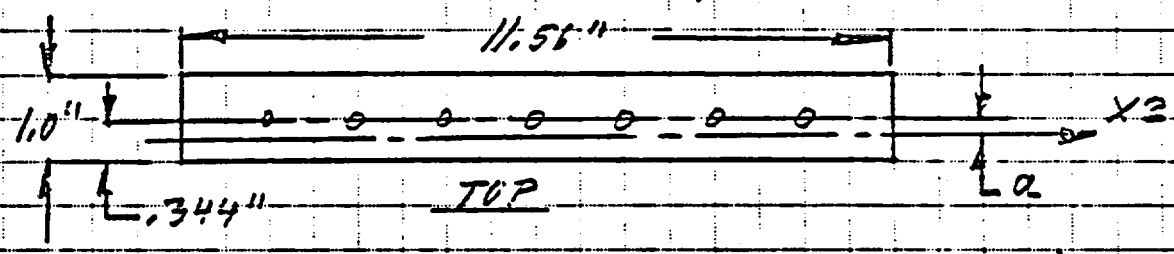

(PER PAR. 4.3.1 - BOTTOM VIEW OF SHIELDING NO. 1)

$$a = \frac{(7 \times .0775 + 11.56 \times .344)}{11.56} \pm \sqrt{\left(\frac{7 \times .0775 + 11.56 \times .344}{11.56}\right)^2 - .344^2}$$

$$a = .205 \text{ IN}$$

$$I_{x2} = 7 \times .0775 \times .205^2 + 1/12 \times 11.56 \times (.344 - .205)^3 + 11.56 \times (.344 - .205)^3 \times \frac{1}{4}$$

$$I_{x2} = .033 \text{ IN}^4$$

$$\sigma_{x1} = \frac{P_{a_1}}{A_t} + \frac{M_{a_2} \times a}{I_{x3}} = \frac{.515}{.0775} + \frac{2.18 \times .205}{.033} = 20.20 \text{ KSI}$$

* SEE PAR. 5.0

4.7.1 CONT'D

SHEAR STRESS AT THREADS = $\bar{S}_{x1}$

$$\bar{S}_{x1} = \frac{S_{22,3}}{A_t} = \frac{1.27}{.0775}$$

$$\bar{S}_{x1} = 16.38 \text{ KSI} < .577 \times 33.5 = 19.3 \text{ KSI}$$

THE EFFECTIVE STRESS AT TOPPLATE-LIDAVIUM PLATE = σ_e

$$\sigma_e = \frac{1}{\sqrt{2}} \times \sqrt{2 \times 20.20^2 + 6 \times 16.38^2}$$

$$\sigma_e = 34.83 \text{ KSI} < S_u = 79.0 \text{ KSI}$$

4.3.1 CONT'D

STRESS IN URANIUM PLATE OF SHIELDING NO'S 1 & 2.

THE MAXIMUM STRESS OCCUR IN BEAM NO'S 462 AND 463 WITH PROPERTY NO. 13

BEAMS 462 & 463

S_{yu} = 46.0 KSI AT 450°F (PER APPENDIX B - TABLE 3)

$\sigma_{462,592}$ = 9.64 KSI < 46.0 KSI

SHEAR STRESSES ARE NEGLIGIBLE.

STRESS IN TOPPLATE - PLATE ELEMENTS.

THE MAXIMUM STRESS IN THE ELEMENTS OF THE TOP-PLATE OCCUR IN ELEMENT NO'S 10 & 30.
FOR THE AREA OF THE TOPPLATE HAVING THE MAXIMUM STRESS SEE TOPPLATE MODEL APPENDIX C.

ELEMENTS 10 & 30

(PER REF. 9-P.102 FOR SX, SY & SXY)

$$\sigma_e = \frac{1}{\sqrt{2}} \times \sqrt{(SX - SY)^2 + SY^2 + SX^2 + 6 \times SXY^2}$$

$$\sigma_{e_{10}} = \frac{1}{\sqrt{2}} \times \sqrt{(7.29 + 54.64)^2 + 54.64^2 + 7.29^2 + 6 \times 4.77^2}$$

$$\sigma_{e_{10}} = 59.20 \text{ KSI}$$

IN ORDER TO COMPARE THIS STRESS WITH THE STRESSES IN THE ADJACENT ELEMENTS, A PLOT OF THE STRESSES (σ_{ei}) VS. ELEMENT NO. i

4.3.1 CONT'D

IS PRODUCED. (PER REF. 3 OF 4.3.1 FOR TPLT.)

$\sigma_{e_1} = \frac{1}{\sqrt{2}} \times \sqrt{(-21.68+7.02)^2 + 21.68^2 + 7.02^2 + 6 \times 9.13^2} = 24.34$ KSI

$\sigma_{e_2} = \frac{1}{\sqrt{2}} \times \sqrt{(6.46+4.36)^2 + 6.46^2 + 4.36^2 + 6 \times 2.15^2} = 10.14$ KSI

$\sigma_{e_3} = \frac{1}{\sqrt{2}} \times \sqrt{(-11.59+3.0)^2 + 11.59^2 + 3.0^2 + 6 \times 6.31^2} = 15.10$ KSI

$\sigma_{e_9} = \frac{1}{\sqrt{2}} \times \sqrt{(-14.39+15.78)^2 + 14.39^2 + 15.78^2 + 6 \times 26.78^2} = 48.79$ KSI

$\sigma_{e_{13}} = \frac{1}{\sqrt{2}} \times \sqrt{(-32.94-6.91)^2 + 32.94^2 + 6.91^2 + 6 \times 2.12^2} = 37.10$ KSI

$\sigma_{e_{21}} = 19.18$ KSI (PER REF. 3 OF PAR. 4.3.1 FOR QUAD-PLT.)

$\sigma_{e_{22}} = 14.82$ KSI

$\sigma_{e_{33}} = 46.01$ KSI

$\sigma_{e_{34}} = 22.58$ KSI

$\sigma_{e_{35}} = 11.30$ KSI

$\sigma_{e_{47}} = 11.19$ KSI

$\sigma_{e_{48}} = 14.16$ KSI

$\sigma_{49} = 12.88$ KSI

$\sigma_{65} = 13.05$ KSI

$\sigma_{e_{66}} = 8.93$ KSI

JOB NO. _____ DATE _____ BY [illegible] CH'K _____

CUSTOMER _____ PROJECT _____

SUBJECT _____

4.3.1 CONT'D

THE STRESSES COMPUTED IN PAR. 4.3.1 WERE BASED ON A G-LOAD OF 159.0 G. PER PAR. 4.2 THE ACTUAL G-LOAD = 214. G. THE STRESSES FOR THE VARIOUS ELEMENTS ARE INCREASED BY THE FACTOR C=214./159.=1.34

ELEMENT NO.	$(\sigma_A+\sigma_B)$ [KSI]	σ_A [KSI]	304 S.S. S_u	304 S.S. S_y	$(\sigma_A+\sigma_B)\times C$ S_y	$\sigma_A\times C$ S_y	$\sigma_A\times C$ [KSI]	$\sigma_B\times C$ [KSI]	NITRONIC-60-S_u	17-4 PH. S_y	TITANIUM S_y
52 & 55	33.79	4.51		20.1	2.25	.3					
62 & 70	41.8	5.3		20.1	2.78	.35					
88 & 154	33.75	.34		20.1	2.25	.02					
104 & 170	52.3	.84		20.1	3.48	.05					
111 & 176		21.9	64.0	20.1			29.3	31.9			
SHIELDING		20.2					27.06	46.67		123.0	
NO. 1 STUDS		29.9					40.0	54.64		123.0	
462 & 463	9.64			1.0	12.9						46.0

PLATE	ELEMENTS OF TOPPLATE	$\sigma_B\times C$	304SS-S_u	216SS-S_y
2		13.6	64.0	89.7
3		20.2		
9		65.4		
10		79.3		
13		49.7		
21		25.7		
22		19.8		
33		61.6		
34		30.2		
35		15.1		
47		15.0		
48		18.9		
49		17.2		
65		17.4		
66		11.9		
1		33.3		

4.3.1 CONT'D

CURVE FOR σ_e VS. ELEMENTS

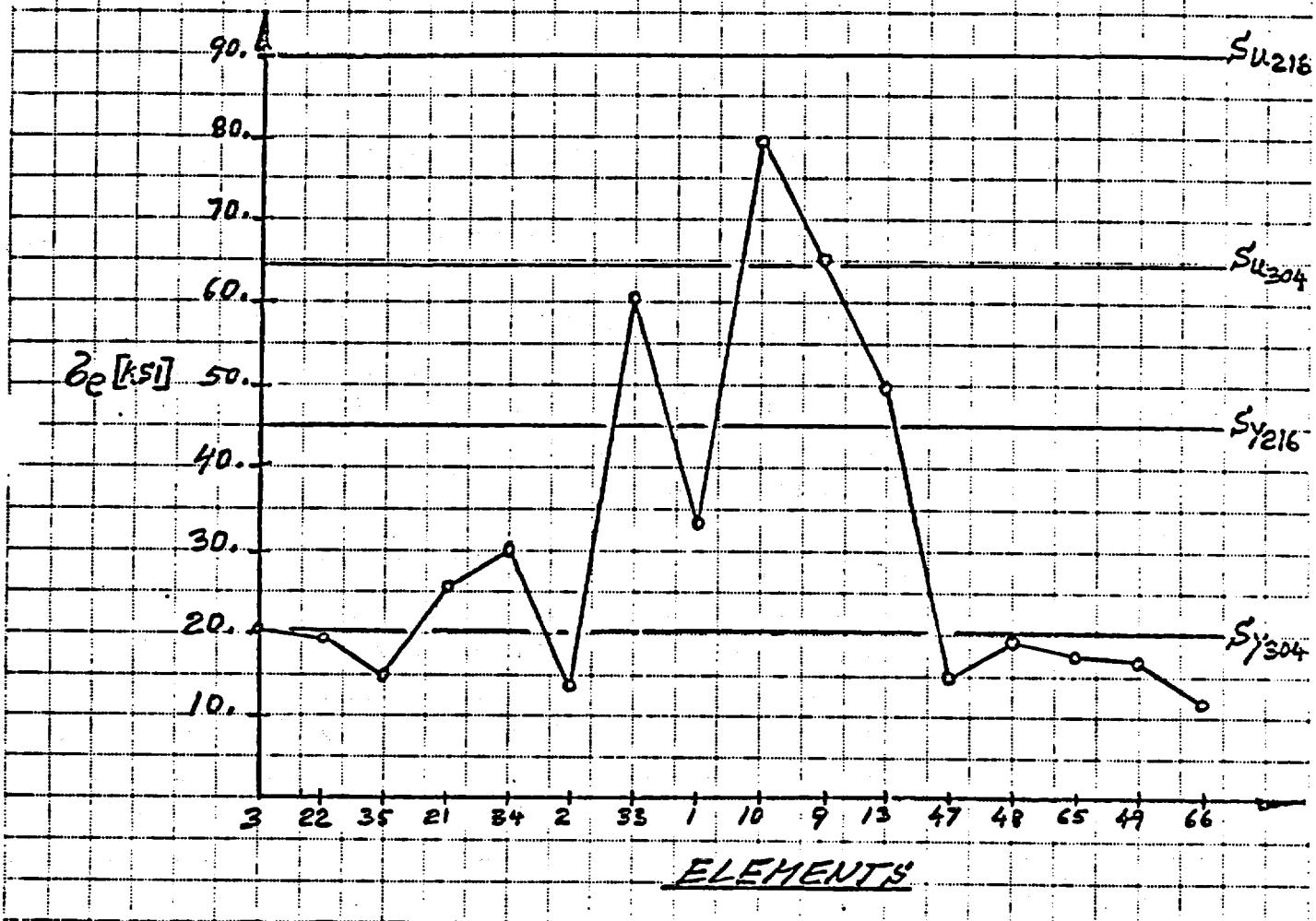

EXAMINING THE PLOT, IT BECOMES OBVIOUS THAT THE ADJACENT ELEMENTS AND THE ELEMENTS BEYOND THE GEOMETRICAL BOUNDARY SHOWN ABOVE ARE CAPABEL OF REDISTRIBUTING AND ABSORBING THE LOAD FROM THE ELEMENTS IN WHICH YIELDING OCCUR. FOR THE AREA OF THE TOPPLATE HAVING THE 216 S.S. MATERIAL SEE APPENDIX C.

4.3.2 DROP ORIENTATION - 90 DEGREES.

THE TOPPLATE SHIELDING ASSEMBLY IS ANALYSED AS DESCRIBED IN PAR. 4.3

THE G-LOAD = G_{qD} = 137.0 (PER PAR. 4.2)

PLOTTING THE DEFLECTIONS OF THE NODES (REF. 3-LOAD CASE # 3) VS. THE UNDEFLECTED CLEARANCE AT THE NODES BETWEEN THE TOPPLATE AND THE INNER SURFACE OF THE SHELL, IT CAN BE SEEN THAT THE COMBINED RESULT OF THE DEFLECTIONS IN THE X1-, X2-DIRECTIONS IS LESS THAN THE CLEARANCE. FOR IMPACT ORIENTATION CONTACT FORCES ALONG THE EDGE OF THE TOPPLATE ARE NOT PRESENT DURING THE ENTIRE TIME OF LOAD APPLICATION.

FOR ELEMENT LOADS & STRESSES SEE REF. 3 - LOAD CASE # 3.

4.3.2 CONT'D

FOR STRESS LIMITS OF THE BEAM ELEMENTS SEE PAR. 4.3.1

MOMENTS, FORCES & STRESSES ARE IDENTIFIED AS PER PAR. 4.3.1.

THE MAXIMUM STRESS FOR BEAMS WITH PROPERTY NO. 1 OCCUR IN BEAM NO.'S 5-6 & 84-85

BEAMS 5-6 & 84-85

(PER PAR 2.0 - PROPERTY NO. 1)

$I_{x20} = .0091 \ IN^4$

$I_{x30} = .028 \ IN^4$

$AREA = .44 \ IN^2$

$$\sigma_{5,22} = \frac{P_5}{.44} + \frac{M_{5,22,2} \times C3}{.0091} + \frac{M_{5,22,3} \times C2}{.028}$$

$$\sigma_{5,22} = \frac{.499}{.44} + \frac{.496 \times .5}{.0091 \times 2} + \frac{1.53 \times .875}{.028 \times 2}$$

$\sigma_{5,22} = 38.67 \ KSI$

$(\sigma_B + \sigma_A) = \sigma_{5,22}$

$\sigma_A = \frac{P_5}{.44} = \frac{.499}{.44} = 1.134 \ KSI$

$(\sigma_B + \sigma_A)/S_y = 38.67/20.1 = 1.92$, $\sigma_A/S_y = 1.134/20.1 = .056$

THE COORD. (.056, 1.92) IS WITHIN THE ENVELOPE

THE EFFECT OF SHEAR IS NEGLIGIBLE.

4.3.2 CONT'D

THE MAXIMUM STRESS FOR BEAMS WITH PROPERTY NO. 25 OCCUR IN BEAM NO.'S

BEAMS 214, 217, 360 & 363

(PER PAR. 2.0 – PROPERTY NO. 25)

$(\sigma_B + \sigma_A) = \sigma_{214,419} = 33.95$ KSI

$\sigma_A = 6.68$ KSI

$(\sigma_A + \sigma_B)/S_y = 33.95/20.1 = 1.69$

$\sigma_A/S_y = 6.68/20.1 = .33$

THE COORD. (.33, 1.69) IS WITHIN THE ENVELOPE

THE EFFECT OF SHEAR IS NEGLIGIBLE

THE MAXIMUM STRESS FOR BEAMS WITH PROPERTY NO. 26 OCCUR IN BEAM NO.'S 218, 221, 364 & 367.

BEAMS 218, 221, 364 & 367

(PER PAR. 2.0 – PROPERTY NO. 26)

$I_{x2} = 1/12 \times 2.0^3 \times .875 = .58 \ IN^4$

$I_{x3} = 1/12 \times .875^3 \times 2.0 = .11 \ IN^4$

$AREA = .875 \times 2.0 = 1.75 \ IN^2$

NOTE: RIB THICKNESS INCREASED TO 1.0 IN. FOR BEAMS 218, 221, 364 & 367 ONLY. THE CHANGE IS CONSIDERED NEGLIGIBLE.

4.3.2 CONT'D

$$\sigma_{218,427} = \frac{P_{218}}{1.12} + \frac{M_{218,427,3} \times C3}{.58} + \frac{M_{218,427,3} \times C2}{.11}$$

$$\sigma_{218,427} = \frac{10.02}{1.75} + \frac{.80 \times 1.12}{.58 \times 2} + \frac{3.62 \times 1.0}{.11 \times 2}$$

$$\sigma_{218,427} = 22.95 \text{ KSI}$$

$$(\sigma_A + \sigma_B) = \sigma_{218,427}$$

$$\sigma_A = \frac{10.02}{1.75} = 5.73 \text{ KSI}$$

$$(\sigma_A + \sigma_B)/S_y = 22.95/20.1 = 1.14$$

$$\sigma_A/S_y = 5.73/20.1 = .29$$

THE COORD. (.29 , 1.14) IS WITHIN THE ENVELOPE.

THE EFFECT OF SHEAR IS NEGLIGIBLE

4.3.2 CONT'D

THE MAXIMUM STRESS FOR BEAMS WITH PROPERTY NO. 9 OCCUR IN BEAM NO.'S 406, 407, 420, 421.

BEAMS 406, 407, 420 & 421

(PER PAR. 2.0 - PROPERTY NO. 9)

$I_{X20} = .042\ IN.^4$

$I_{X30} = .01\ IN.^4$

$AREA = .5\ IN.^2$

$$\sigma_{406,580} = \frac{P_{406}}{.5} + \frac{M_{406,580.2} \times C3}{.042} + \frac{M_{406,580.3} \times C2}{.01}$$

$$\sigma_{406,580} = \frac{1.99}{.5} + \frac{3.45 \times 1.0}{.042 \times 2} + \frac{.451 \times .50}{.01 \quad 2}$$

$\sigma_{406,580} = 56.3\ KSI$

$(\sigma_A + \sigma_B) = \sigma_{406,580}$

$\sigma_A = \frac{1.99}{.5} = 3.98\ KSI$

$(\sigma_A + \sigma_B)/S_y = 56.3/20.1 = 2.8$

$\sigma_A/S_y = 3.98/20.1 = .20$

THE COORD. (.20, 2.8) IS WITHIN THE ENVELOPE

THE EFFECT OF SHEAR IS NEGLIGIBLE

4.3.2 CONT'D

SHIELDING NO. 2 - STUD ANALYSIS

SEE PAR. 4.3.1 - SHIELDING NO. 1 & 2 STUD ANALYSIS DESCRIBTION FOR METHOD & STRESS LIMITS USED.

THE AVERAGE MOMENT = Ma_i
THE AVERAGE AXIAL TENSILE FORCE = Pa_i
THE AVERAGE SHEAR FORCE = $Sa_{i,j}$

$Ma_2 = \frac{\Sigma M2}{N_S} = \frac{4.26}{7} = .610$ KIN. NO. STUDS = $N_S = 7$

$Pa_1 = \frac{7.21}{7} = 1.03$ K

$Sa_{2,3} = \frac{V3}{7} = \frac{4.63}{7} = .661$ K, WHERE V2 ~ 0.0 K

TENSILE STRESS IN THREADS AT RIB-URANIUM PLATE = σ_{x1}

STUD SIZE: 7/16 IN. - 14 UNC ⇒ $A_t = .106$ IN^2

$N_S = 7$, MATERIAL: 304 S.S.

AT 450°F, $S_y = 20.10$ KSI & $S_u = 64.0$ KSI

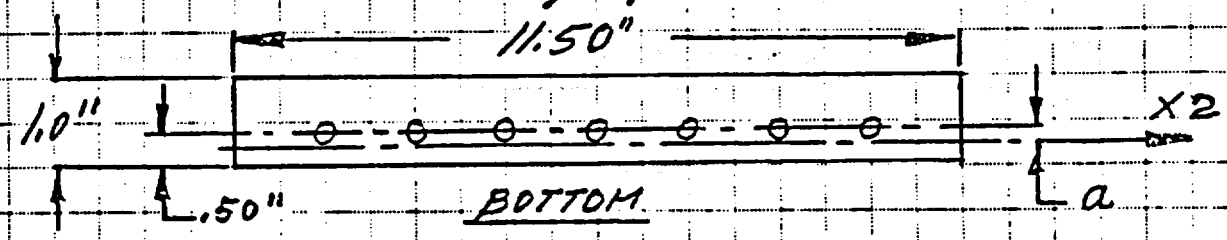

ASSUME $\sum_{i=1}^{n} A_{t_i} \times X_i = 0$

$N_S \times A_t \times a - 11.5 \times (.50 - a)^2 \times \frac{1}{2} = 0$

$a = \frac{(N_S \times A_t + 11.5 \times .50)}{11.5} \pm \sqrt{\left(\frac{N_S \times A_t + 11.5 \times .50}{11.5}\right)^2 - .50^2}$

4.3.2 CONT'D

$$a = \left(\frac{7\times.106+11.5\times.50}{11.5}\right) \pm \sqrt{\left(\frac{7\times.106+11.5\times.50}{11.5}\right)^2 - .5^2}$$

$$a = .302 IN$$

$$I_{x2} = 7\times.106\times.302^2 + 1/12\times11.5\times(.50-.302)^3 + 11.5\times(.50-.302)^3\times\frac{1}{4}$$

$$I_{x2} = .097 IN^4$$

$$\sigma_{x1} = \frac{P_{a1}}{A_t} + \frac{M_{x2}\times a}{I_{x2}} = \frac{1.03}{.106} + \frac{.610\times.302}{.097}$$

$$\sigma_{x1} = 11.62 KSI$$

SHEAR STRESS AT THREADS = τ_{x1}

$$\tau_{x1} = \frac{S_{a2,3}}{A_t} = \frac{.661}{.106} = 6.24 KSI < .577\times20.1 = 11.6 KSI$$

THE EFFECTIVE STRESS = σ_e IN THREADS AT RIB-URANIUM PL.

$$\sigma_e = \frac{1}{\sqrt{2}}\times\sqrt{2\times11.62^2+6\times6.24^2}$$

$$\sigma_e = 15.37 KSI < S_y = 20.1 KSI$$

4.3.2 CONT'D

TENSILE STRESS IN THREADS AT TOPPLATE-URANIUM PLATE CONNECTION = σ_{x1}

$M_{a2} = \frac{EM2}{N_S} = \frac{10.30}{7} = 1.5$ KIN, NO. STUDS $= N_S = 7$

$P_{a1} = \frac{7.2}{7} = 1.03$ K

$S_{a2,3} = \sqrt{\left(\frac{1.5}{7}\right)^2 + \left(\frac{9.4}{7}\right)^2} = 1.40$ K

STUD SIZE: 3/8 IN. - 16 UNC ⇒ $A_t = .0775$ IN^2

MATERIAL: NITRONIC-60 - AT 450°F $S_y = 33.5$ KSI & $S_u = 79.0$ KSI

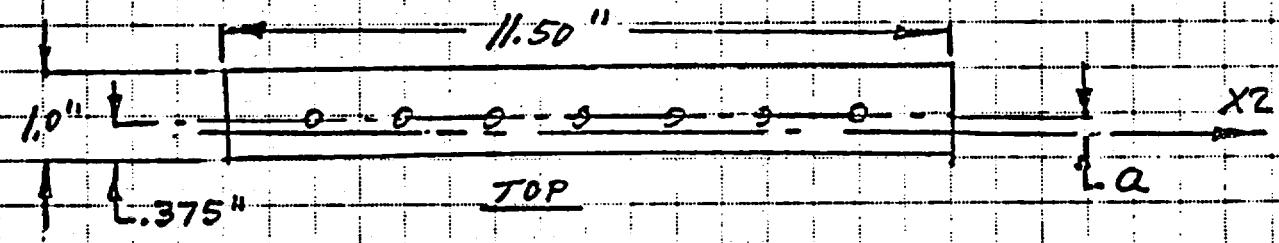

$$a = \frac{(7 \times .0775 + 11.5 \times .375)}{11.5} \pm \sqrt{\left(\frac{7 \times .0775 + 11.5 \times .375}{11.5}\right)^2 - .375^2}$$

$a = .228$ IN.

$$I_{x2} = 7 \times .0775 \times .228^2 + 1/12 \times 11.5 \times (.375 - .228)^3 + 11.5 \times (.375 - .228)^3 \times \frac{1}{4}$$

$I_{x2} = .040$ IN^4

$$\sigma_{x1} = \frac{P_{a1}}{A_t} + \frac{M_{a2} \times a}{I_{x2}} = \frac{1.03}{.0775} + \frac{1.5 \times .228}{.040} = 21.84 \text{ KSI}$$

SHEAR STRESS IN THREAD = τ_{x1}

$$\tau_{x1} = \frac{S_{a2,3}}{A_t} = \frac{1.40}{.0775} = 18.06 \text{ KSI}$$

4.3.2 CONT'D

THE EFFECTIVE STRESS = σ_e IN THREADS AT TOPPLATE-UPWIND.

$$\sigma_e = \frac{1}{\sqrt{2}} \times \sqrt{2 \times 21.87^2 + 6 \times 18.06^2}$$

$$\sigma_e = 38.15 \text{ KSI} < S_u = 79.0 \text{ KSI}$$

4.3.2 CONT'D

SHIELDING NO. 1 - STUD ANALYSIS

SEE PAR. 4.3.1 - SHIELDING NO. 1 & 2 STUD ANALYSIS DESCRIBTION FOR METHOD & STRESS LIMITS USED.
THE MAXIMUM FORCES OCCUR AT THE RIB-URANIUM CONNECTION.
THE AVERAGE MOMENT = M_{a_i}
THE AVERAGE AXIAL TENSILE FORCE = P_{a_i}
THE AVERAGE SHEAR FORCE = $S_{a_{i,j}}$

$$M_{a_2} = \frac{\Sigma M_2}{N_s} = \frac{30.80}{7} = 4.40 \text{ KIN.}, \quad \text{NO. STUDS} = N_s = 7$$

$$P_{a_1} = \frac{\Sigma P_1}{4} = \frac{20.36}{4} = 5.09 \text{ K.}$$

$$S_{a_{2,3}} = \sqrt{\left(\frac{15.44}{7}\right)^2 + \left(\frac{6.22}{7}\right)^2} = 2.38 \text{ K.}$$

TENSILE STRESS IN THREADS AT RIB - URANIUM = σ_{x1}

STUD SIZE: 3/8 IN.-16 UNC $\Rightarrow A_t = .0775 \text{ IN}^2$

MATERIAL: 17-4 PH SS - CONDITION "A" $\Rightarrow S_y = 123.0$ KSI & $S_u = 128.6$ KSI

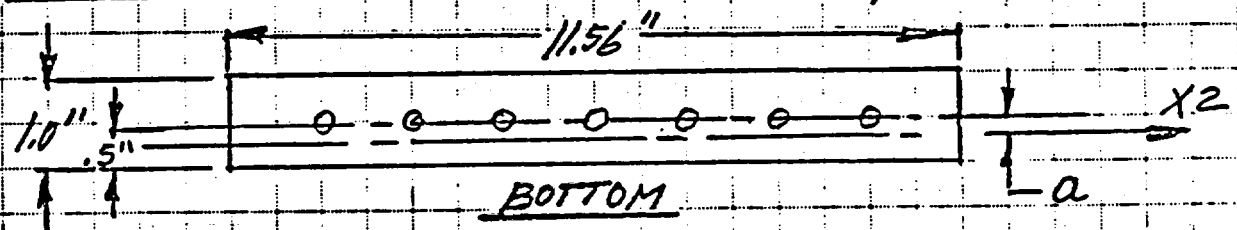

(PER 4.3.1 - SHIELDING NO. 1 STUD ANALYSIS)

$a = .325$ IN

$I_{x2} = .078 \text{ IN}^4$

4.3.2 CONT'D

$$\sigma_{x1} = \frac{P_{a1}}{A_t} + \frac{M_{a2} \times a}{I_{x2}} = \frac{5.09}{.0775} + \frac{4.4 \times .225}{.078} = 84.01 \text{ KSI}$$

SHEAR STRESS AT THREADS = τ_{x1}

$$\tau_{x1} = \frac{S_{a2,3}}{A_t} = \frac{2.38}{.0775} = 30.71 \text{ KSI} < .577 \times 123.0 = 70.97 \text{ (KSI)}$$

THE EFFECTIVE STRESS AT RIB-URANIUM PLATE = σ_e

$$\sigma_e = \frac{1}{\sqrt{2}} \times \sqrt{2 \times 84.01^2 + 6 \times 30.71^2}$$

$$\sigma_e = 99.4 \text{ KSI} < S_u = 128.6 \text{ KSI}$$

TENSILE STRESS IN THREADS AT TOPPLATE-URANIUM PLATE CONNECTION = σ_{x1}

$$M_{a2} = \frac{\Sigma M_2}{n_s} = \frac{7.24}{7} = 1.03 \text{ KIN}$$

$$P_{a1} = \frac{\Sigma P_1}{3} = \frac{10.66}{3} = 3.55 \text{ K}$$

$$S_{a2,3} = \sqrt{\left(\frac{3.54}{7}\right)^2 + \left(\frac{.589}{7}\right)^2} = .513 \text{ K}$$

STUD SIZE: 3/8 IN.-16 UNC $\Rightarrow A_t = .0775 \text{ IN}^2$

* MATERIAL: NITRONIC-60 AT 450°F $S_y = 33.5$ KSI & $S_u = 79.0$ KSI

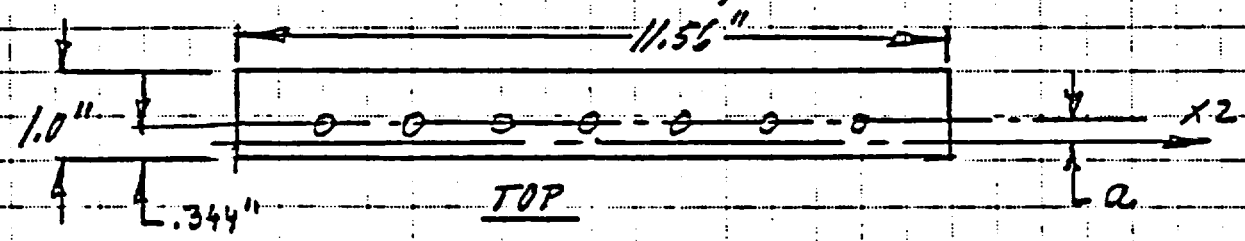

(PER PAR. 4.3.1 - SHIELDING NO. 1 STUD ANALYSIS)

$a = .205$ IN. $\therefore I_{x2} = .033 \text{ IN}^4$ * SEE PAR. 5.0

4.3.2 CONT'D

$$\sigma_{x1} = \frac{P_{a1}}{A_t} + \frac{M_{az} \times D}{I_{xz}} = \frac{3.55}{.0775} + \frac{403 \times 1.05}{.033} = 52.20 \text{ KSI}$$

SHEAR STRESS IN THREADS = τ_{x1}

$$\tau_{x1} = \frac{S_{xz,3}}{A_t} = \frac{.513}{.0775}$$

$$\tau_{x1} = 6.62 \text{ KSI} < .577 \times 33.5 = 19.3 \text{ KSI}$$

THE EFFECTIVE STRESS AT TOPPLATE URANIUM PLATE CONNECTION = σ_e

$$\sigma_e = \frac{1}{\sqrt{2}} \times \sqrt{2 \times 52.2^2 + 6 \times 6.62^2}$$

$$\sigma_e = 53.44 \text{ KSI} < S_u = 79.0 \text{ KSI}$$

STRESS IN TOPPLATE - PLATE ELEMENTS

THE MAXIMUM STRESS IN THE ELEMENTS OF THE TOPPLATE OCCUR IN ELEMENT NO.'S 10, 12, 30 & 32.
FOR THE AREA OF THE TOPPLATE HAVING THE MAXIMUM STRESS SEE TOPPLATE MODEL APPENDIX C.

ELEMENTS 10, 12, 30 & 32

(PER REF. 9 - P. 102 FOR SX, SY, SXY)

$$\sigma_e = \frac{1}{\sqrt{2}} \times \sqrt{(S_x - S_y)^2 + S_y^2 + S_x^2 + 6 \times S_{xy}^2}$$

$$\sigma_e = \frac{1}{\sqrt{2}} \times \sqrt{(-1.56 + 22.15)^2 + 22.15^2 + 1.56^2 + 6 \times 6.83^2} = 24.46 \text{ KSI}$$

4.3.2 CONT'D

THE ELEMENTS ARE LOCATED IN THE AREA OF THE TOPPLATE WHERE THE MATERIAL IS 216 S.S. SEE TOPPLATE MODEL APPENDIX C FOR EXTENSION OF AREA FOR 216 S.S.

MATERIAL: 216 S.S. AT 450 F°

$S_y = 44.9$ KSI & $S_u = 89.9$ KSI

MATERIAL: 304 S.S AT 450 F°

$S_y = 20.1$ KSI & $S_u = 64.0$ KSI

MAXIMUM STRESS IN TOPPLATE HAVING MATERIAL 216SS.

$\sigma_e = 24.5$ KSI $< S_y = 44.9$ KSI

MAXIMUM STRESS IN TOPPLATE HAVING MATERIAL 304SS.

ALL STRESSES [σ_e] ARE $< S_y = 20.1$ KSI

4.3.3 INTRODUCTION TO 45-DEGREES DROP ORIENTATION.

THE GAP BETWEEN THE CIRCLE SEGMENT AND THE INNER SURFACE OF THE ADJACENT SHELL DOES CLOSE DURING THE TIME OF LOAD APPLICATION. THE MOST SEVERE CONDITION IS CONSIDERED TO BE WHEN CONTACT FORCES ARE ACTING ALONG THE EDGE DURING THE ENTIRE TIME OF LOAD APPLICATION RATHER THAN THE RESIDUAL LOAD ACTING AT TIME OF CONTACT AND A FUNCTION OF ΣP VS. TIME DURING THE REMAINING TIME OF DECELERATION OF THE CASK.

DROP ORIENTATION - 45 DEGREES.
(PER REF. 3 - LOAD CASE # 5)
CONTACT AREA & FORCE DIAGRAM.

(PER PAR. 4.3.1)

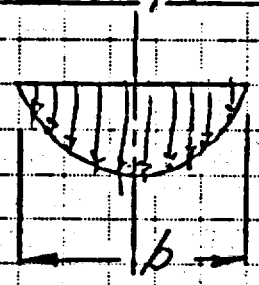

THE G-LOAD = G_{45} = 184.0
PER PAR. 4.2

$$b = 2.15 \times \sqrt{\frac{\pi}{E} \times \frac{D_1 \times D_2}{D_1 - D_2}}, \quad E \cong 26.0 \times 10^6 \ LB/IN^2 \text{ AT } 450°F.$$

INNER DIA. OF SHELL = D_1 = 37.46 IN

SEGMENT DIA. = D_2 = 37.31 IN

CONTACT PRESSURE PER IN. = $p_{x2} = \frac{\Sigma P_{x2}}{t_{PL}}$ [LB/IN]

t_{PL} = .5 IN.

4.3.3 CONT'D

TOTAL CONTACT FORCE FOR THE NODES BELOW $= \Sigma P_{X2}$

$p_{X2} = \frac{48 \times 10^3}{.5} = 96 \times 10^3$ LB/IN, (ΣP_{X2} PER REF. 3 - CASE #5 EQUILIBRIUM CHECK.)

$b = 2.15 \times \sqrt{\frac{96.0 \times 10^3}{26.0 \times 10^6} \times \frac{37.46 \times 37.31}{(37.46 - 37.31)}}$

$b = 12.6$ IN. FOR A SOLID DISC.

ASSUMED CONTACT LENGTH $= b_2$

LENGTH OF CHORD BETWEEN NODE NO. 129 & 256 = 16.4 IN

$b_2 = 16.4$ IN

BY INTERPOLATION THE COMBINED RESULT OF THE DEFLECTIONS IS OBTAINED IN THE X1-X2-DIRECTIONS, BETWEEN NODE # 129 AND THE ADJACENT NODE # 128 AND BETWEEN NODE # 256 AND THE ADJACENT NODE # 257 (REF. TOPPLATE MODEL APPENDIX C AND REF. 3 - LOAD CASE # 5 - NODE DEFLECTIONS).
CONTACT OCCUR BETWEEN NODE 129 & 128 AND BETWEEN NODE 256 & 257.

LENGTH OF CHORD BETWEEN NODE NO. 128 AND 257 = 18.1 IN.

RESULTING IN: $12.6 \text{ IN} < b_2 < 18.1 \text{ IN.} \Rightarrow b_2$ CONSERVATIVE

NODES 129-133, 116, 182, 207, 223, 224, 237, 238, 254-256 ARE FIXED WIT. RESPECT TO TRANSLATION IN THEIR INDIVIDUAL X2-COORD. DIRECTIONS WHERE THE X1-AXIS IS TANGENT TO THE CIRCLE AT THE NODE.
THE TOPPLATE ASSEMBLY IS ANALYSED AS DESCRIBED IN PAR. 4.3 AND STRESS LIMITS PER PAR 4.3.1.

4.3.3 CONT'D

THE MAXIMUM STRESS FOR BEAMS WITH PROPERTY NO. 15 OCCUR IN BEAM NO. 48

BEAM 48

(PER PAR. 2.0 - PROPERTY NO. 15)

$I_{X20} = .009\ IN^4$

$I_{X30} = .028\ IN^4$

$AREA_0 = .438\ IN^2$

$$\sigma_{48,284} = \frac{P_{48}}{.438} + \frac{M_{48,284,2} \times C3}{.009} + \frac{M_{48,284,3} \times C2}{.028}$$

$$\sigma_{48,284} = \frac{.5}{.438} + \frac{.190 \times .5}{.009 \times 2} + \frac{2.15 \times .875}{.028 \times 2}$$

$\sigma_{48,284} = 40.01\ KSI$

$(\sigma_A + \sigma_B) = \sigma_{48,284}$

$\sigma_A = \sigma_{48} = \frac{P_{48}}{.438} = \frac{.5}{.438} = 1.14\ KSI$

$(\sigma_A + \sigma_B)/\sigma_y = 40.01/20.1 = 1.99$

$\sigma_A/\sigma_y = 1.14/20.1 = .06$

THE COORD. (.06, 1.99) IS WITHIN THE ENVELOPE.

THE EFFECT OF SHEAR IS NEGLIGIBLE

4.3.3 CONT'D

THE MAXIMUM STRESS FOR BEAMS WITH PROPERTY NO. 14 OCCUR IN BEAM NO. 76.

BEAM 76

(PER PAR. 2.0 - PROPERTY NO. 14)

$I_{x20} = .014\ IN^4$

$I_{x30} = .090\ IN^4$

$AREA_0 = .65\ IN^4$

$$\sigma_{76,281} = \frac{P_{76}}{.65} + \frac{M_{76,281,2} \times C3}{.014} + \frac{M_{76,281,3} \times C2}{.09}$$

$$\sigma_{76,281} = \frac{1.42}{.65} + \frac{.092 \times .5}{.014 \times 2} + \frac{3.09 \times 1.29}{.09 \times 2} = 25.97\ KSI$$

$$(\sigma_A + \sigma_B) = \sigma_{76,281}$$

$$\sigma_A = \sigma_{76} = \frac{P_{76}}{.65} = \frac{1.42}{.65} = 2.18\ KSI$$

$$(\sigma_A + \sigma_B)/S_y = 25.97/20.1 = 1.30$$

$$\sigma_A/S_y = 2.18/20.1 = .11$$

THE COORD. (.11, 1.3) IS WITHIN THE ENVELOPE.

THE EFFECT OF SHEAR IS NEGLIGIBLE.

4.3.3 CONT'D

THE MAXIMUM STRESS FOR BEAMS WITH PROPERTY NO. 4 OCCUR IN BEAM NO. 89.

BEAM 89

(PER PAR. 2D - PROPERTY NO. 4)

NOTE: RIB THICKNESS IS INCREASED TO 7/8 IN THE CHANGE IS CONSIDERED NEGLIGIBLE.

$I_{x2} = 1/12 \times 1.5^3 \times .875 = .25\ IN^4$

$I_{x3} = 1/12 \times 1.5 \times .875^3 = .084\ IN^4$

$AREA = 1.5 \times .875 = 1.31\ IN^2$

$$\sigma_{89,313} = \frac{P_{89}}{1.31} + \frac{M_{89,313,2} \times C3}{.25} + \frac{M_{89,313,3} \times C2}{.084}$$

$$\sigma_{89,313} = \frac{3.45}{1.31} + \frac{7.83 \times 1.5}{.25 \times 2} + \frac{4.95 \times .875}{.084 \times 2} = 51.80\ KSI$$

$(\sigma_A + \sigma_B)/S_y = 51.80/20.1 = 2.58$

$$\sigma_A = \sigma_{89} = \frac{P_{89}}{1.31} = \frac{3.45}{1.31} = 2.63\ KSI$$

$\sigma_A/S_y = 2.63/20.1 = .13$

THE COORD. (.13, 2.58) IS WITHIN THE ENVELOPE.

THE EFFECT OF SHEAR IS NEGLIGIBLE.

4.3.3 CONT'D

THE MAXIMUM STRESS FOR BEAMS WITH PROPERTY NO. 7 OCCUR IN BEAM NO. 91.

BEAM 91

(PER PAR 2.0 – PROPERTY NO. 7)

$\sigma_{91,312} = 61.33$ KSI

$(\sigma_A + \sigma_B) = \sigma_{91,312}$

$(\sigma_A + \sigma_B)/S_y = 61.33/20.1 = 3.05$

$\sigma_{91} = 1.33$ KSI

$\sigma_A/S_y = 1.33/20.1 = .07$

THE COORD. (.07, 3.05) IS WITHIN THE ENVELOPE.

THE EFFECT OF SHEAR IS NEGLIGIBLE.

4.3.3 CONT'D

THE MAXIMUM STRESS FOR BEAMS WITH PROPERTY NO. 5 OCCUR IN BEAM NO. 93

BEAM 93 (PER PAR. 2.0-PROPERTY NO. 5)

$I_{x2} = 1/12 \times 1.125^3 \times .875 = .10 \ IN^4$

$I_{x3} = 1/12 \times .875^3 \times 1.125 = .06 \ IN^4$

NOTE! RIB THICKNESS PER BEAM NO. 89 ANALYSIS INCREASED TO 7/8 IN.

$AREA = .875 \times 1.125 = .98 \ IN^2$

$$\sigma_{93,318} = \frac{P_{93}}{.98} + \frac{M_{93,318,2} \times C3}{.10} + \frac{M_{93,318,3} \times C2}{.06}$$

$$\sigma_{93,318} = \frac{3.44}{.98} + \frac{1.13 \times 1.125}{.10 \times 2} + \frac{3.54 \times .75}{.06 \times 2} = 32.0 \ KSI$$

$(\sigma_A + \sigma_B) = \sigma_{93,318}$

$(\sigma_A + \sigma_B)/S_y = 32.0/20.1 = 1.59$

$$\sigma_{93} = \frac{P_{93}}{.98} = \frac{3.44}{.98} = 3.51 \ KSI$$

$\sigma_A = \sigma_{93}$

$\sigma_A/S_y = 3.51/20.1 = .17$

THE COORD. (.17, 1.59) IS WITHIN THE ENVELOPE.

THE EFFECT OF SHEAR FORCES IS NEGLIGIBLE.

4.3.3 CONT'D

THE MAXIMUM STRESS FOR BEAMS WITH PROPERTY NO. 9 OCCUR IN BEAM NO. 102

BEAM 102

(PER PAR. 2.0 - PROPERTY NO. 9)

$I_{x20} = .042\ IN^4$

$I_{x30} = .010\ IN^4$

$AREA = .5\ IN^2$

$$\sigma_{102,321} = \frac{P_{102}}{.5} + \frac{M_{102,321,2} \times C_3}{.042} + \frac{M_{102,321,3} \times C_2}{.010}$$

$$\sigma_{102,321} = \frac{.052}{.5} + \frac{.270 \times 1.0}{.042 \times 2} + \frac{2.37 \times .5}{.010 \times 2} = 62.6\ KSI$$

$$(\sigma_A + \sigma_B) = \sigma_{102,321}$$

$$(\sigma_A + \sigma_B)/S_y = 62.6/20.1 = 3.11$$

$$\sigma_A = \sigma_{102} = \frac{P_{102}}{.5} = \frac{.052}{.5} = .104\ KSI \text{ (NEGLIGIBLE)}$$

$$\sigma_A/S_y = .104/20.1 = .005$$

THE COORD. (.005, 3.11) IS WITHIN THE ENVELOPE.

THE RESULTING SHEAR FORCE = F_R

PER REF. 10 THE SHEAR REDUCTION FACTOR = $\left(1 - \left(\frac{F_R}{V_P}\right)^4\right)$

FOR $\sigma_A/S_y \sim 0.0 \Rightarrow (\sigma_B/S_y)/\left(1 - \left(\frac{F_R}{V_P}\right)^4\right) \leq 3.6$ (PER PAR. 4.3.1)

4.3.3 CONT'D

$F_R = \sqrt{V2^2 + V3^2} = \sqrt{3.35^2 + .390^2}$, TORSION $= M_T \sim 0.0$

$F_R = 3.37$ K, $\sigma_B = 62.46$ KSI

$(\sigma_B / S_Y) / (1 - (F_R / V_P)^4) = (62.46 / 20.1) / (1 - (3.37 / 20.1 \times .577 \times .5)^4) = 3.5$

THE COORD. (0.0, 3.5) IS WITHIN THE ENVELOPE

SHIELDING NO. 2 - STUD ANALYSIS

SEE PAR. 4.3.1 - SHIELDING NO. 1 & 2 STUD ANALYSIS DESCRIBTION FOR METHOD & STRESS LIMITS USED.

THE AVERAGE MOMENT $= M_{a_i}$
THE AVERAGE AXIAL TENSILE FORCE $= P_{a_i}$
THE AVERAGE SHEAR FORCE $= S_{a_{i,j}}$

$M_{a_2} = \frac{\Sigma M_e}{N_S} = \frac{8.90}{7} = 1.27$ KIN., NO. STUDS $= N_S = 7$

$P_{a_1} = \frac{\Sigma P}{5} = \frac{5.44}{5} = 1.10$ K

$S_{a,2,3} = \sqrt{\left(\frac{2.73}{7}\right)^2 + \left(\frac{7.16}{7}\right)^2} = 1.10$ K

TENSILE STRESS IN THE THREADS AT TOPPLATE - URANIUM PL. $= \sigma_{xt}$

STUD SIZE: 3/8 IN - 16 UNC $\Rightarrow A_t = .0775$ IN^2

MATERIAL: NITRONIC - 60 AT 450°F $S_y = 33.5$ KSI & $S_u = 79.0$ KSI

4.3.3 CONT'D

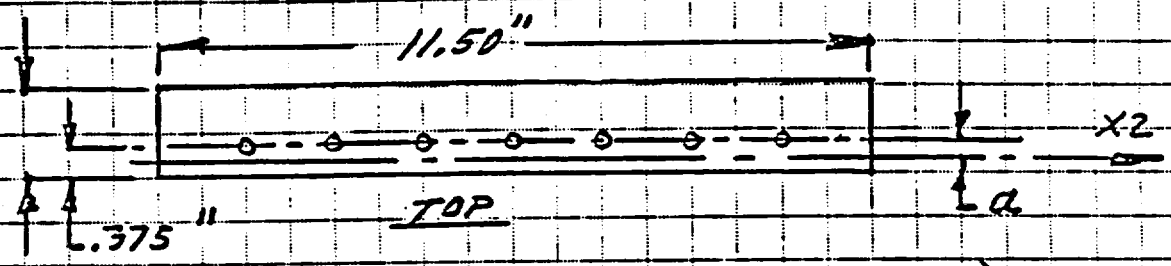

(PER PAR. 4.3.2 - SHIELDING NO. 2 STUD ANALYSIS.)

$a = .228$ IN.

$I_{X2} = .040$ IN^4

$$\sigma_{X1} = \frac{P_{a1}}{A_t} + \frac{M_{a2} \times a}{I_{X2}} = \frac{1.10}{.0775} + \frac{1.27 \times .228}{.040}$$

$\sigma_{X1} = 21.43$ KSI

SHEAR STRESS AT THREADS $= \tau_{X1}$

$$\tau_{X1} = \frac{S_{a2,3}}{A_t} = \frac{1.10}{.0775}$$

$\tau_{X1} = 14.20$ KSI $< .577 \times 33.5 = 19.3$ KSI

THE EFFECTIVE STRESS AT TOPPLATE-URANIUM $= \sigma_e$

$$\sigma_e = \frac{1}{\sqrt{2}} \times \sqrt{2 \times 21.43^2 + 6 \times 14.20^2}$$

$\sigma_e = 32.62$ KSI $< S_u = 79.0$ KSI (SEE PAR. 4.3.1)

4.3.3 CONT'D

TENSILE STRESS IN THE THREADS AT THE RIB-URANIUM PLATE CONNECTION = σ_{x1}

$$M_{a2} = \frac{\Sigma M_2}{N_s} = \frac{4.34}{7} = .620 \text{ KIN} \quad \text{NO. STUDS} = N_s = 7$$

$$P_{a1} = \frac{\Sigma P_1}{5} = \frac{5.5}{5} = 1.10 \text{ K}$$

$$S_{a2,3} = \sqrt{\left(\frac{4.95}{7}\right)^2 + \left(\frac{4.15}{7}\right)^2} = .923 \text{ K}$$

STUD SIZE: 7/16 IN - 14 UNC. $\Rightarrow A_t = .106 \text{ IN}^2$

MATERIAL: 304 S.S. - AT 450°F $S_y = 20.1$ KSI & $S_u = 64.0$ KSI

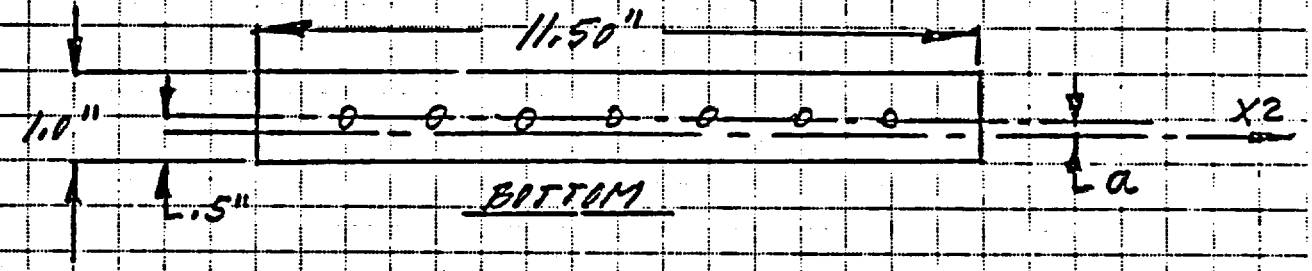

(PER PAR. 4.3.2 - SHIELDING NO. 2 STUD ANALYSIS.)

$a = .302$ IN

$I_{x2} = .047 \text{ IN}^4$

$$\sigma_{x1} = \frac{P_{a1}}{A_t} + \frac{M_{a2} \times a}{I_{x2}} = \frac{1.10}{.106} + \frac{.620 \times .302}{.047} = 12.31 \text{ KSI}$$

SHEAR STRESS IN THREADS = τ_{x1}

$$\tau_{x1} = \frac{S_{a2,3}}{A_t} = \frac{.923}{.106}$$

$\tau_{x1} = 8.71$ KSI $< .577 \times 20.1 = 11.60$ KSI

4.3.3 CONT'D

THE EFFECTIVE STRESS AT RIB-URANIUM PLATE = σ_e

$$\sigma_e = \frac{1}{\sqrt{2}} \times \sqrt{2 \times 12.31^2 + 6 \times 8.71^2}$$

$$\sigma_e = 19.5 \text{ KSI} < S_y = 20.1 \text{ KSI}$$

4.3.3 CONT'D

SHIELDING NO. 1 – STUD ANALYSIS

SEE PAR. 4.3.1 – SHIELDING NO. 1 & 2 STUD ANALYSIS DESCRIPTION FOR METHOD & STRESS LIMITS USED.

THE AVERAGE MOMENT = M_{a_i}
THE AVERAGE AXIAL TENSILE FORCE = P_{a_i}
THE AVERAGE SHEAR FORCE = $S_{a_{i,j}}$

$$M_{a_2} = \frac{\Sigma M_2}{N_s} = \frac{49.4}{7} = 7.06 \text{ KIN}, \quad \text{NO. STUDS} = N_s = 7$$

$$P_{a_1} = \frac{\Sigma P_1}{3} = \frac{9.12}{3} = 3.04 \text{ K}$$

$$S_{a_{2,3}} = \sqrt{\left(\frac{6.52}{7}\right)^2 + \left(\frac{11.2}{7}\right)^2} = 1.73 \text{ K}$$

TENSILE STRESS IN THREADS AT RIB-URANIUM PLATE = b_{x_1}

STUD SIZE: 3/8 IN – 16 UNC ⇒ $A_t = .0775 \text{ IN}^2$

MATERIAL: 17-4 PH. SS-"A" AT 450°F $S_y = 123.0$ KSI & $S_u = 120.6$ KSI

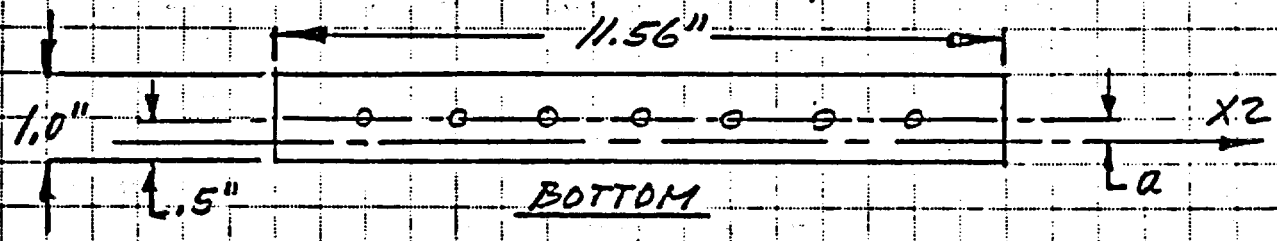

(PER PAR. 4.3.1 – SHIELDING NO. 1 STUD ANALYSIS.)

$a = .325$ IN.

$I_{x2} = .078 \text{ IN}^4$

4.3.3 CONT'D

$$\sigma_{x1} = \frac{Pa_1}{A_t} + \frac{Ma_2 \times a}{I_{x2}} = \frac{3.04}{.0775} + \frac{7.04 \times .325}{.078}$$

$$\sigma_{x1} = 68.64 \text{ KSI}$$

SHEAR STRESS AT THREADS = τ_{x1}

$$\tau_{x1} = \frac{Sa_{2,3}}{A_t} = \frac{1.73}{.0775}$$

$$\tau_{x1} = 22.32 \text{ KSI} < .577 \times 123.0 = 70.97 \text{ KSI}$$

THE EFFECTIVE STRESS AT BIE-URANIUM PLATE = σ_e

$$\sigma_e = \frac{1}{\sqrt{2}} \times \sqrt{3 \times 68.64^2 + 6 \times 22.32^2}$$

$$\sigma_e = 78.8 \text{ KSI} < S_y = 128.6 \text{ KSI (SEE PAR. 4.3.1)}$$

TENSILE STRESS IN THREADS AT TOPPLATE-URANIUM PLATE CONNECTION = σ_{x1}

$$Ma_2 = \frac{\Sigma M_2}{N_s} = \frac{104.4}{7} = 14.91 \text{ KIN}$$

* SEE PAR. 5.0

$$Pa_1 = \frac{\Sigma P_1}{1} = \frac{1.01}{1} = 1.01 \text{ K}$$

$$S_{a2,3} = \frac{1}{7} \times \sqrt{4.53^2 + 7.12^2} = 1.21 \text{ K}$$

STUD SIZE: 3/8 IN - 16 UNC ⇒ $A_t = .0775 \text{ IN}^2$

* MATERIAL: NITRONIC-60 AT 450°F ⇒ $S_y = 33.5$ KSI & $S_u = 77.0$ KSI

4.3.3 CONT'D

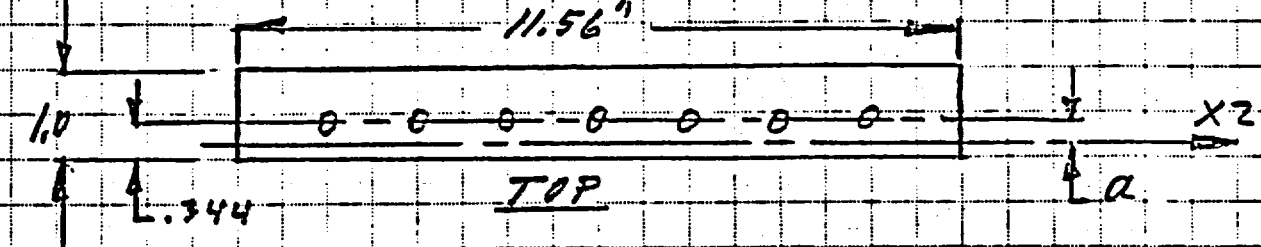

(PER PAR. 4.3.1 - SHIELDING NO. 1 STUD ANALYSIS)

$a = .205$ IN , $I_{X2} = .033$ IN^4

$$\sigma_{X1} = \frac{P_{X1}}{A_t} + \frac{M_{X2} \times a}{I_{X2}} = \frac{1.01}{.0775} + \frac{14.91 \times .205}{.033} = 105.6 \text{ KSI}$$

BREAK STRESS IN THREADS = τ_{X1}

$$\tau_{X1} = \frac{S_{Z2,3}}{A_t} = \frac{1.21}{.0775} = 15.61 \text{ KSI} < .577 \times 33.5 = 19.3 \text{ KSI}$$

THE EFFECTIVE STRESS AT TOP PLATE - HEMISPHERICAL PLATE CONNECTION = σ_e

$$\sigma_e = \frac{1}{\sqrt{2}} \times \sqrt{2 \times 105.6^2 + 6 \times 15.61^2}$$

$$\sigma_e = 109.0 \text{ KSI} < S_u = 128.6 \text{ KSI}$$

4.3.3 CONT'D

THE MAXIMUM STRESS FOR BEAMS WITH PROPERTY NO. 3 OCCUR IN BEAM NO. 526

BEAM 526

(PER PAR. 2.0 - PROPERTY NO. 3)

$I_{X2,S} = .031$ KIN. AT SLOTS

$I_{X3,S} = 6.63$ KIN.

$AREA = 3.0 - (1. \times .5) \times 3 = 1.50\ IN^2$

$$\sigma_{526,673} = \frac{P_{526}}{1.50} + \frac{M_{526,673,2} \times C3}{.031} + \frac{M_{526,673,3} \times C3}{6.63}$$

$$\sigma_{526,673} = \frac{4.12}{1.5} + \frac{2.94 \times .5}{.031 \times 2} + \frac{40.63 \times 6.0}{6.63 \times 2} = 44.86\ KSI$$

$(\sigma_A + \sigma_B) = \sigma_{526,673}$

$$\sigma_{526} = \frac{P_{526}}{1.5} = \frac{4.12}{1.5} = 2.75\ KSI$$

$\sigma_A = \sigma_{526}$

$(\sigma_A + \sigma_B)/S_Y = 44.86/20.1 = 2.23$

$\sigma_A/S_Y = 2.75/20.1 = .14$

THE COORD. (.14, 2.23) IS WITHIN THE ENVELOPE.

∴ THE EFFECT OF SHEAR IS NEGLIGIBLE.

4.3.3 CONT'D

THE MAXIMUM STRESS FOR BEAMS WITH PROPERY NO. 25 OCCUR IN BEAM NO. 360.

BEAM 360

(PER PAR. 2.0 - PROPERTY NO. 25)

$I_{x2} = 1/12 \times 2.0^3 \times 1.0 = .67 \ IN^4$

NOTE: SEE PAR. 4.3.2 (P.54) FOR INCREASE IN RIB THICKNESS TO 1.0 IN.

$I_{x3} = 1/12 \times 2.0 = .17 \ IN^4$

$AREA = 2.0 \ IN^2$

$$\sigma_{360,545} = \frac{P_{360}}{2.0} + \frac{M_{360,545,2} \times C3}{.67} + \frac{M_{360,545,3} \times C2}{.17}$$

$$\sigma_{360,545} = \frac{6.7}{2.0} + \frac{6.94 \times 2.0}{.67 \times 2} + \frac{4.43 \times 1.0}{.17 \times 2} = 26.74 \ KSI$$

$(\sigma_A + \sigma_B) = \sigma_{360,545}$

$$\sigma_A = \sigma_{360} = \frac{P_{360}}{2.0} = \frac{6.7}{2.0} = 3.35 \ KSI$$

$(\sigma_A + \sigma_B)/S_y = 26.74/20.1 = 1.33$

$\sigma_A/S_y = 3.35/20.1 = .17$

THE COORD. (.17, 1.33) IS WITHIN THE ENVELOPE.

THE EFFECT OF SHEAR IS NEGLIGIBLE.

4.3.3 CONT'D

STRESS IN TOPPLATE - PLATE ELEMENTS.

THE MAXIMUM STRESS IN THE ELEMENTS OF THE TOPPLATE OCCUR IN ELEMENT #. 30 (MATERIAL: 216 SS) & ELEMENT #35 (MATERIAL: 304 S.S.)

ELEMENT 30 (Δ) (SEE PAR. 4.3.2 - STRESS IN TOPPLATE-PLATE ELEMENTS)

$$\sigma_e = \frac{1}{\sqrt{2}} \times \sqrt{(S_x - S_y)^2 + S_y^2 + S_x^2 - 6 \times S_{xy}^2}$$

$$\sigma_e = \frac{1}{\sqrt{2}} \times \sqrt{(-20.35 + 36.24)^2 + 20.35^2 + 36.24^2 + 6 \times 19.02^2}$$

$$\sigma_e = 45.6 \text{ KSI}$$

MATERIAL 216 SS ⇒ AT 450°F S_y = 44.4 KSI & S_u = 87.9 KSI

σ_e = 45.6 KSI < S_u = 87.9 KSI ←

ELEMENT 35 (Δ)

$$\sigma_e = \frac{1}{\sqrt{2}} \times \sqrt{(-9.52 + 3.86)^2 + 9.52^2 + 3.86^2 + 6 \times 2.07^2}$$

σ_e = 9.04 < S_y = 20.1 KSI (304 S.S AT 450°F) ←

IN THE AREA OF 216 S.S. PLATE ELEMENT NO. 30 IS THE ONLY ELEMENT HAVING AN EFFECTIVE STRESS

σ_e = 45.6 KSI > S_y = 44.4 KSI ←

(SEE ALSO COMMENTS FOR PLOT OF σ_e VS. ELEMENTS PER PAR. 4.3.1)

4.4 SHIELDING NO. 3

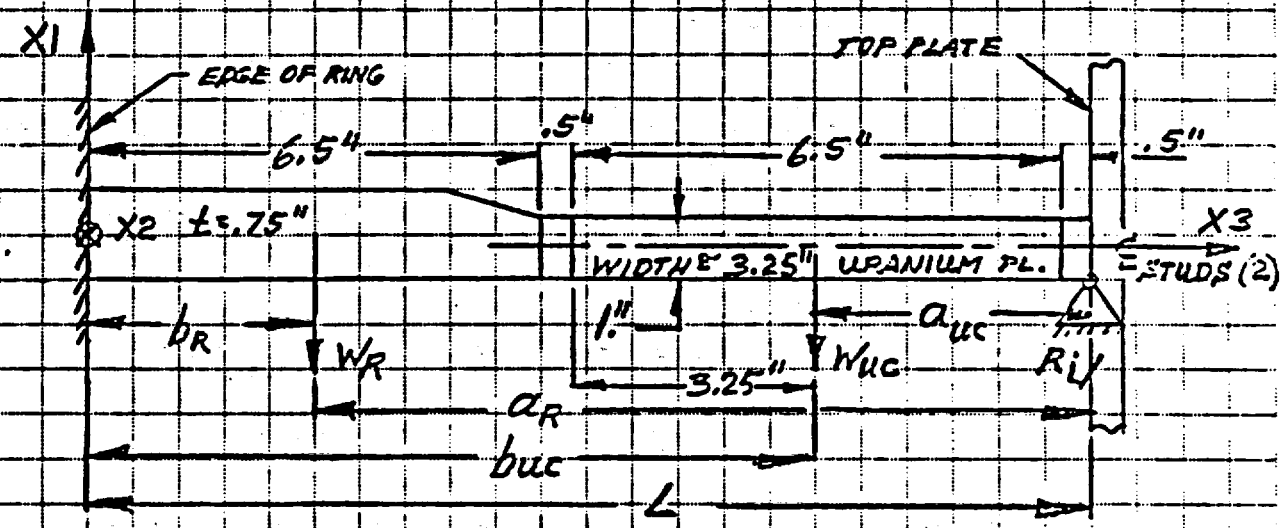

b_R = 3.25 IN. ; b_{uc} = 10.25 IN. ; L = 14.0 IN.
a_R = 10.75 IN. ; a_{uc} = 3.75 IN.

WEIGHT OF URANIUM = 14.0 LB
WEIGHT OF CLADDING = 3.0 LB
W_{uc} = 17.0 LB
WEIGHT OF RIB (1) = W_R = 3.0 LB

THE DYNAMIC LOAD FACTOR FOR DROP ORIENTATION (i) = DLF_i
PER PAR. 4.2 DLF_0 = 1.0 ; DLF_{45} = 1.14 ; DLF_{90} = .975

THE DESIGN G-LOAD FOR THE VARIOUS IMPACT ORIENTATIONS = G_i (PER PAR. 4.2)

THE STUDS AT THE TOP PLATE CONNECTION ARE CONSIDERED TO HAVE NEGLIGIBLE MOMENT CARRYING CAPABILITY.
REACTION AT SIMPLY SUPPORTED END = R_i

$$R_i = G_i \times DLF_i \times \left[\frac{W_{uc} \times b_{uc}^2 \times (a_{uc} + 2 \times L)}{2 \times L^3} + \frac{W_R \times b_R^2 \times (a_R + 2 \times L)}{2 \times L^3} \right]$$

4.4 CONT'D

$$R_i = G_i \times DLF_i \times \left[W_{UC} \times \frac{10.25^2 \times (3.75 + 2 \times 14.)}{2 \times 14.^3} + W_R \times \frac{3.25^2 \times (10.75 + 2 \times 14.)}{2 \times 14.^3} \right]$$

$$R_i = G_i \times DLF_i \times (W_{UC} \times .608 + W_R \times .075) \times 10^{-3} \quad [K]$$

4.4.1 DROP ORIENTATION - 90 DEGREES

$$G_i = G_{90} = 140., \quad DLF_i = DLF_{90} = .975$$

A. STRESS IN RIB AT THE STRUCTURAL RING $= \sigma_{R_{90}}$

NO. OF RIBS = 1

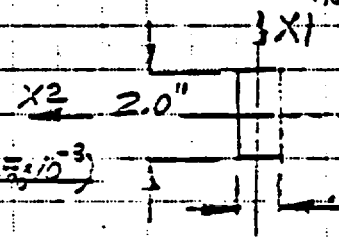

$$\sigma_{R_{90}} = \frac{(R_{90} \times L - (W_{UC} \times b_{UC} + W_R \times b_R) \times G_{90} \times DLF_{90} \times 10^{-3})}{S_{X2}}$$

$$R_{90} = 140. \times .975 \times (17.0 \times .608 + 3.0 \times .075) \times 10^{-3}$$

$$R_{90} = 1.44\ K, \quad C = 1.0\ IN, \quad S_{X2} = \frac{1/12 \times 2.^3 \times .75}{C} = .50\ IN^3$$

$$\sigma_{R_{90}} = \frac{(1.44 \times 14. - (17. \times 10.25 + 3. \times 3.25) \times 140. \times .975 \times 10^{-3})}{.50}$$

$$\sigma_{R_{90}} = 9.92\ KSI < S_Y = 20.1\ KSI$$

B. STRESS IN URANIUM $= \sigma_{U_{90}}$

$$W_{UC_{90}} = \frac{W_{UC} \times G_{90} \times DLF_{90}}{6.5} \times 10^{-3} = \frac{17. \times 140. \times .975}{6.5} \times 10^{-3} = .357\ K/IN$$

MAX. MOMENT AT X3 [IN]

$$X3 = L - \left(.5 + \frac{R_{90}}{W_{UC_{90}}}\right) = 14. - \left(.5 + \frac{1.44}{.357}\right) = 9.47\ IN$$

4.4.1 CONT'D

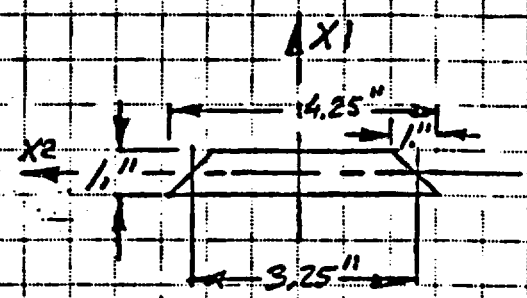

$$S_{x2} = \frac{1/12 \times 3.25}{.5} = .54 \text{ IN}^3$$

$$\sigma_{u_{90}} = \frac{(P_a \times (L - X3) - (W_{uc_{90}} \times (L - .5 - X3)^2/2))}{S_{x2}}$$

$$\sigma_{u_{90}} = \frac{(1.44 \times (14. - 9.47) - (.357 \times (14. - .5 - 9.47)^2/2))}{.54}$$

$$\sigma_{u_{90}} = 6.71 \text{ KSI} < S_{yu} = 46.0 \text{ KSI}$$

C. STUDS

STRESS IN STUDS AT RIB - URANIUM CONNECTION = $\sigma_{S_{90}}$

STUD SIZE: 3/8 IN.-16 UNC

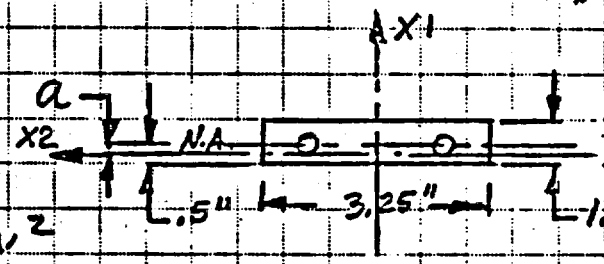

$$A_S = \pi/4 \times .375^2 = .110 \text{ IN}^2$$

TENSILE STRESS AREA = .0775 IN^2

CONSIDER $\sum_{i=1}^{n} A \times X_i = 0$ ($E_{SS304} \sim E_{URANIUM}$ [LB/IN^2])

NO. OF STUDS = n = 2. MATERIAL: NITRONIC-60 → S_y = 33.5 KSI &

$$n \times A \times a - 3.25 \times (.5 - a)^2 \times \frac{1}{2} = 0 \quad \therefore \quad S_u = 79.0 \text{ KSI AT } 450°F$$

$$a = \frac{(n \times A + 3.25 \times .5)}{3.25} \pm \sqrt{\left(\frac{n \times A + 3.25 \times .5}{3.25}\right)^2 - (.5)^2}$$

$$a = \frac{(2 \times .0775 + 3.25 \times .5)}{3.25} \pm \sqrt{\left(\frac{2 \times .0775 + 3.25 \times .5}{3.25}\right)^2 - .25}$$

$$a = .324 \text{ IN}$$

$$I_{x2} = 2 \times .0775 \times .324^2 + 1/12 \times 3.25 \times (.5 - .324)^3 + 3.25 \times (.5 - .324)^3 \times \frac{1}{4}$$

4.4.1 CONT'D

$I_{x2} = .022\ IN^4$; $S_{x2} = \frac{.022}{a} = \frac{.022}{.324} = .068\ IN^3$

$$\sigma_{S_{90}} = \frac{(R_{90} \times (.5+6.5) - W_{uc} \times 3.25 \times G_{90} \times DLF_{90} \times 10^{-3})}{S_{x2}}$$

$$\sigma_{S_{90}} = \frac{(1.44 \times 7. - 17. \times 3.25 \times 140. \times .975 \times 10^{-3})}{.068}$$

$$\sigma_{S_{90}} = 37.32\ KSI$$

CHECK THREAD ENGAGEMENT LENGTH IN URANIUM AT RIB-URANIUM CONNECTION.

(PER REF. 2 - PAGE 1142)

STUD ENGAGEMENT LENGTH $= L_{Se} = .75\ IN$

$$L_e = \frac{2 \times A_t}{3.1416 \times K_{nmax} \times \left(\frac{1}{2} + .57735 \times n \times (E_{S_{MIN}} - K_{nmax})\right)}$$

$A_t = .0775\ IN^2$; $K_{nmax} = .3073\ IN.$; $E_{S_{MIN}} = .3344\ IN.$

$$L_e = \frac{2 \times .0775}{3.1416 \times .3073 \times (.5 + .57735 \times 16 \times (.3344 - .3073))} ; \quad n = 16$$

$L_e = .214\ IN < L_{Se} = .75\ IN$

SHEAR STRESS IN STUDS AT RIB-URANIUM CONNECTION $= \tau_{S_{90}}$

$$\tau_{S_{90}} = \frac{W_{uc} \times G_{90} \times DLF_{90} \times 10^{-3} - R_{90}}{2 \times .0775} = \frac{17. \times 140. \times .975 \times 10^{-3} - 1.44}{2 \times .0775}$$

$$\tau_{S_{90}} = 5.68\ KSI < 33.5 \times \frac{1}{\sqrt{3}} = 19.30\ KSI$$

4.4.1 CONT'D

COMBINED STRESS IN STUDS DUE TO TENSION & SHEAR AT RIB-URANIUM CONNECTION = $\sigma_{C_{90}}$

$$\sigma_{C_{90}} = \frac{\sigma_{S_{90}}}{2} \pm \frac{1}{2}\sqrt{\sigma_{S_{90}}^2 + 4 \times \tau_{S_{90}}^2}$$

$$\sigma_{C_{90}} = \frac{37.32}{2} + \frac{1}{2} \times \sqrt{37.32^2 + 4 \times 5.68^2}$$

$$\sigma_{C_{90}} = 38.16\,KSI < \sigma_u = 79.0\,KSI \text{ (SEE PAR. 4.4.1)}$$

SHEAR STRESS IN STUDS AT URANIUM-TOP PLATE CONNECTION = $\tau_{T_{90}}$

$$\tau_{T_{90}} = \frac{R_{90}}{2 \times .0775} = \frac{1.44}{2 \times .0775}$$

$$\tau_{T_{90}} = 9.30\,KSI < 33.5 \times \frac{1}{\sqrt{3}} = 19.3\,KSI$$

D. WELDS

AS THE WELDS ALL ARE FULL PENETRATIONS THE STRENGTH OF THE WELDS ARE EQUAL TO THE RIBS ANALYSED THROUGH PAR. 4.4.1.

4.4.2 DROP ORIENTATION - 0 DEGREE

THE G_i-LOAD AND S_x [IN^3] CHANGES WITH THE DROP ORIENTATION. THE STRESSES FOR 0-DEGREE DROP ORIENTATION ARE COMPUTED FROM THE 90-DEGREES STRESSES (4.4.1) BASED ON THE RATIO OF THE RESPECTIVE G_i, DLF_i & S_x.

$G_i = G_0 = 214.$, $DLF_i = DLF_0 = 1.0$

A. STRESS IN RIB AT THE STRUCTURAL RING = σ_{R_0}

$$S_{X1} = \frac{1/12 \times .75^3 \times 2.0}{(.75/2)} = .190 \text{ IN}^3$$

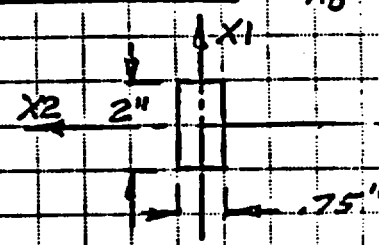

$S_{X2} = .50 \text{ IN}^3$ (PAR. 4.4.1 - A.)

$$\sigma_{R_0} = \sigma_{R_{90}} \times \frac{S_{X2}}{S_{X1}} \times \frac{G_0}{G_{90}} \times \frac{DLF_0}{DLF_{90}}$$

$$\sigma_{R_0} = 9.92 \times \frac{.50}{.190} \times \frac{214.}{140.} \times \frac{1.0}{.975} = 41.0 \text{ KSI}. \quad \sigma_{B_0}/S_y = 41./20.1 = 2.04$$

THE COORD (0., 2.04) IS WITHIN THE ENVELOPE (PAR. 4.3.1)

B. STRESS IN ALUMINUM PLATE = σ_{u_0}

MAX. MOMENT AT X3 [IN]

X3 = 9.47 IN (PAR. 4.4.1 - B.)

$$S_{X1} = \frac{1/12 \times 3.25^3 \times 1.0}{(4.25/2)} = 1.35 \text{ IN}^3$$

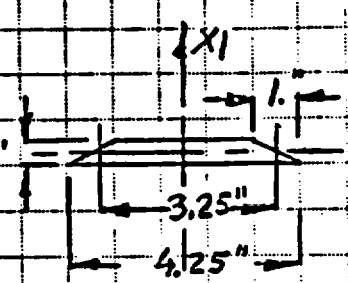

$S_{X2} = .54 \text{ IN}^3$ (PAR. 4.4.1 - B.)

$$\sigma_{u_0} = \sigma_{u_{90}} \times \frac{S_{X2}}{S_{X1}} \times \frac{G_0}{G_{90}} \times \frac{DLF_0}{DLF_{90}}$$

$$\sigma_{u_0} = 6.71 \times \frac{.54}{1.35} \times \frac{214.}{140.} \times \frac{1.0}{.975}$$

$\sigma_{u_c} = 4.21$ KSI $< S_{yu} = 46.0$ KSI

4.4.2 CONT'D

C. STUDS

STRESS IN STUDS AT RIB-URANIUM CONNECTION = σ_{S_0}

(PER 4.4.1 - C)

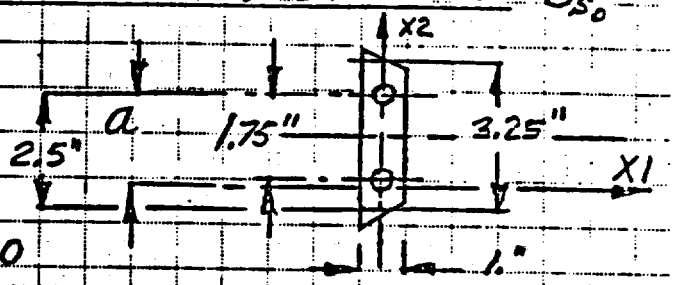

$n \cong 1$; $A = .0775\ IN^2$

$n \times A \times a - 1. \times (2.5 - a)^2 \times \frac{1}{2} \cong 0$

$a = \frac{(n \times A + 1. \times 2.5)}{1.} \pm \sqrt{\left(\frac{n \times A + 1. \times 2.5}{1.}\right)^2 - (2.5)^2}$

$a = \frac{.0775 + 2.5}{1.} \pm \sqrt{(.0775 + 2.5)^2 - 2.5^2}$

$a = 1.95\ IN$

$I_{x_1} = .0775 \times 1.95^2 + 1/12 \times 1. \times (2.5 - 1.95)^3 + 1. \times (2.5 - 1.95)^3 \times \frac{1}{4}$

$I_{x_1} = .35\ IN^4$; $S_{x_1} = \frac{I_{x_1}}{a} = \frac{.35}{1.95} = .18\ IN^3$

$S_{x_2} = .068\ IN^3$ (PAR. 4.5.1 - C)

$\sigma_{S_0} = \sigma_{S_{90}} \times \frac{S_{x2}}{S_{x1}} \times \frac{G_0}{G_{90}} \times \frac{DLF_0}{DLF_{90}} = 37.32 \times \frac{.068}{.18} \times \frac{214.}{140.} \times \frac{1.0}{.975}$

$\sigma_{S_0} = 22.10\ KSI$

SHEAR STRESS IN STUDS AT RIB-URANIUM CONNECTION = τ_{S_0}

$\tau_{S_0} = \tau_{S_{90}} \times \frac{G_0}{G_{90}} \times \frac{DLF_0}{DLF_{90}} = 5.68 \times \frac{214.}{140.} \times \frac{1.0}{.975}$

$\tau_{S_0} = 8.9\ KSI < 33.5 \times \frac{1}{\sqrt{3}} = 19.5\ KSI$

4.4.2 CONT'D

COMBINED STRESS IN STUDS DUE TO TENSION & SHEAR AT RIB-URANIUM PLATE CONNECTION = σ_{C_0}

$$\sigma_{C_0} = \frac{\sigma_{S_0}}{2} \pm \frac{1}{2} \times \sqrt{\sigma_{S_0}^2 + 4 \times \tau_{S_0}^2}$$

$$\sigma_{C_0} = \frac{22.1}{2} + \frac{1}{2} \times \sqrt{22.1^2 + 4 \times 8.9^2}$$

$$\sigma_{C_0} = 25.24 \text{ KSI} < \sigma_u = 79.0 \text{ KSI (SEE PAR. 4.3.1)}$$

SHEAR STRESS IN STUDS AT URANIUM-TOP PLATE CONNECTION = τ_{T_0}

$$\tau_{T_0} = \tau_{T_{90}} \times \frac{G_0}{G_{90}} \times \frac{DLF_0}{DLF_{90}} = 9.30 \times \frac{214.}{140.} \times \frac{1.0}{.975}$$

$$\tau_{T_0} = 14.60 \text{ KSI} < 33.5 \times \frac{1}{\sqrt{3}} = 19.3 \text{ KSI}$$

STUD MATERIAL FOR ALL STUDS IN SHIELDING NO. 3 & 4 PER PAR. 4.3.1

MATERIAL: NITRONIC-60 AT 450°F

$S_y = 33.5$ KSI & $S_u = 79.0$ KSI

D. WELD

PER PAR. 4.4.1

4.4.3 DROP ORIENTATION - 45 DEGREES

THE STRESSES FOR 45 DEGREES DROP ORIENTATION ARE COMPUTED FROM THE 90 DEGREES STRESSES (4.4.1) BASED ON THE RATIO OF THE RESPECTIVE G_i, DLF_i & S_x

$G_i = G_{45} = 161.$, $DLF_i = DLF_{45} = 1.14$

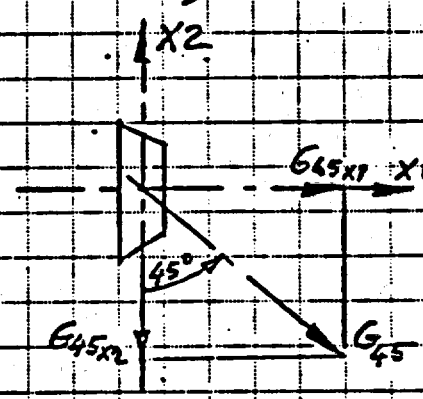

$G_{45x1} = G_{45x2} = G_{45} \times \cos 45 = 161 \times \cos 45 = 114.$

A. STRESS IN RIB AT THE STRUCTURAL RING = σ_{R45}

$S_{x1} = .190\ IN^3$ (PAR. 4.4.2-A.)

$S_{x2} = .50\ IN^3$ (PAR. 4.4.1-A.)

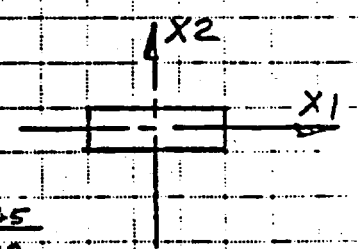

$$\sigma_{R45} = \sigma_{R90} \times \left(\frac{G_{45x1}}{G_{90}} + \frac{G_{45x2}}{G_{90}} \times \frac{S_{x2}}{S_{x1}} \right) \times \frac{DLF_{45}}{DLF_{90}}$$

$$\sigma_{R45} = 9.92 \times \left(\frac{114.}{140.} + \frac{114.}{140.} \times \frac{.50}{.19} \right) \times \frac{1.14}{.975} = 34.3\ KSI$$

$\sigma_{B45} = \sigma_{R45}$

$\sigma_{B45} / S_y = 34.3 / 20.1 = 1.71$, $\sigma_{A45} = 0.\ KSI$

THE COORD. (0., 1.71) IS WITHIN THE ENVELOPE (PAR. 4.3.1)

4.4.3 CONT'D

B. STRESS IN URANIUM = σ_{U45}

MAX. MOMENT AT X3 [IN]

$X3 = 9.47$ IN (PAR. 4.4.1 - B.)

$S_{x1} = 1.35\ IN^4$ (PAR. 4.4.2 - B.)

$S_{x2} = .54\ IN^4$ (PAR. 4.4.1 - B)

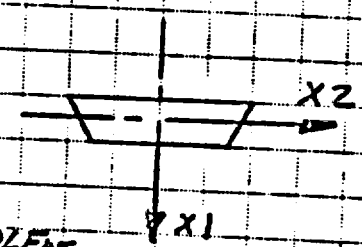

$$\sigma_{U45} = \sigma_{U90} \times \left(\frac{G_{45x1}}{G_{90}} + \frac{G_{45x2}}{G_{90}} \times \frac{S_{x2}}{S_{x1}} \right) \times \frac{DLF_{45}}{DLF_{90}}$$

$$\sigma_{U45} = 6.71 \times \left(\frac{114.}{140.} + \frac{114.}{140.} \times \frac{.54}{1.35} \right) \times \frac{1.14}{.975}$$

$\sigma_{U45} = 8.94$ KSI $< S_{yu} = 46.0$ KSI

C. STUDS

STRESS IN STUDS AT RIB-URANIUM CONNECTION = σ_{S45}

$S_{x1} = .18\ IN^4$ (PAR. 4.4.2 - C.)

$S_{x2} = .068\ IN^4$ (PAR. 4.4.1 - C.)

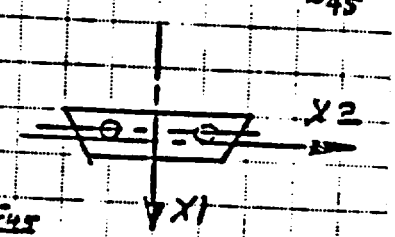

$$\sigma_{S45} = \sigma_{S90} \times \left(\frac{G_{45x1}}{G_{90}} + \frac{G_{45x2}}{G_{90}} \times \frac{S_{x2}}{S_{x1}} \right) \times \frac{DLF_{45}}{DLF_{90}}$$

$$\sigma_{S45} = 37.32 \times \left(\frac{114.}{140.} + \frac{114.}{140.} \times \frac{.068}{.18} \right) \times \frac{1.14}{.975} = 48.96\ KSI$$

SHEAR STRESS IN STUDS AT RIB-URANIUM CONNECTION = τ_{S45}

$$\tau_{S45} = \tau_{S90} \times \frac{G_{45}}{G_{90}} \times \frac{DLF_{45}}{DLF_{90}} = 5.68 \times \frac{161.}{140.} \times \frac{1.14}{.975} = 7.64\ KSI$$

4.4.3 CONT'D

$\tau_{S45} = 7.64$ KSI $< 33.5 \times 1/\sqrt{3} = 19.3$ KSI

COMBINED STRESS DUE TO TENSION AND SHEAR AT IN STUDS AT RIB-URANIUM PLATE CONNECTION = σ_{C45}

$$\sigma_{S45} = \frac{\sigma_{S45}}{2} \pm \frac{1}{2} \times \sqrt{\sigma_{S45}^2 + 4 \times \tau_{S45}^2}$$

$$\sigma_{S45} = \frac{48.96}{2} \pm \frac{1}{2} \times \sqrt{48.96^2 + 4 \times 7.64^2}$$

$\sigma_{S45} = 50.1$ KSI $< \sigma_u = 79.0$ KSI (SEE PAR. 4.3.1)

SHEAR STRESS IN STUDS AT URANIUM-TOP PLATE CONNECTION = τ_{T45}

$$\tau_{T45} = \tau_{T90} \times \frac{G_{45}}{G_{90}} \times \frac{DLF_{45}}{DLF_{90}} = 9.30 \times \frac{161.}{140.} \times \frac{1.14}{.975}$$

$\tau_{T45} = 12.50$ KSI $< 33.5 \times 1/\sqrt{3} = 19.3$ KSI

D. WELDS

SEE 4.4.1 - D.

4.5 SHIELDING NO. 4

WEIGHT OF URANIUM = 9.7 LB
WEIGHT OF CLADDING = 1.8 LB
W_{UC} = 11.5 LB

WEIGHT OF RIB (2) = W_R = 1.3 LB

THE BOUNDARY CONDITIONS AND X3-DIMENSIONS ARE THE SAME AS FOR SHIELDING NO. 3 - PAR. 4.4.

REACTION AT SIMPLY SUPPORTED END = $R_{i_{X_3}}$

$$R_{i_{X_3}} = G_i \times DLF_i \times \left[\frac{W_{UC} \times b_{UC}^2 \times (a_{UC} + 2 \times L)}{2 \times L^3} + \frac{W_R \times b_R^2 \times (a_R + 2 \times L)}{2 \times L^3} \right]$$

$$R_{i_{X_3}} = 1.0 \times DLF_i \times (W_{UC} \times .608 + W_R \times .075) \times 10^{-3} \; [K/G_i]$$

4.5.1 DROP ORIENTATION - 90 DEGREES

$G_i = G_{90} = 140.$; $DLF_i = DLF_{90} = .975$

A. STRESS IN RIBS AT THE STRUCTURAL RING = $\sigma_{R_{70}}$

NO. OF RIBS = 2

$$R_{90_{X_3}} = 1.0 \times .975 \times (11.5 \times .608 + 1.3 \times .075) \times 10^{-3} \; [K/G_i]$$

$$R_{90_{X_3}} = .0069 \; K/G_{90_{X_3}}$$

4.5.1 CONT'D

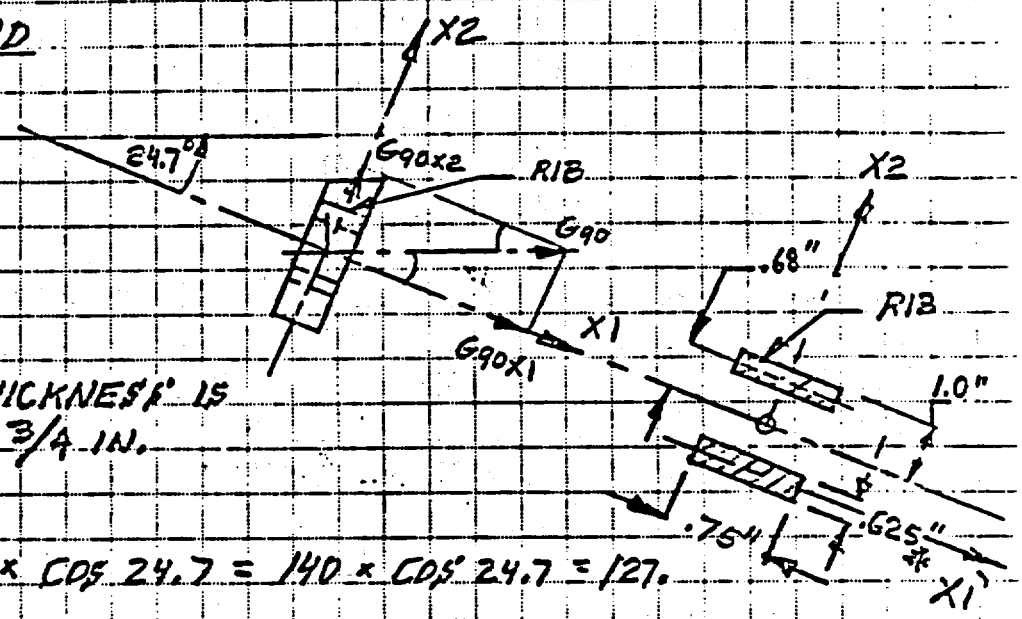

*ACTUAL RIB THICKNESS IS INCREASED TO 3/4 IN.

$G_{90X1} = G_{90} \times \cos 24.7 = 140 \times \cos 24.7 = 127.$

$G_{90X2} = 140 \times \sin 24.7 = 59.$

SHEAR FORCE AT RIB-URANIUM PLATE CONNECTION TRANSFERED EQUALLY TO THE 2 RIBS = F_{iXJ}

$F_{90XJ} = (W_{uc} \times DLF_{90} \times 10^{-3} - R_{90XJ})/2 \; [K/G_{90XJ}]$ (SEE PAR. 4.4)

G_{90X2} - COMPONENT

STRESS IN EACH RIB DUE TO MOMENT FROM $F_{90X2} = \sigma_{F90X2}$

$S_{X1}' = \dfrac{1/12 \times .625^3 \times .75}{(.68/2)} = .05 \; IN^3$

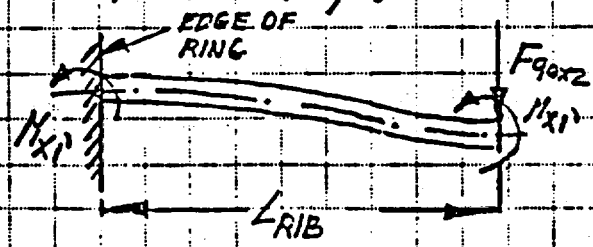

$L_{RIB} = 6.5 \; IN.$

$M_{X1}' = \dfrac{F_{90X2} \times L_{RIB}}{2}$

4.5.1 CONT'D

TENSILE STRESS IN RIB DUE TO MOMENT ABOUT THE COMMON AXIS-X1 FOR THE 2 RIBS = σ_{Mx1}

$S'_{x1} = 2 \times (1/12 \times .625^3 \times .75 + .75 \times .625 \times .68^2)/.68$

$S_{x1} = .68 \ IN^3$

COMBINED STRESS IN EACH RIB DUE TO G_{90x2} COMPONENT IS = σ_{90x2}

$\sigma_{90x2} = \sigma_{Mx1} + \sigma_{F90x2}$

$F_{90x3} = F_{90x2} = (W_{uc} \times DLF_{90} \times 10^{-3} - R_{90x2})/2 \quad [K/G_{90x2}]$

$F_{90x2} = (11.5 \times 10^{-3} \times .975 - .0069)/2 = .00215 \ K/G_{90x2}$

$\sigma_{90x2} = \left[\frac{(R_{90x2} \times L - (W_{uc} \times b_{uc} + W_R \times h_R) \times DLF_{90} \times 10^{-3})}{S_{x1}} + \frac{(F_{90x2} \times L_{R12})}{2 \times S'_{x1}}\right] \times G_{90x2}$

$\sigma_{90x2} = \left[\frac{(.0069 \times 14. - (11.5 \times 10.25 + 1.3 \times 3.25) \times .975 \times 10^{-3})}{.68} + \frac{(.00215 \times 6.5)}{2 \times .05}\right] \times 59.$

$\sigma_{90x2} = 10.20 \ KSI$, $\sigma_{A_{90}} = \frac{-(.0069 \times 14. - (11.5 \times 10.25 + 1.3 \times 3.25) \times .975 \times 10^{-3})}{.68} \times 59.$

$= 1.95 \ KSI$

G_{90x1} - COMPONENT

STRESS IN RIBS DUE TO MOMENT ABOUT X2-AXIS = σ_{Mx1}

$S_{x2} = \frac{2 \times 1/12 \times .75^3 \times .625}{(.75/2)} = .120 \ IN^3$

$\sigma_{90x1} = \left[\frac{(R_{90x1} \times L - (W_{uc} \times b_{uc} + W_R \times b_R) \times DLF_{90} \times 10^{-3})}{S_{x2}}\right] \times G_{90x1}$

$\sigma_{90x1} = \left[\frac{.0069 \times 14. - (11.5 \times 10.25 + 1.3 \times 3.25) \times .975 \times 10^{-3})}{.120}\right] \times 127.$

4.5.1 CONT'D

$\sigma_{90x1} = 23.75$ KSI

$\sigma_{R90} = \sigma_{90x1} + \sigma_{90x2} = 23.75 + 10.20 = 33.95$ KSI

$(\sigma_{A90} + \sigma_B)/S_y = 33.95/20.1 = 1.69$ & $\sigma_{A90}/S_y = 1.95/20.1 = .10$

COORD. (.10, 1.69) WITHIN ENVELOPE PAR. 4.3.1

B. STRESS IN URANIUM = σ_{u90}

$W_{uc} = \frac{W_{uc} \times DLF_{90}}{6.5} = \frac{11.5 \times .975}{6.5} \times 10^{-3} = .001725$ K/IN/G_{90x3}

MAX. MOMENT AT X3 [IN]

$X3 = L - \left(.5 + \frac{R_{90x3}}{W_{uc}}\right) = 14. - \left(.5 + \frac{.0069}{.001725}\right)$

$X3 = 9.50$ IN.

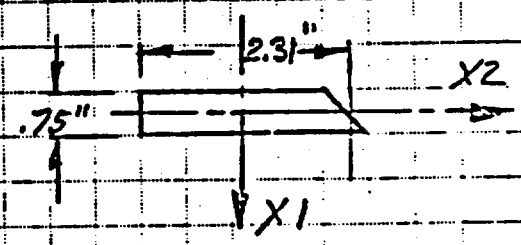

G_{90x1} - COMPONENT

$S_{x2} = \frac{1/12 \times .75^3 \times 2.31}{(.75/2)} = .22$ IN^3

STRESS IN URANIUM DUE TO MOMENT ABOUT X2-AXIS = σ_{90x1}

$\sigma_{90x1} = \frac{(R_{90x1} \times (L - X3) - (W_{uc} \times (L - .5 - X3)^2/2))}{S_{x2}} \times G_{90x1}$

$\sigma_{90x1} = \frac{(.0069 \times (14. - 9.5) - (.001725 \times (14. - .5 - 9.5)^2/2))}{.22} \times 127.$

$\sigma_{90x1} = 9.96$ KSI

4.5.1 CONT'D

G_{90X2} - COMPONENT

STRESS IN URANIUM DUE TO MOMENT ABOUT X1-AXIS = σ_{90X2}

$$S_{X1} \cong \frac{1/12 \times 2.31^3 \times .75}{(2.31/2)} = .67 \text{ IN}^3$$

$$\sigma_{90X2} = \sigma_{90X1} \times \frac{S_{X2}}{S_{X1}} \times \frac{G_{90X2}}{G_{90X1}} = 9.96 \times \frac{.22}{.67} \times \frac{59.}{127.}$$

$$\sigma_{90X2} = 1.52 \text{ KSI}$$

$$\sigma_{U90} = \sigma_{90X1} + \sigma_{90X2} = 9.96 + 1.52$$

$$\sigma_{U90} = 11.5 \text{ KSI} < S_{YU} = 46.0 \text{ KSI}$$

C. STUDS (SEE PAR. 4.5.4)

STRESS IN STUD AT RIB-URANIUM CONNECTION = σ_{S90}

STUD SIZE: 7/16 IN - 14 UNC

TENSILE STRESS AREA = A_t = .106 IN^2

NO. OF STUDS = n = 1. MATERIAL: NITRONIC - 60 AT 450°F

S_y = 33.5 & S_u = 79.0 KSI

G_{90X1} - COMPONENT

$$n \times A_t \times a - 2.31 \times (.375 - a)^2 \times \frac{1}{2} = 0$$

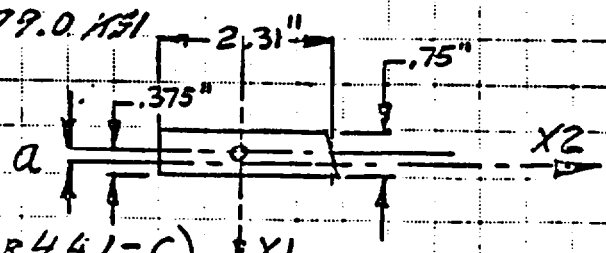

(PAR. 4.4.1-C)

4.5.1 CONT'D

$$a = \frac{(n \times A_t + 2.31 \times .375)}{2.31} \pm \sqrt{\left(\frac{n \times A_t + 2.31 \times .375}{2.31}\right)^2 - .375^2}$$

$$a = \frac{(.106 + 2.31 \times .375)}{2.31} \pm \sqrt{\left(\frac{.106 + 2.31 \times .375}{2.31}\right)^2 - .375^2}$$

$$a = .230 \text{ IN.}$$

$$S_{x2} = \frac{.106 \times .230^2 + 1/12 \times 2.31 \times (.375 - .230)^3 + 2.31 \times (.375 - .230)^3 \times \frac{1}{4}}{.23}$$

$$S_{x2} = .035 \text{ IN}^3$$

STRESS IN STUD DUE TO MOMENT ABOUT X2-AXIS = σ_{90x1}

$$\sigma_{90x1} = \left[\frac{(P_{90x1} \times (.5 + 6.5) - W_{UC} \times 3.25 \times DLF_{90} \times 10^{-3})}{S_{x2}}\right] \times G_{90x1}$$

$$\sigma_{90x1} = \left[\frac{.0069 \times 7. - 11.5 \times 3.25 \times .975 \times 10^{-3}}{.035}\right] \times 127. = 43.0 \text{ K}$$

G_{90x2} = COMPONENT

$n = 1$; $A_t = .0775 \text{ IN}^2$

$$a \times n \times A_t - .75 \times (1.125 - a)^2 \times \frac{1}{2} \sim 0$$

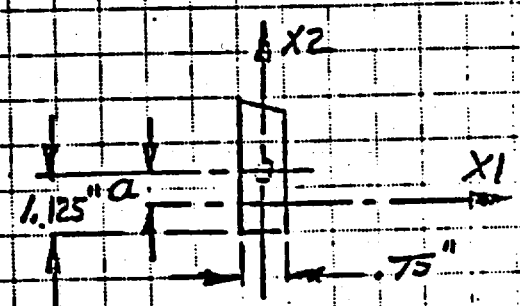

$$a = \frac{n \times A_t + .75 \times 1.125}{.75} \pm \sqrt{\left(\frac{n \times A_t + .75 \times 1.125}{.75}\right)^2 - 1.125^2}$$

$$a = \frac{.106 + .75 \times 1.125}{.75} \pm \sqrt{\left(\frac{.106 + .75 \times 1.125}{.75}\right)^2 - 1.125^2}$$

$$a = .685 \text{ IN}$$

4.5.1 CONT'D

$$S_{x1} = \frac{.106 \times .685^2 + 1/12 \times .75 \times (1.125 - .595)^3 + .75 \times (1.125 - .635)^3 \times \frac{1}{4}}{.685}$$

$$S_{x1} = .104 \text{ IN}^3$$

STRESS IN STUD DUE TO MOMENT ABOUT X1-AXIS = σ_{90x2}

$$\sigma_{90x2} = \sigma_{90x1} \times \frac{S_{x2}}{S_{x1}} \times \frac{G_{90x2}}{G_{90x1}} = 43.0 \times \frac{.035}{.104} \times \frac{59.}{127.}$$

$$\sigma_{90x2} = 6.72 \text{ KSI}$$

$$\sigma_{S_{90}} = \sigma_{90x1} + \sigma_{90x2} = 43.0 + 6.72$$

$$\sigma_{S_{90}} = 49.72 \text{ KSI}$$

SHEAR STRESS IN STUD AT RIB-URANIUM CONNECTION = $\tau_{S_{90}}$

$$\tau_{S_{90}} = \frac{W_{HCC} \times DLF \times 10^{-3} - R_{90}}{.106} \times G_{90} \quad \text{(SEE 4.5.1 - A.)}$$

$$\tau_{S_{90}} = \frac{11.5 \times 10^{-3} \times .975 - .0069}{.106} \times 140.$$

$$\tau_{S_{90}} = 5.70 \text{ KSI} < 33.5 \times 1/\sqrt{3} = 19.3 \text{ KSI}$$

COMBINED STRESS IN STUD DUE TO TENSION & SHEAR AT RIB-URANIUM CONNECTION = σ_{C90}

$$\sigma_{C90} = \frac{49.72}{2} \pm \frac{1}{2} \times \sqrt{49.72^2 + 4 \times 5.7^2}$$

$$\sigma_{C90} = 50.37 \text{ KSI} < S_u = 79.0 \text{ KSI} \quad \text{(SEE PAR. 4.3.1)}$$

4.5.1 CONT'D

CHECK THREAD ENGAGEMENT LENGTH IN URANIUM

STUD ENGAGEMENT LENGTH = L_{se} = .75 IN

PER PAR. 4.4.1 L_e = .214 IN < L_{se} = .75 IN

SHEAR STRESS IN STUD AT URANIUM - TOP PLATE CONNECTION = $\tau_{T_{90}}$

$$\tau_{T_{90}} = \frac{R_{90}}{.106} \times G_{90} = \frac{.0069}{.106} \times 140.$$

$$\tau_{T_{90}} = 9.11 \text{ KSI} < 33.5 \times 1/\sqrt{3} = 19.3 \text{ KSI}$$

D. WELDS

SEE PAR. 4.4.1 - D.

4.5.2 DROP ORIENTATION - 0 DEGREE

THE STRESSES FOR THE 0-DEGREE DROP ORIENTATION ARE COMPUTED FROM THE 90-DEGREES STRESSES (PAR. 4.5.1) BASED ON THE RATIO OF THE RESPECTIVE G_i & DLF_i.

$G_i = G_0 = 214.$

$DLF_i = DLF_0 = 1.0$

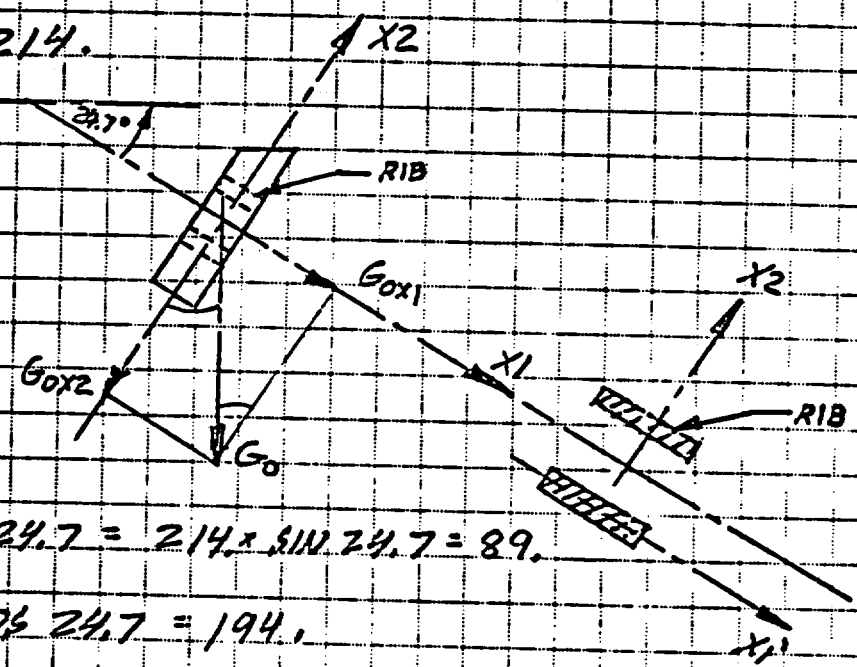

$G_{0x1} = G_0 \times \sin 24.7 = 214 \times \sin 24.7 = 89.$

$G_{0x2} = 214. \times \cos 24.7 = 194.$

A. STRESS IN RIBS AT THE STRUCTURAL RING $= \sigma_{R0}$
(PER PAR. 4.5.1 - A.)

G_{0x2} - COMPONENT

COMBINED STRESS IN EACH RIB DUE TO G_{0x2} COMPONENT IS $= \sigma_{0x2}$

$$\sigma_{0x2} = \sigma_{90x2} \times \frac{G_{0x2}}{G_{90x2}} \times \frac{DLF_0}{DLF_{90}} = 10.2 \times \frac{194.}{59.} \times \frac{1.0}{.975}$$

$$\sigma_{0x2} = 34.4 \text{ KSI}, \quad \sigma_{A0} = \sigma_{A90} \times \frac{194.}{59.} \times \frac{1.0}{.975} = 1.95 \times 3.37 = 6.57 \text{ KSI}$$

4.5.2 CONT'D

G_{0X1} - COMPONENT

STRESS IN RIBS DUE TO MOMENT ABOUT X2-AXIS = σ_{0X1}

$$\sigma_{0X1} = \sigma_{90X1} \times \frac{G_{0X1}}{G_{90X1}} \times \frac{DLF_0}{DLF_{90}} = 23.75 \times \frac{89.}{127.} \times \frac{1.0}{.975}$$

$$\sigma_{0X1} = 17.1 \text{ KSI}$$

$$\sigma_{R0} = \sigma_{0X1} + \sigma_{0X2} = 17.1 + 34.4 = 51.5 \quad \sigma_{R0}/S_Y = 6.57/20.1 = .33$$

$(\sigma_{R0} + \sigma_U)/S_Y = 51.5/20.1 = 2.56 \Rightarrow$ CODED (.33, 2.56) IS WITHIN ENVELOPE

B. STRESS IN URANIUM = σ_{U0}
(PER PAR. 4.5.1 - B.)

MAX. MOMENT AT X3 [IN]

X3 = 9.5 IN

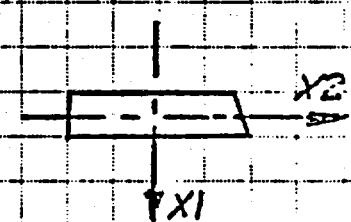

G_{0X1} - COMPONENT

STRESS IN URANIUM DUE TO MOMENT ABOUT X2-AXIS = σ_{0X1}

$$\sigma_{0X1} = \sigma_{90X1} \times \frac{G_{0X1}}{G_{90X1}} \times \frac{DLF_0}{DLF_{90}} = 9.96 \times \frac{89.}{127.} \times \frac{1.0}{.975}$$

$$\sigma_{0X1} = 7.2 \text{ KSI}$$

4.5.2 CONT'D

G_{0X2} - COMPONENT

STRESS IN URANIUM DUE TO MOMENT ABOUT X1-AXIS = σ_{0X2}

$$\sigma_{0X2} = \sigma_{90X2} \times \frac{G_{0X2}}{G_{90X2}} \times \frac{DLF_0}{DLF_{90}} = 1.52 \times \frac{194.}{59.} \times \frac{1.0}{.475}$$

$$\sigma_{0X2} = 5.1 \text{ KSI}$$

$$\sigma_{U_0} = \sigma_{0X1} + \sigma_{0X2} = 7.2 + 5.1$$

$$\sigma_{U_0} = 12.3 \text{ KSI} < S_{y_U} = 46.0 \text{ KSI}$$

C. STUDS (PAR. 4.5.1 - C & PAR. 4.5.4)

STRESS IN STUD AT RIE-URANIUM CONNECTION = σ_{S0}

G_{0X1} - COMPONENT

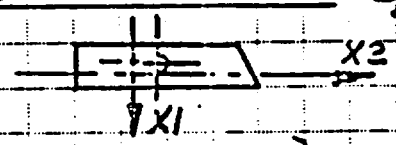

STRESS IN STUD DUE TO MOMENT ABOUT X2-AXIS = σ_{0X1}

$$\sigma_{0X1} = \sigma_{90X1} \times \frac{G_{0X1}}{G_{90X1}} \times \frac{DLF_0}{DLF_{90}} = 43.0 \times \frac{99.}{127.} \times \frac{1.0}{.975}$$

$$\sigma_{0X1} = 30.91 \text{ KSI}$$

G_{0X2} - COMPONENT

STRESS IN STUD DUE TO MOMENT ABOUT X1-AXIS = σ_{0X2}

$$\sigma_{0X2} = \sigma_{90X2} \times \frac{G_{0X2}}{G_{90X2}} \times \frac{DLF_0}{DLF_{90}} = 6.72 \times \frac{194.}{59.} \times \frac{1.0}{.975} = 22.66 \text{ KSI}$$

4.5.2 CONT'D

$\sigma_{S_0} = \sigma_{0x_1} + \sigma_{0x_2} = 30.91 + 22.66$

$\sigma_{S_0} = 53.57$ KSI

SHEAR STRESS IN STUD AT RIB-URANIUM CONNECTION = τ_{S_0}

$\tau_{S_0} = \tau_{S_{90}} \times \frac{G_0}{G_{90}} \times \frac{DLF_0}{DLF_{90}} = 5.7 \times \frac{214.}{140.} \times \frac{1.0}{.975}$

$\tau_{S_0} = 8.94$ KSI $< 33.5 \times 1/\sqrt{3} = 19.3$ KSI

COMBINED STRESS IN STUD DUE TO TENSION & SHEAR AT RIB-URANIUM PLATE CONNECTION = σ_{C_0}

$\sigma_{C_0} = \frac{53.57}{2} \pm \frac{1}{2} \times \sqrt{53.57^2 + 4 \times 8.94^2}$

$\sigma_{C_0} = 55.02$ KSI $< S_U = 79.0$ KSI (SEE PAR. 4.3.1)

SHEAR STRESS IN STUD AT URANIUM - TOP PLATE CONNECTION = τ_{T_0}

$\tau_{T_0} = \tau_{T_{90}} \times \frac{G_0}{G_{90}} \times \frac{DLF_0}{DLF_{90}} = 9.11 \times \frac{214.}{140.} \times \frac{1.0}{.975}$

$\tau_{T_0} = 14.3$ KSI $< 33.5 \times 1/\sqrt{3} = 19.3$ KSI

D. WELDS

SEE PAR. 4.4.1 - D.

4.5.3 DROP ORIENTATION - 45 DEGREES

THE STRESSES FOR THE 45-DEGREES DROP ORIENTATION ARE COMPUTED FROM THE 90-DEGREES STRESSES (PAR. 4.5.1) BASED ON THE RATIO OF THE RESPECTIVE G_i & DLF_i.

$G_i = G_{45} = 161.$ $\qquad DLF_i = DLF_{45} = 1.14$

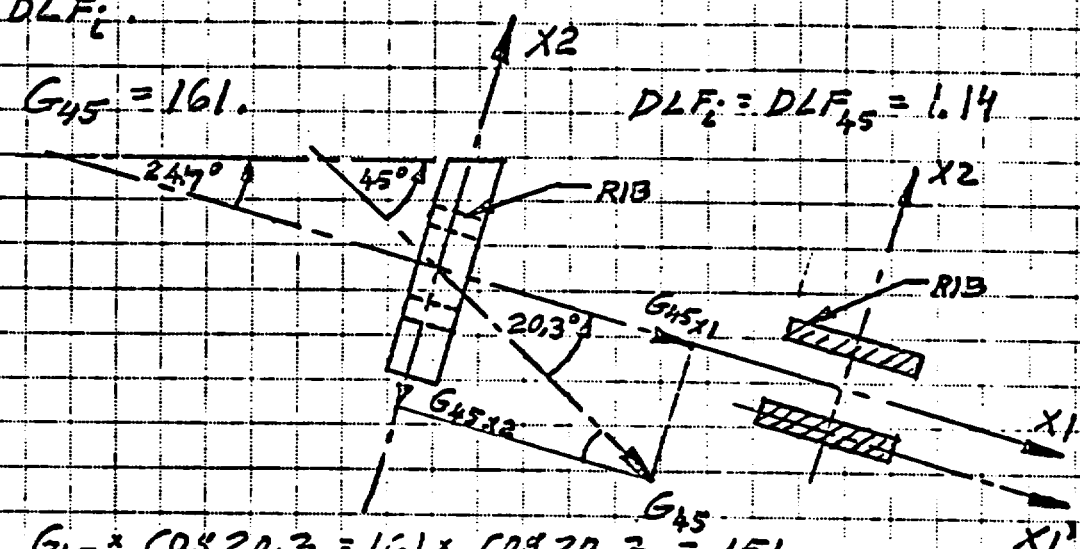

$G_{45x1} = G_{45} \times \cos 20.3 = 161 \times \cos 20.3 = 151.$

$G_{45x2} = 161 \times \sin 20.3 = 56.$

A. STRESS IN RIBS AT THE STRUCTURAL RINGS $= \sigma_{R45}$
(PER PAR. 4.5.1 - A.)

G_{45x2} - COMPONENT

COMBINED STRESS IN EACH RIB DUE TO G_{45x2} COMPONENT IS $= \sigma_{45x2}$

$$\sigma_{45x2} = \sigma_{90x2} \times \frac{G_{45x2}}{G_{90x2}} \times \frac{DLF_{45}}{DLF_{90}} = 10.2 \times \frac{56.}{59.} \times \frac{1.14}{.975}$$

$\sigma_{45x2} = 11.32$ KSI

4.5.3 CONT'D

G_{45X1} - COMPONENT

STRESS IN RIBS DUE TO MOMENT ABOUT X2-AXIS = σ_{45X1}

$$\sigma_{45X1} = \sigma_{90X1} \times \frac{G_{45X1}}{G_{90X1}} \times \frac{DLF_{45}}{DLF_{90}} = 23.75 \times \frac{151.}{127.} \times \frac{1.14}{.975}$$

$\sigma_{45X1} = 33.0$ KSI. $\sigma_{A45} = \sigma_{A90} \times \frac{151.}{127.} \times \frac{1.14}{.975} = 1.9 \times 1.39 = 2.64$ K

$\sigma_{R45} = \sigma_{45X1} + \sigma_{45X2} = 33.0 + 11.32 = 44.32$. $\sigma_{A90}/S_y = 2.64/20.1 = .13$

$(\sigma_{A45} + \sigma_{R45})/S_y = 44.32/20.1 = 2.2 \Rightarrow$ COORD. (.13, 2.2) WITHIN ENVELOPE

B. STRESS IN URANIUM = σ_{U45}
(PAR. 4.5.1 - B)

MAX. MOMENT AT X3 [IN]

X3 = 9.5 IN

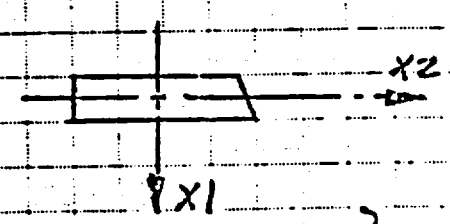

G_{45X1} - COMPONENT

STRESS IN URANIUM DUE TO MOMENT ABOUT X2-AXIS = σ_{45X1}

$$\sigma_{45X1} = \sigma_{90X1} \times \frac{G_{45X1}}{G_{90X1}} \times \frac{DLF_{45}}{DLF_{90}} = 9.96 \times \frac{151.}{127.} \times \frac{1.14}{.975}$$

$\sigma_{45X1} = 13.85$ KSI

4.5.3. CONT'D

G_{45x2} - COMPONENT

STRESS IN URANIUM DUE TO MOMENT ABOUT X1-AXIS = σ_{45x2}

$$\sigma_{45x2} = \sigma_{90x2} \times \frac{G_{45x2}}{G_{90x2}} \times \frac{DLF_{45}}{DLF_{90}} = 1.52 \times \frac{56.}{59} \times \frac{1.14}{.975}$$

$$\sigma_{45x2} = 1.70 \text{ KSI}$$

$$\sigma_{u45} = \sigma_{45x1} + \sigma_{45x2} = 13.85 + 1.70$$

$$\sigma_{u45} = 15.55 \text{ KSI} < S_{yu} = 46.0 \text{ KSI}$$

C. STUDS (PAR. 4.5.1-C & 4.5.4)

STRESS IN STUD AT RIB-URANIUM CONNECTION = σ_{S45}

G_{45x1} - COMPONENT

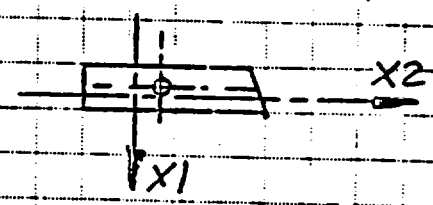

STRESS IN STUD DUE TO MOMENT ABOUT X2-AXIS = σ_{45x1}

$$\sigma_{45x1} = \sigma_{90x1} \times \frac{G_{45x1}}{G_{90x1}} \times \frac{DLF_{45}}{DLF_{90}} = 43.0 \times \frac{151.}{127.} \times \frac{1.14}{.975}$$

$$\sigma_{45x1} = 59.78 \text{ KSI}$$

G_{45x2} - COMPONENT

STRESS IN STUD DUE TO MOMENT ABOUT X1-AXIS = σ_{45x2}

$$\sigma_{45x2} = \sigma_{90x2} \times \frac{G_{45x2}}{G_{90x2}} \times \frac{DLF_{45}}{DLF_{90}} = 6.72 \times \frac{56.}{59.} \times \frac{1.14}{.975} = 7.46 \text{ KSI}$$

4.5.3 CONT'D

$\sigma_{S_{45}} = \sigma_{45x1} + \sigma_{45x2} = 59.78 + 7.46$

$\sigma_{S_{45}} = 67.24$ KSI

SHEAR STRESS IN STUD AT RIB-URANIUM CONNECTION $= \tau_{S_{45}}$

$\tau_{S_{45}} = \tau_{S_{90}} \times \frac{G_{45}}{G_{90}} \times \frac{DLF_{45}}{DLF_{90}} = 5.70 \times \frac{161.}{140.} \times \frac{1.14}{.978}$

$\tau_{S_{45}} = 7.66$ KSI $< 33.5 \times 1/\sqrt{3} = 19.3$ KSI

COMBINED STRESS IN STUD DUE TO TENSION & SHEAR AT RIB-URANIUM PLATE CONNECTION $= \sigma_{C_{45}}$

$\sigma_{C_{45}} = \frac{67.24}{2} \pm \frac{1}{2} \times \sqrt{67.24^2 + 4 \times 7.66^2}$

$\sigma_{C_{45}} = 68.10$ KSI $< \sigma_u = 79.0$ (SEE PAR. 4.3.1)

SHEAR STRESS IN STUD AT URANIUM - TOP PLATE CONNECTION $= \tau_{T_{45}}$

$\tau_{T_{45}} = \tau_{T_{90}} \times \frac{G_{45}}{G_{90}} \times \frac{DLF_{45}}{DLF_{90}} = 9.11 \times \frac{161.}{140.} \times \frac{1.14}{.978}$

$\tau_{T_{45}} = 12.25$ KSI $< 33.5 \times 1/\sqrt{3} = 19.3$ KSI

D. WELDS

SEE PAR. 4.4.1 - D.

4.5.4 SHIELDING NO. 4 - STUD SIZE TABLE
(PER PAR. 4.5.1-C THROUGH 4.5.3-C)

DEG. ORIENTATION	STUD SIZE AT BOTTOM	A_t [IN²]	a_{x1} & a_{x2} [IN]	S_{x2} [IN³]	S_{x1} [IN³]	σ_{s_i} [KSI] (i-DEG.)	σ_{c_i} [KSI] (i-DEG.)	BOTTOM STUD MATERIAL: 17-4 PH-A Sy [KSI]	Su [KSI]	L (450°F) NITRONIC-50 Sy [KSI]	Su [KSI]
90						49.72	50.37				
0	7/16-14 UNC	.106	.23 & .685	.035	.104	53.57	55.02	—	—	33.5	79.0
45						67.24	68.10				
90						66.98	67.88				
0	3/8-16 UNC	.0775	.246 & .735	.026	.077	72.24	74.25	123.0	128.6	—	—
45						90.6	91.8				

DEG. ORIENTATION	STUD SIZE AT TOP	A_t [IN²]	SHEAR STRESS = τ_{T_i} [KSI] (i-DEG.)		TOP STUD $\tau_p = S_y \times .577$ [KSI]	$\tau_p = S_y \times .57$ [KSI]
90			9.11	(NO WELD AT STUD TO TOP-PLATE)		
0	7/16-14 UNC	.106	14.3		—	19.3
45			12.25			
90			12.46	(NO WELD AT STUD TO TOP-PLATE)		
0	3/8-16 UNC	.0775	19.55		—	19.3
45			16.75			